TECHNISCHE UNIVERSITÄT
CHEMNITZ

Faculty of Natural Science

Workshop Ellipsometry

March 19 - 21, 2018
in Chemnitz, Germany

Abstract - Book

(with space for your notes)

Arbeitskreis Ellipsometrie (AKE) - Paul Drude e. V.

➡ www.ake-pdv.org/

www.WSE10.de

Impressum

Chemnitz University of Technology
Reichenhainer Straße 70
D-09126 Chemnitz / Germany

Phone: +49 371 531-33005

Fax: +49 371 531-833005

Email: secretary@wse10.de

Web: www.WSE10.de

Print: PrintService at Print and Media Technology at TU Chemnitz

Cover-Photo: TUC / St. Conrad
Conference-Logo: Lutz Feige

Table of Contents

Welcome address 2

Committees 4

List of Sponsors and Exhibitors 7

Technical Information 9

Program Overview 10

List of Oral Sessions

- Monday 13
- Tuesday 51
- Wednesday 73

Poster Contributions 104

Authors 201

City Map Chemnitz 210

Campus Map 212

Welcome Address

Dear Colleagues,

welcome to Chemnitz! The city, more than 800 years old, is situated in the heart of Saxony and is the third-largest in the new Federal States; about 245,000 people live here. Fascinating architecture reflects the changing times and spirit of those things which have shaped the city: industrial monuments, redeveloped Gründerzeit residential quarters such as the Kassberg, Villa Esche or the city centre, which has been completely modified since Re-unification, bridge the gap from yesterday to today and tomorrow. Just as famous is the 7.10-metres-high Karl-Marx bust made of bronze by Lew Kerbel in 1971, locally known as "Nischel" (head).
Probably no other city in Germany fits the description "City of Modernity" quite so well as Chemnitz does. Developed at the time of Classical Modernism, which still gives impetus to the development of business and science, the influences of the cultural and architectural Modernism are visible and perceptible. In 2006, the new centre was awarded the DIFA award for inner-city quarters for its successful mixture of retail, offices, catering trades, residential areas, leisure activities, and culture.
Chemnitz is a capital of culture. The city theatre is nationally and internationally prized along with the Opera House and the Playhouse with exceptional productions as well as the Robert-Schumann Philharmonic Orchestra. The City Art Collections on Theaterplatz are regularly included in the Federal German feature pages with their exhibitions. Moreover, one of the largest private German art collections found its place in Chemnitz in 2007: In the Gunzenhauser Museum almost 2,500 eminent works await the visitors in a former Sparkasse building. The works are of the Classic Modernism period, the art between the World Wars and the second half of the 20th century, among which is one of the largest Otto-Dix collections worldwide.
Chemnitz was, and still is, a city with a flourishing economy and inventive talent. And Chemnitz today is once again a competitive centre for technological innovation, for which it owes its numerous entrepreneurs and their proximity to the research centres. Since 2004, Chemnitz has been counted among the ten strongest growing cities of Germany every year.

Situated in the center of the Chemnitz “Wissenschaftsregion” (“science region”), the Technische Universität (TU) Chemnitz is home to more than 11,000 students from 90 countries. With approximately 2,300 employees in science, engineering, and management, the TU Chemnitz is among the most important employers in the region. Today, TU Chemnitz stands for outstanding research. Within the core competencies “Materials and Smart Systems”, “Resource-efficient Production and Lightweight Structures” and “Humans and Technology”, solutions for the challenges of tomorrow are developed. The profile of TU Chemnitz is characterized by a unique constellation of competencies across eight faculties. Thanks to this constellation, Chemnitz is emerging as an internationally visible research hub for future value creation processes and sustainable growth for the future.

Within the core competency “Materials and Smart Systems”, scientists at the TU Chemnitz are, for instance, involved in the Federal Cluster of Excellence “Center for Advancing Electronics Dresden” (cfAED). Several DFG Research Groups (Towards Molecular Spintronics, Sensorical Micro- and Nanosystems, and Twin Poymerisation) composed of physicists, chemists, and engineers work in the field nanotechnology. In addition, TU Chemnitz is the home of the “Center for Materials, Architectures and Integration of Nanomembranes” (MAIN), which is unique in Europe.

The Faculty of Natural Science as a faculty with strong connections between the Institute of Chemistry and the Physics Institute on the basis of experimental and theoretical methods is devoted both to fundamental research as well as applied science. The faculty concentrates on the following four research topics: Complex Materials, Molecular Systems, Scientific Modelling and Simulation, and Sensors and Cognition. Traditionally, research in the Institute of Physics was and still is focused on condensed matter systems and, in particular thin films and surfaces. Even well before reunification Physics in Chemnitz was well-recognised for the work on e.g. hard coatings. Later this work was continued and strongly extended in large-scale projects like “Thin Films and Non-Crystalline Materials”, “Methods and Materials for the Nanometer Scale”, “Micromechanical Sensor and Actor Arrays”, or the “Nano System Integration Network of Excellence”. Today two-dimensional materials like graphene and transition metal dichalcogenides and low-dimensional materials such as carbon nanotubes and semiconductor quantum dots belong to the research interests in the Institute of Physics. We are proud of an excellent infrastructure and you are all welcome to visit our facilities in the Physics building which was opened in 2008.

The Workshop of Ellipsometry (WSE) has taken place since 2000, gathering an increasing number of scientists from all over the world. The 10th edition now takes place in Chemnitz (Germany) from March 19th - 21st 2018 and follows the previous workshops held in Stuttgart (2000 and 2004), Berlin (2002, 2006, and 2011), Zweibrücken (2009), Leipzig (2012), Dresden (2014), and Enschede (2015).

The aim of this workshop is to provide a platform to present new advances and developments in ellipsometric application, science, and technology and related methods of metrology as well as to encourage interdisciplinary research. The topics discussed at the workshop are intended to span from science to industrial applications. This workshop allows young researchers to exchange experiences and gain knowledge on basics of ellipsometry and related methods as well as on a wide field of ellipsometry applications. There are 10 invited talks as well as 35 oral and 46 poster contributions.

Enjoy the scientific and the social program with the excursion to terra mineralia and Freiberg!

Chemnitz, March 2018

Dietrich RT Zahn

Organizing Committee

Dietrich R. T. Zahn
(Chemnitz University of Technology)

with **Local Support** by

Lutz Feige (Chemnitz University of Technology)
Sybille Raschke (Chemnitz University of Technology)
Jane Eisentraut (Chemnitz University of Technology)
Constance Schmidt (Chemnitz University of Technology)

Program Committee

Klaus-Jochen Eichhorn (Leibniz-Institut für Polymerforschung Dresden e.V.)

Norbert Esser (Leibniz-Institut für Analytische Wissenschaften e.V. / ISAS)

Karsten Hinrichs (Leibniz-Institut für Analytische Wissenschaften e.V. / ISAS)

Heidemarie Schmidt (Chemnitz University of Technology)

Rüdiger Schmidt-Grund (Universität Leipzig)

Herbert Wormeester (University of Twente)

Dietrich R. T. Zahn (Chemnitz University of Technology)

International Advisory Board

Hans Arwin (Linköping University,Sweden)

Uwe Beck (Bundesanstalt für Materialforschung und -prüfung, Germany)

Christian Bernhard (Université de Fribourg, Swiss)

Christoph Cobet (Johannes-Kepler-Universität Linz, Austria)

Bernard Drevillon (Centre national de la recherche scientifique, France)

Kurt Hingerl (Johannes-Kepler-Universität Linz, Austria)

Josef Humlicek (Masaryk Univerity, Czech Republic)

Stergios Logothetidis (Aristotle University of Thessaloniki, Greece)

Maria Losurdo (CNR-NANOTEC, Institut of Nanotechnology, Italy)

Peter Petrik (Centre for Energy Research, Institute of Techn. Physics and Materials Science, Hungary)

Kamil Postava (Technical University of Ostrava, Czech Republic)

Mathias Schubert (University of Nebraska-Lincoln, USA)

List of Sponsors and Exhibitors

ACCURION

www.accurion.de

HORIBA Scientific

www.horiba.com/de/scientific

LOT

www.lot-q.de

Schaefer Technologie GmbH

www.schaefer-tec.com

SEMILAB

www.semilab.hu

SENTECH

www.sentech.com

Chemnitz University of Technology

www.tu-chemnitz.de

Brewery “Freiberger Brauhaus”

www.freiberger-pils.de

Technical Information

- **for Talks:**

The venue of the WSE 10 conference is the Central Lecture Hall Building on the campus. Address: Reichenhainer Str. 90, 09126 Chemnitz, near tram stop line 3, or cityline 13, 14, 15.

We provide a notebook with Win10, MS Office 2013, and Adobe Acrobat XI. If you will use your own computer please connect your computer prior to the session and check whether your presentation works properly. As video connection VGA and HDMI connections are available. In case of questions please contact our technical team or
call **✆ +49 371 531-29884** or **✆ +49 151 11 64 28 90**.

- **for Posters:**

The poster boards have the size DIN A0 (vertical: 841 mm x 1189 mm). The poster session will take place in the 1st floor in the Central Lecture Hall Building. Please leave your poster at the registration desk until the lunch break on Monday. We will fix all posters on the boards. On Wednesday afternoon the posters will be removed.

- **Excursion and Conference Dinner:**

We will go by bus to the City Freiberg. There we will visit the brewery “Freiberger Brauhaus” and the mineral exhibition of the TU Bergakademie Freiberg "terra mineralia" (↗ www.terra-mineralia.de/).

The dinner takes place in the Brauhof Freiberg.

After the conference dinner we will all return by bus to Chemnitz.

- **for WLAN:**

Access to WLAN is available in the entire Central Lecture Hall Building. Two nets are available: >eduroam< (login with the access data of your institute) and >tu-chemnitz.de< (for this network open your web browser, go to the tab ‘Event’ and enter the following key: WSE10chemnitz) .

- **Contacts:**

If you have any problems or trouble please contact our support team at the registration desk or call one of the following numbers:

Conference Desk:	✆ +49 371 531-29884
DI DI(FH) L. Feige:	✆ +49 151 11 64 28 90
Prof. Dr. DRT Zahn:	✆ +49 171 74 20 29 3
S. Raschke:	✆ +49 152 53 93 96 76

Program Overview

18th March - Sunday		
18:00 - 20:00	Pre-Registration Stand assembly	Organization Office N106 Lecture Hall Building

19th March - Monday		
07:30 - 08:55	Registration	Organization Office N106
08:55 - 09:10	Opening session	N112
09:10 - 09:40	K. Hingerl	
09:40 - 10:00	C. Walder	
10:00 - 10:20	W. Ogieglo	
10:20 - 10:50	Coffee break	Foyer
10:50 - 11:20	Z. Pápa	N112
11:20 - 11:40	M. Canepa	
11:40 - 12:00	A. Hertwig	
12:00 - 12:20	J. Rappich	
12:20 - 12 :40	E. Bittrich	
12:40 - 13:40	Break for lunch	Foyer Lecture Hall Building
13:40 - 14:10	G. Salvan	N112
14:10 - 14:30	S. Espinoza	
14:30 - 14:50	A. Sharma	
14:50 - 15:10	E. Baron	
15:10 - 15:30	E. Krüger	
15:30 - 16:00	Coffee break	Foyer
16:00 - 16:30	R. Goldhahn	N112
16:30 - 16:50	R. Reineke-Koch	
16:50 - 17:10	C. Sturm	
17:10 - 17:30	V. Zviagin	
17:30 - 17:50	A. Mock	
18:00 - 20:00	Poster session, Exhibition, Beer	Foyer Lecture Hall Building
20:00 - 21:00	Mitgliederversammlung des AKE - Paul Drude e. V. Assembly of Paul Drude Association	N113

20th March - Tuesday		
08:30 - 09:00	B. Gompf	N112
09:00 - 09:20	M. Hammerschmidt	
09:20 - 09:40	W. Shen	
09:40 - 10:00	S. A. Jensen	
10:00 - 10:20	R. Sachse	
10:20 - 10:50	Coffee break	Foyer
10:50 - 11:20	T. Shaykhutdinov	N112
11:20 - 11:40	M. Duwe	
11:40 - 12:00	S. Funke	
12:00 - 12:20	M. Magnozzi	
12:20 - 12:40	U. Beck	
12:40 - 13:30	Break for lunch	Foyer Lecture Hall Building
13:30 - 18:30	Excursion - Freiberg	
18:30 - 22:00	Social dinner Freiberg	

21st March - Wednesday		
08:30 - 09:00	T. Hofmann	N112
09:00 - 09:20	L. Skowronski	
09:20 - 09:40	M. Fried	
09:40 - 10:00	P. Basa	
10:00 - 10:20	L. Jansen	
10:20 - 10:50	Coffee break	Foyer
10:50 - 11:20	S. Richter	N112
11:20 - 11:40	J. Budai	
11:40 - 12:00	A. Horn	
12:00 - 12:20	A. Blümich	
12:20 - 12:40	D. V. Likhachev	
12:40 - 13:40	Break for lunch	Foyer Lecture Hall Building
13:40 - 14:10	S. Zollner	N112
14:10 - 14:30	M. Stoica	
14:30 - 14:50	I. Alonso	
14:50 - 15:10	P. Kühne	
15:10 - 15:40	A. Furchner	
15:40 - 16:10	Awards, Concluding remarks	

List of Oral Sessions & Abstracts

Sunday:

18.00 – 20:00	Pre-Registration Stand Assembly

Monday:

07:30	Registration
	N112
08:55	Opening session
09:10	*Invited Talk*: K. Hingerl
09:40	C. Walder
10:00	W. Ogieglo
10:50	*Invited Talk*: Z. Pápa
11:20	M. Canepa
11:40	A. Hertwig
12:00	J. Rappich
12:20	E. Bittrich
13:40	*Invited Talk*: G. Salvan
14:10	S. Espinoza
14:30	A. Sharma
14:50	E. Baron
15:10	E. Krüger
16:00	*Invited Talk*: R. Goldhahn
16:30	R. Reineke-Koch
16:50	C. Sturm
17:10	V. Zviagin
17:30	A. Mock

18:00	Poster session, Exhibition, Beer
20:00	Assembly of Paul Drude Association

A classical model for depolarization by temporal and spatial decoherence

Kurt Hingerl
Center for Surface- and Nanoanalytics, University Linz , Austria
Kurt.Hingerl@jku.at

A finite spectral resolution and/or an imperfectly collimated beam /and or an (areal) extended light source / and or an (areal) extended detector and/ or a sample with a varying thickness can produce depolarization in any ellipsometric or polarization measurement. Despite these experimental findings, there are to our knowledge no physical models published which trace the origin of depolarization back to the atomic properties. Therefore, in the talk I will explain crosspolarization - and subsequently depolarization by considering the ***common- not separable-*** effect between the light beam and the sample, described by **coherence length and coherence area**.
For inhomogeneous samples with dimensions smaller than the coherence area, the fields have to be added coherently. However, inner and non-planar boundaries give rise to evanescent fields in the vicinity of these boundaries. Parallel and perpendicular field components oscillate and decay differently in the vicinity of the boundaries, therefore cross- polarization (incident s- polarized light excites reflected p-polarized light and vice versa) occurs.[1] In inhomogeneous samples the Fresnel reflectances are not correct any more, these strictly rely on homogeneity (i.e. arbitrary shifts of the sample along any surface direction change the measurement).

However, in optics we never measure the electric fields, because our available detectors are much too slow, but we measure their ***statistical*** second moments. In homogeneous samples with thick transparent overlayers it turns out that depolarization arises through the temporal decoherence of photons, and the measured Müller matrix (MM) elements are given by a convolution of the spectral width of the light source and a sample property: the thickness of the transparent overlayer.

For inhomogeneous samples, when the sample sizes or structures are larger than the coherence area, then the different local polarization states in reflection coming from different materials have to be added incoherently- partially depolarized light results.[2] Also here the measured Müller matrix is given by a convolution of a light source property (i.e. the coherence area) and a sample property: the structure size). For both depolarization mechanisms mathematical models[3] will be presented, allowing to predict the polarization response, i.e. all MM elements for periodic structures, metamaterials and thick films.

---

[1] J. -P. Perin, K. Hingerl, Appl. Surf. Sci. **421**, 738, (2017)

[2] The mathematical formulations- which will be largely avoided in the talk- are given through the coherency matrix / respectively the Stokes vectors, and decoherence shows up by the Cittert- Zernike theorem (M. Born & E. Wolf, *Principles of Optics*, chapter X.9).

[3] K. Hingerl, R. Ossikovski, Opt. Lett., **41**, 219, (2016)
and R. Ossikovski, K. Hingerl, Opt. Lett., **41**, 4044, (2016)

INFRARED SPECTROSCOPIC ELLIPSOMETRY OF SiO_2 TRAPEZOIDS AND BIOHYBRID SiO_2/PROTEIN INTERFACES

C. Walder[a], A. Furchner[a], M. Zellmeier[b], J. Rappich[b], H. Ketelsen[c] and K. Hinrichs[a]

[a]ISAS Berlin, Schwarzschildstraße 8, 12489 Berlin, Leibniz-Institut für Analytische Wissenschaften - ISAS - e.V., Germany
[b]Institut für Silizium Photovoltaik, Kekuléstraße 5, 12489 Berlin, Helmholtz-Zentrum Berlin für Materialien und Energie GmbH, Germany
[c]SENTECH Instruments GmbH, Schwarzschildstraße 2, 12489 Berlin, Germany

Infrared spectroscopic ellipsometry yields in-situ information about the micrometer-sized surface structure and surface chemistry of components relevant for solar cells, LEDs, biotemplates and biosensors. While ellipsometric scatterometry is already established in the UV/VIS spectral range for the integrated circuit industry, our approach combines the investigation of micrometer-sized periodic structures with the analysis of molecular vibrations [1, 2].

We measured the Mueller matrices of trapezoidal SiO_2 columns on Si with periods from 10 to 20 μm in both lateral directions (Fig. 1.). The modeling by Rigorous Coupled Wave Analysis shows good agreement for two different azimuth angles of sample rotation and geometrical lengths which correspond to SEM results. Moreover, simulations suggest that the off-diagonal Müller matrix elements are especially sensitive to variations of the azimuth angles and the trapezoidal baseline length.

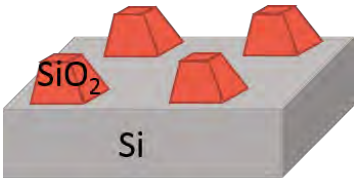

Fig. 1. Sketch of SiO_2 trapezoids

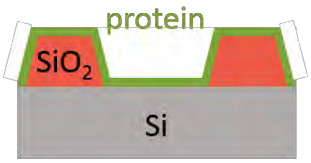

Fig. 2. Cross section of protein coated SiO_2 stripes

To describe a system with a biohybrid interface, micrometer-sized lamellar SiO_2 gratings were produced on Si and coated with a nanometer-thin monolayer of human serum albumin (HSA, protein, Fig. 2.). The infrared ellipsometric spectra were recorded before and after the protein coating. The comparison of the spectra shows geometrical characteristics as well as protein related vibrational peaks which, in principle, can elucidate the secondary protein structure.

Keywords: Infrared Ellipsometry; Scatterometry; Mueller Matrix; Biohybrid Interface

References

[1] H.T. Huang, F.L. Terry, Thin Solid Films 455-456 (2004) 828-836.
[2] C. Walder, M. Zellmeier, J. Rappich, H. Ketelsen, K. Hinrichs, Applied Surface Science 416 (2017) 397-401.

ULTRA-THIN POLYMERS OF INTRINSIC MICROPOROSITY IN FLUIDS

Wojciech Ogieglo[a,b], Bader Ghanem[b], Xiaohua Ma[b], Matthias Wessling[a] and Ingo Pinnau[b]

[a] DWI Leibniz Institute for Interactive Materials, Forckenbeckstr. 50, 52074 Aachen, Germany
[b]Advanced Membranes and Porous Materials Center, 4700 King Abdullah University of Science and Technology (KAUST), Thuwal 23955-6900, Kingdom of Saudi Arabia

Polymers of Intrinsic Microporosity (PIMs) are widely regarded as having the potential to revolutionize such fields as molecular separations, catalysis or energy storage [1]. PIMs possess high microporosity often with pores similar to sizes of small gas molecules (3 – 6 Å) that enable effective "sieving" of gases and vapors. Such a structure forms naturally as a result of PIMs extremely rigid backbones that pack inefficiently in a solid state following deposition from a polymer solution. The easy processing of PIMs allows their introduction on a large industrial scale using the existing manufacturing facilities.

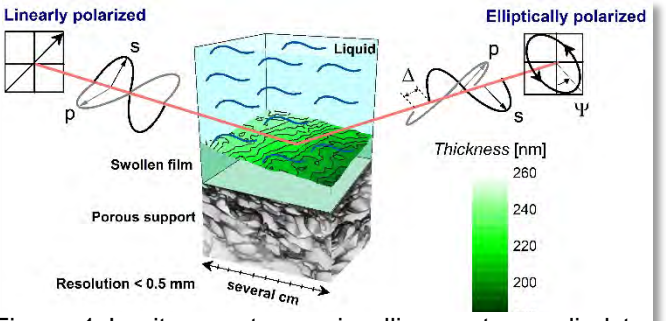

Figure 1 In-situ spectroscopic ellipsometry applied to directly image thin film composite

In this contribution, *in-situ* interference-enhanced ellipsometry is used to characterize ultra-thin (down to 6-7 nm) PIMs interacting with a variety of fundamentally and technologically important fluids including high pressure gases, liquids or vapors [2–4]. Next to characterization of thin PIM films ellipsometry is applied to study thin film composite membranes consisting of a selective skin deposited on a porous substrate [5]. Such geometry, highly unusual in typical ellipsometry analysis, mimics an actual highly efficient membrane that could be used in a large scale molecular separation plant.

Keywords: Polymers of Intrinsic Microporosity; In-situ Ellipsometry; Industrial Membranes

References

[1] N.B. McKeown, P.M. Budd, Polymers of intrinsic microporosity (PIMs): organic materials for membrane separations, heterogeneous catalysis and hydrogen storage, Chem. Soc. Rev. 35 (2006) 675.
[2] W. Ogieglo, K. Rahimi, S.B. Rauer, B. Ghanem, X. Ma, I. Pinnau, M. Wessling, How Do Organic Vapors Swell Ultrathin Films of Polymer of Intrinsic Microporosity PIM-1?, J. Phys. Chem. B. 121 (2017) 7210–7220.
[3] W. Ogieglo, B. Ghanem, X. Ma, I. Pinnau, M. Wessling, How Much Do Ultrathin Polymers with Intrinsic Microporosity Swell in Liquids?, J. Phys. Chem. B. 120 (2016) 10403–10410.
[4] W. Ogieglo, A. Furchner, B.S. Ghanem, X.-H. Ma, I. Pinnau, M. Wessling, Mixed-Penetrant Sorption in Ultra-Thin Films of Polymer of Intrinsic Microporosity PIM-1, J. Phys. Chem. B. (2017) acs.jpcb.7b10061.
[5] W. Ogieglo, I. Pinnau, M. Wessling, In-situ Non-Invasive Imaging of Liquid-Immersed Thin Film Composite Membranes, J. Memb. Sci. 546 (2017) 206–214.

ELLIPSOMETRY OF THIN PEPTIDE FILMS

Z. Pápa [a,b] and J. Budai [a,b]

[a]University of Szeged, Department of Optics and Quantum Electronics, H-6720 Szeged, Dóm tér 9., Hungary
[b]ELI-HU Non-Profit Ltd, Szeged, Hungary

Spectroscopic ellipsometry is increasingly used for investigation of biofilms and biological materials because of its non-invasive manner. In the case of biofilms, the investigated material might be present on the surface only in small amounts forming an island-like coating. In this work, we used various types of peptides which adhesion differences in the case of deposition to n- and p-type silicon were determined in [1]. We investigate the applicability of different ellipsometric models for such peptide films. We also present which models lead to unphysical result and how it is possible to choose the correct ones utilizing only ellipsometric measurements.

Three different approaches were built to model our peptide films: i) a perfect layer which optical properties are modeled with Sellmeier-dispersion, ii) Sellmeier-dispersion extended with Gaussian absorption, iii) Sellmeier-dispersion assuming a non-continuous layer. Although the peptides are transparent in the visible spectral range as supported by absorption measurements, the first model failed. The second and the third approaches described the measured data with almost the same fitting quality, although their physical background is completely different. The second model applies a perfect layer with a slight absorption, and the third deals with a transparent layer which does not cover the substrate perfectly. To resolve this contradiction the results of a simulation will be presented that show the compatibility of the last two models, and explain why both models can describe the measured data. We will show that the absorption obtained in the second model can originate from the discontinuity of the layer. According to theory and simulations, the patterned character of the layer should lead to depolarization, which could ease the finding of the correct model [2].

However, in most cases depolarization is an undesired feature since it deteriorates degree of polarization, limiting the applicability of classical models. Therefore, through the examples of different sample types we emphasize the importance of handling depolarization in general [3,4].

Keywords: Peptide; Depolarization; Patterned layer ellipsometric model

References

[1] Z. Pápa*, S. K. Ramakrishnan*, M. Martin, T. Cloitre, L. Zimányi, J. Márquez, J. Budai, Z. Tóth, C. Gergely, Langmuir 32 (28) (2016) 7250-7258 (* equal contribution)
[2] Z. Pápa, S. K. Ramakrishnan, M. Martin, T. Cloitre, L. Zimányi, Z. Tóth, C. Gergely, J. Budai, Applied Surface Science 421 (2017) 707-713
[3] Z. Pápa, J. Budai, I. Hanyecz, J. Csontos, Z. Toth, Thin Solid Films 571 (2014) 562-566
[4] Z. Pápa, J. Csontos, T. Smausz, Z. Toth, J. Budai, Applied Surface Science 421 (2017) 714-721

SPECTROSCOPIC ELLIPSOMETRY CHARACTERIZATION OF HYBRIDIZATION OF DNA ON GOLD SURFACES

I. Solano[a], P. Parisse[b], G. Pinto[a], F. Bisio[c], L. Casalis[b], O. Cavalleri[a] , M. Canepa[a]

a OptMatLab, Dipartimento di Fisica, Università di Genova, via Dodecaneso 33, 16146 Genova, Italy
b Elettra Sincrotrone Trieste, Italy
c CNR-SPIN, Genova, Italy

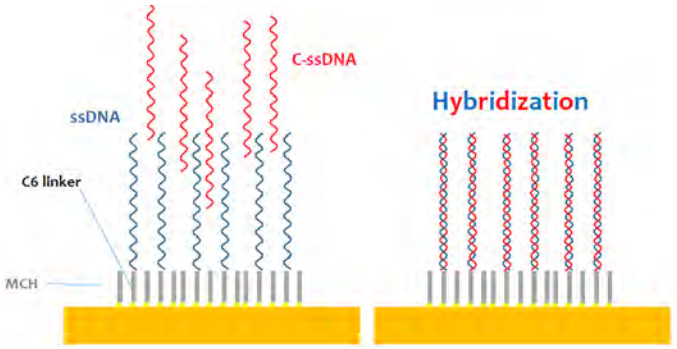

We recently coupled Spectroscopic Ellipsometry (SE) and AFM nanolithography methods to investigate the bonding of biomolecules at gold surfaces functionalized with well-organized compact thiolate Self-Assembled Monolayers (SAMs). AFM nanolithography was employed in so-called nano-shaving and nano-grafting modes [1,2] allowing precise determination of height of SAMs, which is important to feed the SE analysis. We present SE results (in-liquid and ex-situ) on a system of importance in the design of biosensors. Experiments on single-stranded ss-DNA were devoted to the detection of specific bonding through hybridization with complementary strands (c-DNA). The SE analysis of the precursor SAM, performed through the difference spectra method, allowed to disentangle the spectral features characteristic of the ss-DNA molecules and the molecule-surface bond. In particular a strong absorption in the UV range (260-270 nm) was detected in both in-situ and ex-situ data which was reproduced by a multi-oscillator model, consistently with known spectral response of DNA basis. The SE analysis with difference spectra was also able to clearly detect the hybridization process in mixed SAMs of ssDNA with mercaptohexanol (MCH), a short thiolate molecule which, through interaction with the C6 linker of ss-DNA (see cartoon) favors a standing-up organization of ss-DNA on the surface, in turn helping Hybridization. The influence of Hybridization on SE spectra turned out to be equivalent to a thickness increase of the film, which was confirmed by AFM nanoshaving. Control experiments performed by exposing the precursor ss-DNA layer to non-complementary DNA strands revealed no spectral change at all.

Keywords: Spectroscopic ellipsometry, DNA, bio-sensors

[1] I. Solano et al., Spectroscopic ellipsometry meets AFM nanolithography: about hydration of bio-inert oligo(ethylene glycol)-terminated self-assembled monolayers on gold. Phys. Chem. Chem. Phys. 17, 28774 (2015)
[2] I. Solano et al., Investigating organic multilayers by spectroscopic ellipsometry: specific and non-specific interactions of polyhistidine with NTA self-assembled monolayers, Beilstein J. Nanotechnol. 2016, 7, 544–553.

Determination of the glass transition region of PVME by means of spectroscopic ellipsometry

Andreas Hertwig[a], **Sherif Madkour**[b], **Marcel Gawek**[b], **Andreas Schönhals**[b]

[a]Div. 6.7, BAM, Unter den Eichen 87, 12200 Berlin, Germany,
andreas.hertwig@bam.de
[b]Div. 6.6, BAM, Unter den Eichen 87, 12200 Berlin, Germany

In this presentation, we report on the determination of the glass transition temperature of thin layers of Polyvinylmethylether (PVME) depending on the thickness of the polymer layer. The glass transition of thin polymer layers is currently under much investigation due to the nano-confinement effects proposed to appear in dependence on the layer thicknesses in the nm range. The properties of the polymer, the temperature range, as well as the thicknesses range of the polymer layers pose a serious challenge to the investigation by means of spectroscopic ellipsometry. By careful choice of experimental parameters, we were able to investigate the thickness change by temperature of PVME layers in the range between 2 and 300 nm and in the temperature range between 200 K and 340 K. By optimizing the analysis process, we were able to determine T_g values within this parameter range with sufficient accuracy to investigate the T_g change due to confinement effects.

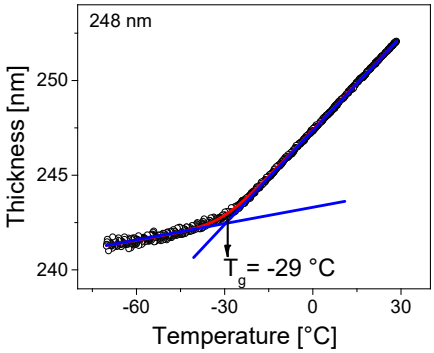

Fig. 1. T_g determination of a PVME layer

Alongside the change of position of the glass transition with thickness, we discuss the details of the ellipsometric analysis and its implications for the resulting thermal properties of the thin polymer layers [1] as well as the accuracy of the T_g value with respect to the method used in the analysis process.

Keywords: Polymers, PVME, temperature dependent ellipsometry, glass transition

References

[1] Madkour, S., et al., Decoupling of Dynamic and Thermal Glass Transition in Thin Films of a PVME/PS Blend. ACS Macro Letters, 2017. **6**(10): p. 1156-1161.

GRAPHENE FUNCTIONALIZED BY ULTRA-THIN ANCHOR LAYERS TOWARDS BIOSENSOR APPLICATION

T. J. Neubert[a], F. Rösicke[a], G. Sun[b], T. Shaykhutdinov[b], C. Kratz[b], K. Hinrichs[b], S. Janietz[c], N. H. Nickel[a], J. Rappich[a]

[a] Helmholtz-Zentrum Berlin für Materialien und Energie GmbH, Institut für Silizium Photovoltaik, Kekuléstr. 5, 12489, Berlin, Germany
[b] Leibniz-Institut für Analytische Wissenschaften - ISAS - e.V., Schwarzschildstr. 8, 12489 Berlin, Germany
[c] Fraunhofer Institute for Applied Polymer Research, Department Polymer Electronics, Geiselbergstr. 69, 14476 Potsdam, Germany

The functionalization of single layer graphene with specifically binding receptor molecules enables the facile fabrication of biosensors. The linkage between graphene and the receptor can be easily achieved by covalently bound molecules. We present the deposition of ultra-thin layers of such linker molecules on large area CVD-grown graphene by the electrochemical reduction of aryl diazonium salts containing amino, maleimide or thiol groups.[1] The successful deposition of the functional groups and the change of the graphene structure were detected by infrared spectroscopic ellipsometry, Raman backscattering, and electrochemical quartz crystal microbalance measurements. The homogeneity of the about 4.5 nm thin electrochemically prepared functional layer was verified by infrared atomic force microscopy.[2] The reactivity of these functional groups was tested by specific wet-chemical modification with small molecules via amidation reaction including immobilization of COOH-modified quantum dots. Finally, the functionalized and modified graphene was transferred from copper to different substrates including glass, silicon and flexible PTFE tape.

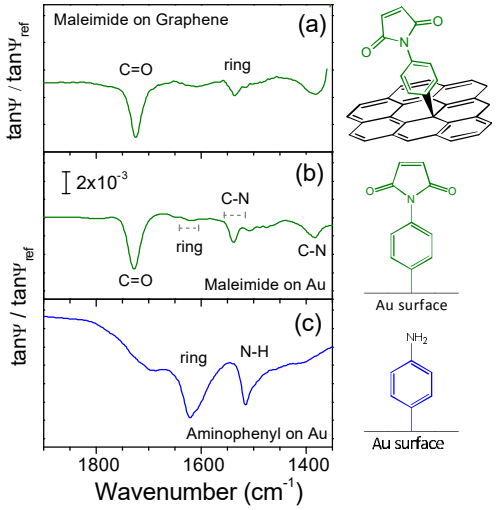

Fig. 1: IRSE spectra of Graphene (a) and Au (b,c) surfaces functionalized by maleimide (a,b) or amino (c) groups.

Keywords: Surface functionalization, biosensing, infrared-spectroscopic ellipsometry

References

[1] F. Rösicke, M.A. Gluba, K. Hinrichs, G. Sun, N.H. Nickel, J. Rappich, *Electrochem. commun.* 57 (2015) 52
[2] F. Rösicke, M.A. Gluba, T. Shaykhutdinov, G. Sun, C. Kratz, J. Rappich, K. Hinrichs, N.H. Nickel, *Chem. Commun.* 53 (2017) 9308

ZWITTERIONIC POLYMER SURFACES BASED ON PHOSPHORYLCHOLINE: SWELLING AND BIOMOLECULE INTERACTION

E. Bittrich[a], C. Naas[a], A. Münch[a], P. Uhlmann[a], K.-J. Eichhorn[a] and B. Voit[a]

[a]Leibniz-Institut für Polymerforschung Dresden e.V., Hohe Str. 6, Dresden, Germany

Zwitterionic polymers with positively and negatively charged molecular groups along the chains are showing excellent biocompatibility and are promising for applications in implant medicines, biosensors, or drug release [1]. Of special interest are coatings based on the zwitterionic phospholipid polymer poly (2-methacryloyloxyethyl phosphorylcholine) (PMPC) due to their biomimetic resemblance of phospholipid bilayers in biomembranes [2].

We prepared MPC – containing polymer layers based on the statistical copolymer MPC-*co*-GMA (Fig. 1a) with different layer thicknesses and analyzed their swelling behavior, protein resistance and phospholipid interaction by in-situ VIS-ellipsometry. We found good resistance to the adsorption of bovine serum albumin (BSA), the most abundant protein in the blood plasma, and considerable adsorption of the phospholipid DPPC (lipid for cell membrane models) (Fig. 1b).

Additionally, we mixed the MPC with the pH-sensitive polymer poly acrylic acid (PAA) aiming at stimuli-responsive blend layers with anti-fouling properties.

Ellipsometric investigations were combined with surface characterization by X-ray photoelectron spectroscopy (XPS), atomic force microscopy (AFM) and contact angle measurements, as well as quartz crystal microbalance (QCMD) analysis.

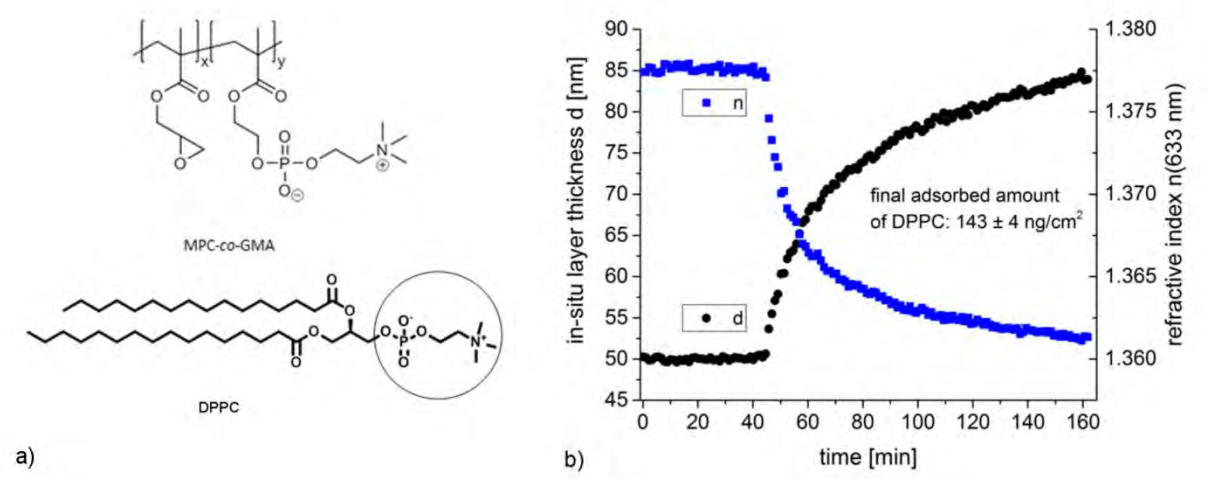

Fig. 1: a) Chemical structures of MPC-*co*-GMA (top) and 1,2-dipalmitoyl-*sn*-glycero-3-phosphocholine (DPPC) (bottom), b) in-situ layer thickness and refractive index at λ=633 nm for DPPC adsorption ($c^{DPPC}_{in\text{-}solution}$ = 0.25 mg/ml) to a MPC-*co*-GMA layer (dry thickness: 15 nm) in 10 mM sodium phosphate buffer solution at pH 5.8 with 1 mM $CaCl_2$.

Keywords: phosphorylcholine; in-situ VIS ellipsometry; protein adsorption

References

[1] J. B. Schlenoff, Langmuir 30 (2014) 9625.
[2] A. L. Lewis, Colloid. Surf. B: Biointerfaces 18 (2000) 261.

MAGNETO-OPTICAL KERR EFFECT SPECTROSCOPY OF MAGNETIC OXIDES AND ORGANIC/OXIDE HETEROSTRUCTURES

Georgeta Salvan

Semiconductor Physics, Chemnitz University of Technology, 09107 Chemnitz, Germany

Recent progress in multiferroic materials and spintronic devices has renewed interest in metal oxide ferromagnetic and ferrimagnetic materials. We recently showed, on the example of $CoFe_2O_4$ (CFO) that the preparation of high-quality thin films of nanocrystalline ferrimagnetic can be achieven by means of an environmentally benign aqueous solution processing route [1]. In addition to the ability to make high quality ferrite films, the aqueous solution processing strategy offers great flexibility for tuning film properties by incorporating or substituting additional transition metal ions. Furthermore, it can also be applied for the preparation of $La_{1-x}Sr_xMnO_3$ films [2], which is in discussion as material with high potential for spintronic applications as such or in combination with organic molecules.

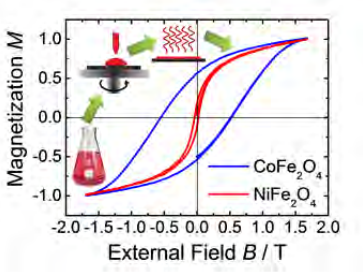

Fig. 1. Magnetization loops obtained by MOKE magnetometry for high-quality ferrite films fabricated by aqueous solution processing

The evolution of the structural, optical, and magnetic properties as a function of post-deposition annealing temperature was performed by HR-TEM and (magneto-)optical techniques: spectroscopic ellipsometry and magneto-optical Kerr effect spectroscopy. The latter methods were also employed to study the effect of the substrate magnetization on the molecular orientation of phthalocyanine molecules impozed during the growth on the ferrite substrates.

Keywords: magnetic oxides, organic molecules, MOKE spectroscopy, spectroscopic ellipsometry

References

[1] Peter Richter, Paul N. Plassmeyer, Julia Harzdorf, Tobias Rüffer, Jana Kalbacova, Nathanael Jöhrmann, Steffen Schulze, Michael Hietschold, Heinrich Lang, Sri Sai Phani Kanth Arekapudi, Manfred Albrecht, Dietrich R.T. Zahn, Catherine J. Page, and Georgeta Salvan, Chem. Mater. 2016, 28, 4917−4927.
[2] Manuel Monecke, PhD Thesis, Chemnitz

VUV MAGNETO-OPTICAL TRANSIENT ELLIPSOMETER: ELIps

S. Espinoza[a], S. Richter[a], M. Rebarz[a] and J. Andreasson[a,b]

[a] ELI Beamlines, Institute of Physics, Czech Academy of Science, Na Slovance 2, 18221 Prague, Czech Republic
[b] Condensed Matter Physics Group, Department of Physics, Chalmers University of Technology, Kemigården 1, 412 96 Göteborg, Sweden

The ELIps instrument being built at the European Extreme Light Infrastructure Beamlines (ELI Beamlines) will combine three advanced techniques of ellipsometry: VUV ellipsometry, transient (Pump-probe) ellipsometry, and magneto-optical ellipsometry [1] The working range of energies in the VUV is between 12 eV and 40 eV, this VUV radiation will be provided by a High Harmonics Generation (HHG) source driven by a high-power femtosecond-laser.

The instrument complements already established VUV ellipsometers at synchrotron light sources [2] by using pulsed laser light sources that can be synchronized allowing the measurement of processes with a time-resolution of a few picoseconds. The pump pulse from a laser hits the sample first, triggering e.g. charge transfer processes; these processes can be observed and quantified by measuring the changes on the optical properties of the material by a probe pulse. The pump beam is a single wavelength beam that can be chosen from 180 nm – 20 um. A Helmholtz coil is also installed in the instrument, which can deliver a field of up to 1.5 T at a rate of up to1 kHz. It would be possible to obtain the transverse magneto-optical Kerr Effect and probe e.g. the excitation of spin-polarized states.

All the components are contained within a single UHV chamber (with a target pressure lower than 10^{-8} mbar) designed with several additional ports to support future upgrades such as a sample preparation chamber. Furthermore, a cryostat allows temperature dependent studies.

Additional to the VUV ellipsometer, at ELI Beamlines, there is table top system for time-resolved ellipsometry utilizing super-continuum white-light pulses ranging from 350 nm – 750 nm that might be combined with the ELIps instrument.

This work is supported by the European Regional Development Fund: ELI Extreme Light Infrastructure Phase 2 (CZ.02.1.01/0.0/0.0/15_008/0000162) and ELIBIO (CZ.02.1.01/0.0/0.0/15_003/0000447).

Keywords: VUV ellipsometry, Pump-probe, Transient, Ultrafast phenomena, UHV

References

[1] S. Espinoza, G. Neuber, C.D. Brooks, B. Besner, M. Hashemi, M. Rübhausen, J. Andreasson. Appl. Surf. Sci. 421, 378-382 (2017)
[2] M.D. Neumann, C. Cobet, H. Kaser, M. Kolbe, A. Gottwald, M. Richter, N. Esser. Rev. Sci. Instrum. 85, 55117 (2014)

MAGNETO-OPTICAL SPECTROSCOPY AND SPECTROSCOPIC ELLIPSOMETRY OF $Co_{60}Fe_{20}B_{20}$ THIN FILMS

Apoorva Sharma[1], Maria Almeida[2], Patrick Matthes[3], Ramona Ecke[3], Dietrich R. T. Zahn[1], Stefan E. Schulz[2,3], and Georgeta Salvan[1]

[1]Semiconductor Physics, Chemnitz University of Technology, D-09107Chemnitz, Germany
[2]Center for Microtechnologies, Chemnitz University of Technology, D-09126Chemnitz, Germany
[3]Department Back-End of Line, Fraunhofer Institute for Electronic Nanosystems, D-09126Chemnitz, Germany

With the increasing interest in CoFeB for the realization of spintronic devices, the magneto-optical and optical transitions in spin-polarized electronic states are of significant importance for the characterization of such devices and further understanding of spin-dependent phenomena. We present the characterization of $Co_{60}Fe_{20}B_{20}$ thin films with combined magneto-optical Kerr effect (MOKE) spectroscopy and spectroscopic ellipsometry (SE).

$Co_{60}Fe_{20}B_{20}$ films with thicknesses ranging from 5 nm to 20 nm and a 3 nm Au capping layer were prepared by magnetron sputtering on glass and on thermally oxidized Si substrates. After a full characterization of the as-deposited samples, these were annealed in vacuum at 350ºC in order to study the changes in the magneto-optical and optical spectra of the samples upon the crystallization of CoFeB.

Variable angle spectroscopic ellipsometry (VASE) measurements were performed in the spectral range from 0.73 eV to 5 eV, in transmission and reflection modes, the latter including measurements at five angles of incidence (Φ = 50º, 55º, 60º, 65º and 70º). This allowed the relevant optical constants and the diagonal component of the dielectric tensor to be derived for CoFeB. The spectral dependence of the dielectric tensor component and the absorption coefficient were deduced from the experimental data for the samples prior and after annealing of CoFeB thin films, allowing further assessing the changes in the spectra due to the crystallization of the layer.

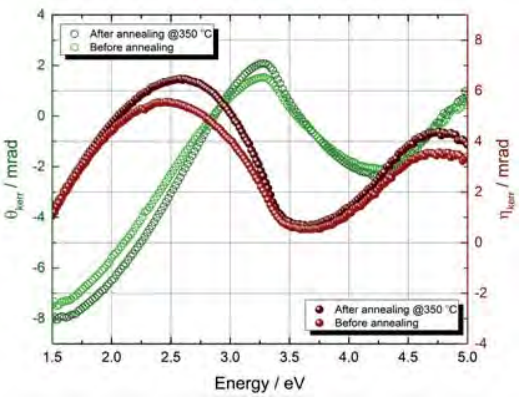

Figure 1: MOKE spectra measured at RT for $Si/SiO_2(100nm)/Co_{60}F_{20}eB_{20}(20nm)/Au(3nm)$ before and after annealing the sample at 350 °C. The hollow circles show the real part (rotation) and solid sphere are the imaginary part (ellipticity) of the polar MOKE spectra.

The MOKE investigations were performed in polar geometry in the spectral range of 1.5 eV to 5.0 eV, under magnetic saturation conditions. The Kerr rotation angle (θ_{Kerr}) and the Kerr ellipticity (η_{Kerr}) were measured as a function of the photon energy for the samples before and after annealing. The features of the θ_{Kerr} and η_{Kerr}–spectra at ~3.25 eV and ~2.5 eV are observed to become narrower after annealing, these spectral features are directly related to the magneto-optical transitions between the spin-polarized electronic states and the narrowing can be ascribed to the crystallization of CoFeB.

Finally, the present study provides access to the magneto-optical and optical characteristics of CoFeB thin films which can be determinant for spintronic device applications.

Keyword—CoFeB, Magneto-Optics, Ellipsometry, and Spintronic.

PLASMONIC PROPERTIES OF DEGENERATELY GE-DOPED CUBIC GAN

E. Baron[a], M. Feneberg[a], R. Goldhahn[a], M. Deppe[b] and D.J. As[b]

[a]Institut für Experimentelle Physik, Otto-von-Guericke-Universität Magdeburg, Germany
[b]Department Physik, Universität Paderborn, Germany

The optical properties of highly-doped zincblende GaN (c-GaN) are investigated. Using germanium, free electron concentrations (n) exceeding 10^{20}cm^{-3} can be achieved while maintaining high structural sample quality [1]. Thin films were deposited by plasma-assisted molecular beam epitaxy on 3C-SiC quasi-substrates. Similar to the case of wurtzite GaN [2], they were studied comprehensively by emission and absorption related optical techniques. Spectroscopic ellipsometry yields the complex dielectric function (DF) of c-GaN from the mid-infrared into the deep ultraviolet spectral region. The transverse optical phonon mode and free carrier concentration dependent plasma frequencies are obtained from the IR-DF. Combined with Hall-effect data, we find a pronounced increase of the effective electron mass with n mirroring the non-parabolicity of the conduction band. The onset energy of interband absorption is determined by the fundamental band gap for lower n and blue-shifts due to phase-space-filling for increased electron density. Quantification of this so-called effective Burstein-Moss shift is possible when taking into account the counteracting band gap renormalization effect and the momentum dependence of the effective electron mass. Photoluminescence spectra reveal a blue-shift of the main recombination feature consisting of a donor-acceptor-pair band at doping levels below the degeneracy limit and a free-electron recombination band above. The lineshape fitting yields parameters emphasizing the values for gap renormalization and band filling obtained from DF.

Keywords: cubic GaN; effective mass; non-parabolicity; transition energy

References

[1] M. Deppe, J.W. Gerlach, D. Reuter, D.J. As, Physica Status Solidi B 254 (2017) 1600700.
[2] M. Feneberg, K. Lange, C. Lidig, B. Garke, R. Goldhahn, E. Richter, C. Netzel, M. Neumann, N. Esser, S. Fritze, H. Witte, J. Bläsing, A. Dadgar, A. Krost, Physical Review B 90 (2014) 075203.

TEMPERATURE DEPENDENT DIELECTRIC FUCTION OF CUI THIN FILMS

E. Krüger, V. Zviagin, C. Yang, R. Schmidt-Grund and M. Grundmann

Universität Leipzig, Felix-Bloch-Institut für Festkörperphysik,
Linnéstraße 5, 04103 Leipzig, Germany

We present optical and structural properties of CuI thin films deposited by DC-sputtering at temperatures varying from 55°C to 310°C on c-sapphire substrate.

Scanning electron microscopy scans reveal a smooth surface morphology for films grown at temperatures above 60°C and large thickness inhomogeneity for films grown at lower temperatures. X-ray diffraction reveals good crystal quality for growth temperatures above 200°C.

The main features in the DF (see Fig. 1.) were assigned to exciton-related optical transitions at various critical points in the Brillouin zone. The observed energy separation of the split-off band is around 630 meV and is consistent with previous investigations [2].

The observed transitions reveal non-monotonic temperature dependence of the energy [1] as well as strong screening for excitons related to higher critical points.

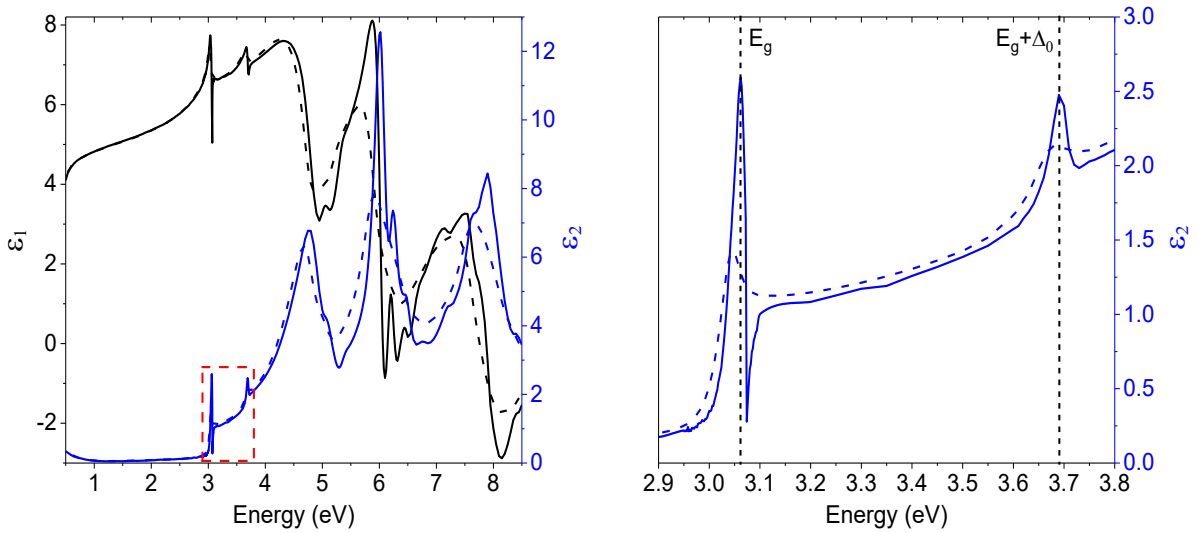

Fig. 1. Real (black) and imaginary part of dielectric function of the investigated CuI film at 10 K (solid) and at 300 K (dashed).

Keywords: Dielectric function; CuI;

References

[1] J. Serrano, Ch. Schweitzer, Physical Review B 65 (2002)
[2] M. Grundmann, F.-L. Schein, Physica Status Solidi A 210 (2013)

ELLIPSOMETRY OF TRANSPARENT CONDUCTING OXIDES FROM MID-INFRARED INTO VACUUM-ULTRAVIOLET

Rüdiger Goldhahn

Institute of Experimental Physics, University of Magdeburg, Germany,

Semiconducting metal oxides such as cubic In_2O_3, the various polytypes of Ga_2O_3, or rutile SnO_2 have attracted much interest in recent years. High-quality bulk crystals and single-crystalline heteroepitaxial films, covering a wide range of electron concentrations, became available allowing the determination of intrinsic optical properties as well as related fundamental band-structure parameters. This talk summarizes recent achievements.

Spectroscopic ellipsometry from the infrared (IR) into the vacuum-ultraviolet (VUV) spectral region is applied for determining the components of the dielectric tensor. The analysis of the IR dielectric function yields the phonon frequencies and the coupled phonon-plasmon modes from which electron effective mass as a function of carrier density (non-parabolicity of the conduction band) is obtained. Many-body effects such as exciton screening, band-gap renormalization, and band filling have a strong impact on the behavior around the fundamental band gaps, a quantitative description of these properties will be presented. Finally, synchrotron-based studies in VUV provide the transition energies related to critical points of the band structure.

Keywords: $(In,Ga,Al)_2O_3$; Band structure; effective mass, many-body effects

MAGNETRON SPUTTERED TiO_X LAYERS: STRUCTURAL, ELECTRICAL, OPTICAL AND THERMOCHROMIC ASPECTS

A. Pazidis[a], R. Reineke-Koch[a]

[a]Institute for Solar Energy Research Hamelin (ISFH), Am Ohrberg 1, 31860 Emmerthal, Germany

Titanium oxide layers were prepared by sputter deposition with plasma emission monitoring in the whole stoichiometry range between Ti and TiO_2 without and with substrate heating to 240 °C. The layers were characterized with regard to their crystal structure and specific resistance. Optical constants were determined in the spectral range between 240 nm and 38 µm by minds of spectral ellipsometry. The thermochromic behavior of a prepared Ti_2O_3 layer was measured and compared to calculations for bulk material.

Sub-stoichiometric titanium oxides and oxynitrides are used as absorber materials for solar thermal collectors [1]. But although a variety of thin film deposition techniques have been reported for the titanium-oxide system, infrared optical properties for these coatings were rarely determined. In recent years additional interest in thermochromic absorber layers has risen, especially for the infrared region as thermochromic absorbers are used to lower the collector stagnation temperature [2]. The Ti_2O_3 material comprising a switching temperature between 130 °C and 200 °C is a potentially interesting candidate for this application [3]. So the scope of this paper is to link the deposition parameters for sputtered titanium oxide layers to their morphology and optical constants, with special interest in the thermochromic phase Ti_2O_3 [4].

Keywords: solar thermal collector; titanium oxide; thermochromic absorber

References

[1] C.E. Kennedy, Technical Report, NREL/TP-520-31267 National Renewable Energy Laboratory, Colorado (2002)
[2] H. Marty, S. Brunold, P. Vogelsanger, 18. OTTI Symposium Thermische Solarenergie, Bad Staffelstein, Germany, 2008, edited by OTTI e.V., Regensburg (2008) 80-85
[3] S.H. Shin, G.V. Chandrashekhar, R.E. Loehman, J.M. Honig, Phys. Rev. B 8 (1973) 1364-1372
[4] A. Pazidis, R. Reineke-Koch, Thin Solid Films (2018) accepted

DIELECTRIC FUNCTION OF ε-$(In,Ga)_2O_3$ THIN FILMS

C. Sturm, A. Werner, V. Zviagin, D. Splith, H. v. Wenckstern, M. Lorenz, J. Lenzner, R. Schmidt-Grund and M. Grundmann

Felix-Bloch-Institut für Festkörperphysik, Linnéstr. 5, Universität Leipzig, Germany

The large band gap energy of about 4.8eV makes Ga_2O_3 interesting as transparent conductive oxide (TCO) since even in the presence of impurities a high transmissivity is sustained in the visible and even in the UV-A/B spectral range. The dielectric function for the β-phase of Ga_2O_3 was recently presented and discussed [1–3]. However, the dielectric function of the ε-phase, being interesting due to its spontaneous polarization, and its alloys with In and Al, which are used for tuning the band-gap energy, is not explored in great detail so far.

Here, we present a detailed analysis of the dielectric function of an ε-phase $(In,Ga)_2O_3$ thin film with lateral In composition spread for In concentrations between 1% and 35% in the infrared ($350cm^{-1}$ – $1500cm^{-1}$) and NIR-VUV (0.5eV – 8.5eV) spectral range. By means of a parametric model dielectric function approach, we derive the refractive index dispersion and the properties of the electronic band-band transitions and phonons. We observe a red shift of the fundamental band-gap energy with increasing In concentration which results in an refractive index increase in the transparent spectral range.

The thin film samples have been grown by means of pulsed laser deposition (PLD), with the use of segmented PLD targets (consisting of half-segments of binary indium oxide respective indium oxide and binary gallium oxide). This resulted in films with a continuous composition spread [4].

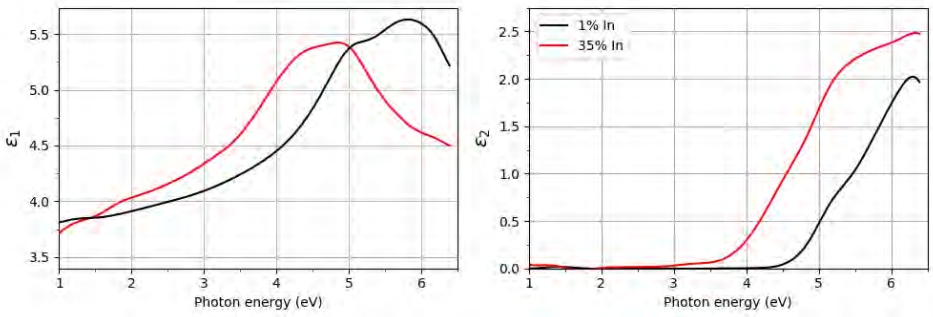

Fig.1. Real (left) and imaginary (right) part of the dielectric function of ε-Ga_2O_3:In for an In concentration of 1% (red line) and 35% (black line).

Keywords: dielectric function; Raman tensor; Ga_2O_3; wide band-gap oxide

References

[1] C. Sturm, J. Furthmüller, F. Bechstedt, R. Schmidt-Grund, and M. Grundmann, Appl. Phys. Lett. Materials **3** (2015) 106106.
[2] C. Sturm, R. Schmidt-Grund, C. Kranert, J. Furthmüller, F. Bechstedt, and M. Grundmann, Phys. Rev. B **94** (2016) 035148.
[3] A. Mock, R. Korlacki, C. Briley, V. Darakchieva, B. Monemar, Y. Kumagai, K. Goto, M. Higashiwaki, and M. Schubert, arXiv: 1704.06711.
[4] H. v. Wenckstern, Z. Zhang, F. Schmidt, J. Lenzner, H. Hochmuth, and M. Grundmann, CrystEngComm **15** (2013) 10020.

SPECTROSCOPIC INVESTIGATION OF CATION CONFIGURATION STATE OF SPINEL FERRITE THIN FILMS

V. Zviagin[a], P. Huth[b], C. Sturm[a], M. Bonholzer[a], J. Lenzner[a], A. Setzer[a], R. Denecke[b], P. Esquinazi[a], M. Grundmann[a] and R. Schmidt-Grund[a]

[a]Felix-Bloch-Institut für Festkörperphysik, Linnéstr. 5, Universität Leipzig, Germany
[b]Wilhelm-Ostwald-Institut für Physikalische und Theoretische Chemie, Linnéstr. 2, Universität Leipzig, Germany

We present a systematic study of cation configurations of spinel type $ZnFe_2O_4$ (ZFO) and $Zn_xFe_{3-x}O_4$ thin films fabricated by pulsed laser deposition. Electronic transitions assigned in the model dielectric function (MDF) correspond to Fe^{2+} interband d-d band and O^{2-} anion 2p to Fe^{3+} cation 4s and 3d band optical transitions [1]. Taking into account the contribution of each optical transition to the MDF, we have estimated the cation concentration ratio corresponding to the disordered state of the normal spinel configuration, and have compared it to the room temperature magnetization saturation of ZFO films before and after annealing in oxygen and argon atmospheres at temperatures to 375°C, (see Fig.1 a). Surface sensitive XPS Fe 2p and 3p core level analysis generally follows the trend, but shows also a deviation in the divalent and trivalent cation ratio as obtained from the bulk MDF for the $Zn_xFe_{3-x}O_4$ films, (Fig. 1 b). Two competing exchange interactions, AFM oxygen mediated super-exchange and FM double-exchange, were determined as a function of annealing temperature in ZFO and of the Zn/Fe ratio in $Zn_xFe_{3-x}O_4$ films. The results clarify their role in weakening the total ferrimagnetic response.

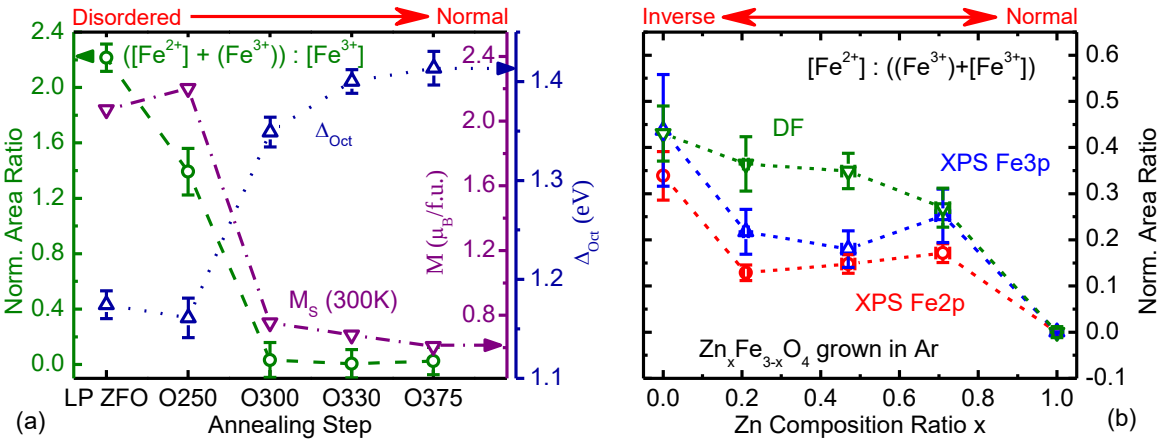

Fig. 1. (a) Area ratio of transitions involving divalent and trivalent Fe cations, representing disorder in a normal spinel structure, octahedral crystal field parameter and room temperature magnetization saturation as a function of annealing step in oxygen atmosphere. (b) Normalized area ratio of divalent and trivalent Fe cation contributions obtained from transitions in the DF and XPS Fe 2p and 3p core levels as a function of Zn composition ratio.

Keywords: Dielectric Function; Ferrimagnetic Material; Spinel Ferrites

References

[1] V. Zviagin, Y. Kumar, I. Lorite, P. Esquinazi, M. Grundmann, R. Schmidt-Grund, Appl. Phys. Lett. 108 (2016) 131901.

OPTICAL AND ELECTRONIC PROPERTIES OF LOW-SYMMETRY MATERIALS

A. Mock,[1] R. Korlacki,[1] S. Knight,[1] V. Darakchieva,[2] and M. Schubert,[1,2,3]

[1]Department of Electrical and Computer Engineering, Univ. of Nebraska-Lincoln, U.S.A.
[2]Department of Physics, Chemistry, and Biology, Linkoping University, Sweden
[3]Leibniz Institute for Polymer Research, Dresden, Germany

We discuss analysis of the dielectric function tensor for monoclinic metal-oxides. Generalized ellipsometry using an eigenpolarization vector summation approach [1] from the terahertz to the vacuum-ultra-violet spectral regions, and as a function of temperature (Fig. 1) [2], along with optical Hall effect, permit us to unravel all infrared active transverse and longitudinal optical phonon modes [3], free carrier excitations [3], band-to-band transitions [4], optical constants [4], exciton properties [4], effective mass parameters [5] and directional dependencies in single crystalline β-Ga_2O_3. We compare our findings with results from density functional theory calculations [4], and we revise and augment previous incomplete assignments [6,7].

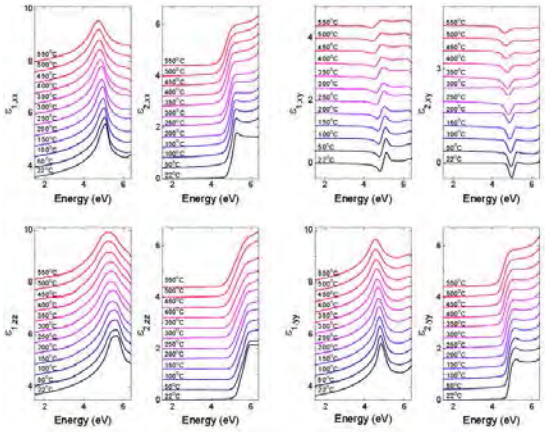

Figure 1: Real and imaginary components of the dielectric tensor elements, ε_{xx}, ε_{yy}, ε_{xy}, and ε_{zz} for room temperature (black) to 550°C (red) determined by generalized ellipsometry. The functions were shifted vertically by increments of 0.4 with respect to each other for convenience. Ref. [2]

We apply this same approach to other monoclinic oxides such as $CdWO_4$ [8] (Fig. 2) and Y_2SiO_5 [9] as well as to triclinic materials.

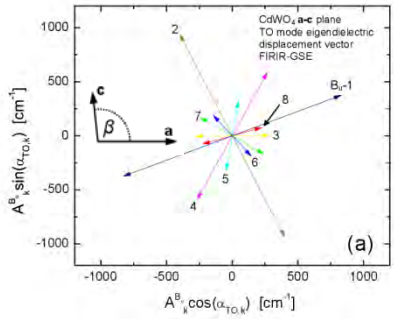

Figure 2: Schematic presentation of the Bu symmetry TO mode eigendielectric displacement unit vectors within the **a-c** plane according to TO mode amplitude parameters $A^{Bu}{}_k$ and orientation angles $\alpha_{TO,k}$ with respect to axis a obtained from generalized ellipsometry analysis. Ref. [8]

Keywords: Low-symmetry, monoclinic, Ga_2O_3

References

[1] M. Schubert, Phys. Rev. Lett. 117 (2016) 215502.
[2] A. Mock et al., arXiv:1710.10314 [cond-mat.mtrl-sci] App. Phys. Lett. (accepted) (2018)
[3] M. Schubert et al., Phys. Rev. B 93 (2016) 125209.
[4] A. Mock et al., Phys. Rev. B 96 (2017) 245205.
[5] S. Knight et al., Appl. Phys. Lett. 112 (2018) 012103
[6] C. Sturm et al., Phys. Rev. B 94 (2016) 035148.
[7] C. Sturm et al., APL Materials 3 (2015) 106106.
[8] A. Mock et al., Phys. Rev. B 95 (2017) 165202
[9] A. Mock et al., arXiv:1711.06336 [cond-mat.mtrl-sci] Phys. Rev. B (Under review) (2018)

Tuesday:

	N112
08:30	*Invited Talk*: G. Gompf
09:00	H. Hammerschmidt
09:20	W. Shen
09:40	S. A. Jensen
10:00	R. Sachse
10:50	*Invited Talk*: T. Shaykhutdinov
11:20	M. Duwe
11:40	S. Funke
12:00	M. Magnozzi
12:20	U. Beck
13:30	Excursion Freiberg
18:30	Social dinner Freiberg

The depolarization in granular media: a Mueller matrix approach

Bruno Gompf

University of Stuttgart, Germany

We describe a general method to disclose the information hidden in Mueller matrices experimentally obtained from depolarizing samples. Although spectroscopic Mueller-matrix ellipsometry allows for a model-free characterization of inhomogeneous samples, i.e., independently from any assumption on the sample structure, the interpretation of the obtained results is often challenging. The proposed method combines three different decomposition techniques applied to the measured Mueller matrices in transmission and reflection of granular thin films with different thicknesses and densities. We demonstrate that the comparative analysis of the respective differential-, product-, and sum-decomposition of the Mueller matrices, together with correlation effects and the visualization as a Poincaré sphere, reveals the particular underlying physical processes of depolarization. As an example, we apply this method on granular BaSO4 thin films. This method is general and can be applied to a wide variety of intrinsically inhomogeneous materials with applications in physics, industry, biology, or medicine.

QUANTIFYING UNCERTAINTIES OF RECONSTRUCTED PARAMETERS IN OPTICAL SCATTEROMETRY OF NANOSTRUCTURED SURFACES

Martin Hammerschmidt[a,b], Philipp-Immanuel Schneider[a], Xavier Garcia Santiago[a,c] , Lin Zschiedrich[a] and Sven Burger[a,b]

[a]JCMwave GmbH, Bolivarallee 22, D-14050 Berlin, Germany
[b]Zuse Institute Berlin (ZIB), Takustraße 7, D-14195 Berlin, Germany
[c]Karlsruher Institut für Technologie (KIT), Kaiserstraße 7, D-76131 Karlsruhe, Germany

Methods for solving Maxwell's equations in three spatial dimensions are an integral part of many optical metrology and ellipsometry setups in technology and science. In critical dimension metrology characterising deviations and uncertainties from (idealised) targets accurately play an important role.

We discuss a method which allows to efficiently compute highly accurate solutions and parameter sensitivities to Maxwell's equations for general scattering targets. The method is based on hp-adaptive finite-elements. Therefore, complex shapes including corner roundings and sidewall angles can be handled without additional computation cost compared to the idealized case of geometries composed from rectangular shapes. We present a combination of machine learning tools and Newton-like methods to solve the inverse problem and quantify parameter uncertainties.

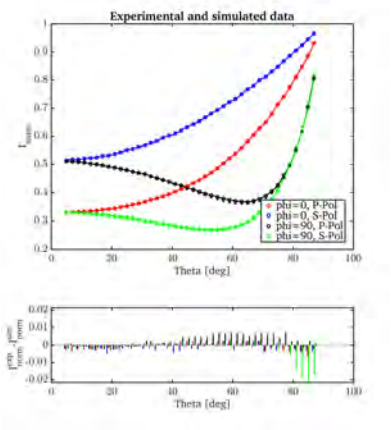

Fig. 1. Experimental and simulated data for a reconstructed line grating with corner roundings and non-rectangular sidewalls

This project has received funding from the European Unions Horizon 2020 research and innovation programme under the Marie Sklodowska-Curie grant agreement No 675745 (MSCA-ITN-EID NOLOSS).

Keywords: Electromagnetic field solver; finite elements, uncertainty quantification; Bayesian optimization, optical metrology

References

[1] Hammerschmidt, Martin, et al. "Quantifying parameter uncertainties in optical scatterometry using Bayesian inversion." Proc. SPIE 10330, 1033004 (2017).
[2] Schneider, Philipp-Immanuel, et al. "Global optimization of complex optical structures using Bayesian optimization based on Gaussian processes." Proc. SPIE 10335, 103350O (2017).

AZIMUTH-DEPENDENT OPTICAL ANISOTROPY AT THE EDGES OF MICROSTRUCTURES

Wanfu Shen[a,b], Chunguang Hu[a*], Shuai Li[a], Zhaoyang Sun[a], Shuchun Huo[a], Lidong Sun[b] and Xiaotang Hu[a]

[a] State Key Laboratory of Precision Measuring Technology and Instruments, Tianjin University, Weijin Road, CN-300072 Tianjin, China.
[b]Institute of Experimental Physics, Johannes Kepler University Linz, A-4040 Linz, Austria
* Corresponding author: cghu@tju.edu.cn

The comprehensive characterization of nanometer thickness microstructures is extremely important and in urgent demands in the area of nanoscience and nanotechnology, particularly for the micro/nano devices. Tremendous optical microscopes were developed for the microstructure characterization including ellipsometric microscope, near-field ellipsometric microscope, differential confocal microscope, scanning optical interfermeter and reflectance difference microscope (RDM). [1] Among them, RDM is a simple and convenient method while possessing the advantages of high optical anisotropy sensitivity, non-destructive and rapid response. Besides, the normal incident light of RDM greatly simplifies the data analysis. [1, 2] Two reasons mainly contribute to the optical anisotropy at the edges of step microstructures. Firstly, the light scattering induced by the tilt edge of step structure, inevitably at process of manufacture, breaks the cylindrical symmetry of the normally incident light and leads to an optical anisotropy signal. Secondly, the discontinuity at the boundary of two different materials composed surface introduces a phase difference between the two halves of the light spot and gives rise to an optical anisotropy signal too. [3] In most cases, it is hard to discriminate the two reasons when the lateral length of the edge of step structure is smaller than the lateral resolution of measurement method. Therefore, ”false” anisotropy signals are probably introduced into the real signals, such as non-uniformity of the sample surface and misalignment of components of instrument setup, which demands rigid challenge for RDM instrumentation.

Here, we present a new type of azimuthal dependence reflectance anisotropy microscopy (ADRDM) based on liquid crystal retarder to meet this urgent challenge. [4] An in-situ and online calibration method was developed to eliminate the testing errors introduced by the asymmetry of the optical system. Using our proposed ADRDM, we directly and precisely image the optical anisotropy at edges of microstructures and demonstrate its polarization-dependence feature.

Keywords: Microstructures; Reflectance difference microscope; Polarization-dependence

References

[1] W. Zhang, Z. Qin and Z. Yang. Journal of applied physics 97 (2005) 074314.
[2] B. Koopmans, P. Santos and M. Cardona. Physica status solidi (a) 170 (1998) 307.
[3] D. Aspnes. Physical Review B 41 (1990) 10334.
[4] C. Hu, S. Huo, W. Shen, Y. Li and X. Hu. (recently accepted by Journal of Microscopy)

ROUGH CIGS SURFACE ANALYZED WITH RAYLEIGH-RICE THEORY

Søren A. Jensen[a], Dana Maria Rosu[b], Andreas Hertwig[b] and Poul-Erik Hansen[a]

[a]Danish Fundamental Metrology A/S, Kogle Allé 5, 2970 Hørsholm, Denmark
[b]BAM - Federal Institute for Materials Research and Testing, Unter den Eichen 87, 12205 Berlin, Germany

We employ Müller matrix ellipsometry to study the high efficiency thin film photovoltaic material copper indium gallium selenide Cu(In,Ga)Se_2 (CIGS) [1]. The analysis is complicated by a surface roughness with an rms value of 68 nm, measured with confocal microscopy. We use Rayleigh-Rice (RR) theory [2] to take the optical effect of this surface roughness into account. The roughness parameters σ (rms height of roughness) and ξ (roughness correlation length) are found from the Müller parameters by comparing them to calculations based on RR theory for a library of structures. Figure 1 shows the measured data and the optimal calculated solution.

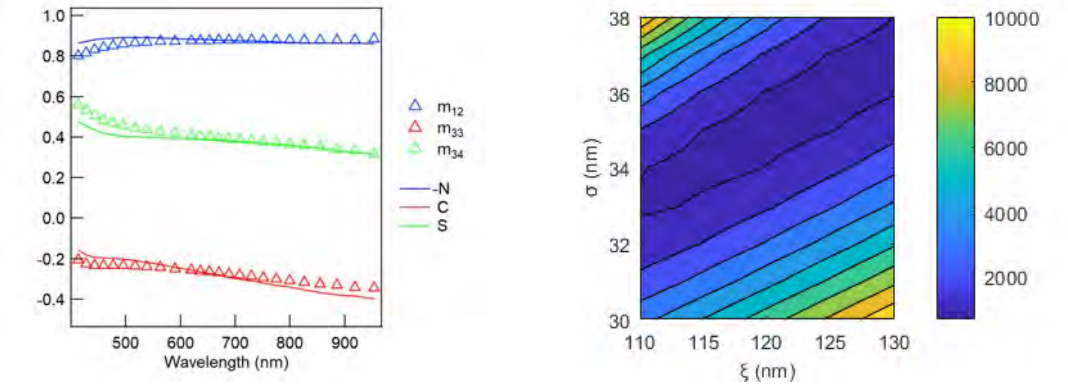

Figure 1. Left: Experimental Müller matrix elements (m_{12}, m_{33}, and m_{34}) and best calculated solution (*N*, *C*, and *S*) corresponding to σ = 36 nm and ξ = 125 nm. Right: Error χ^2 of comparison between experimental data and model as function of the roughness parameters σ and ξ.

The roughness parameters extracted from the analysis are comparable to values found using confocal microscopy and AFM, showing that the Rayleigh-Rice model can be employed to account for roughness effects in ellipsometric measurements. We investigate if the difference between the methods could be due to the fact that ellipsometry is more sensitive to high spatial frequency roughness than low frequency components. We find that the observed ellipsometry sensitivity is almost independently of the spatial frequencies of the roughness.

Keywords: Müller matrix ellipsometry, Copper Indium Gallium Selenide, Rayleigh-Rice theory

References

[1] S.A. Jensen, D.M. Rosu, A. Hertwig, and P.E. Hansen, Phys. Status Solidi C 14 (2017) 1700217.
[2] D. Franta and I. Ohlídal, Opt. Commun. 248 (2005) 459.

Spectroscopic ellipsometry for the determination of thickness and porosity of mesoporous metal oxide films

René Sachse[a], Andreas Hertwig[b], Vasile-Dan Hodoroaba[b], Ralph Kraehnert[a]
[a] Technical University Berlin, Berlin, Germany
[b] Federal Institute for Materials Research and Testing, Berlin, Germany

Thin mesoporous metal oxide films are versatile and attractive candidates for several energy applications like photovoltaics, electrolysis or batteries. Due to their high surface area and ordered pore structure, mesoporous metal oxides demonstrate higher activities. The performance of the porous films is affected by properties like size and shape of the mesopores as well as the crystallinity of the framework. The exact determination and metrological evaluation of the complex morphology of thin mesoporous films requires a new analytical approach employing combined data from different analytical techniques.

In this contribution we present an evaluation procedure based on spectroscopic ellipsometry (SE) to analyze thin mesoporous iridium oxide films. Mesoporous IrO_2 films were prepared via dip-coating from a solution containing a triblock-copolymer and an iridium precursor in ethanol.[1] Deposited films were calcined in air at temperatures between 300 and 600 °C. Their morphology was studied with SEM and electron probe microanalysis (EPMA)[2] and correlated to SE using the Bruggeman effective medium approach (BEMA)[3]. Figure 1a shows a top-view SEM image of mesoporous IrO_2 film calcined at 375 °C. The image reveals that the films exhibit a well-ordered mesopore structure. Figure 1b is a parity plot of film thicknesses determined by cross-section SEM versus SE of IrO_2 film samples prepared at different calcination temperatures. The porosity from the SE model is in good agreement to the porosity values obtained by EPMA (Fig. 1c).

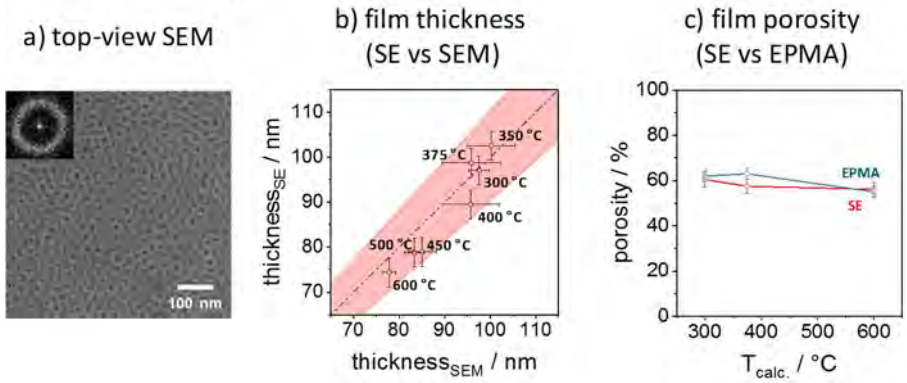

Figure 1: Characterization of mesoporous IrOx thin films via scanning electron microscopy (SEM), spectroscopic ellipsometry (SE) and electron probe microanalysis (EPMA).

The contribution will assess in detail the novel approach to analyses the morphology and porosity of thin metal oxide films. Moreover, the facility of a multi-sample analysis, the sensitivity analysis as well as the mapping of samples will be discussed.

References

[1] E. Ortel et al. ***Chemistry of Materials*** **2011** ***23*** (13), 3201-3209.
[2] E. Ortel et al. ***Analytical Chemistry*** **2016** ***88*** (14), 7083-7090.
[3] D.-M. Rosu et al. ***Applied Surface Science*** **2017** ***421***, 487-493.

ANISOTROPY OF THIN FILMS AND AGGREGATES BY IR NANOPOLARIMETRY

T. Shaykhutdinov and K. Hinrichs

Leibniz-Institut für Analytische Wissenschaften − ISAS − e.V.,
Schwarzschildstr. 8, 12489 Berlin, Germany

Resolving anisotropy at the nanoscale requires new spectroscopic methods overcoming the diffraction limit with high sensitivity to both the in- and out-of-plane optical properties of the sample. IR nanopolarimetry transfers the classical approach to the nanoscale by combining AFM-IR with polarized QCL sources (Fig. 1) [1]. The method uses an AFM tip to directly probe IR absorption via thermal expansion of the sample under p- and s-polarized low-power QCL pulses in ambient conditions allowing for straightforward spectra-structure correlations [2].

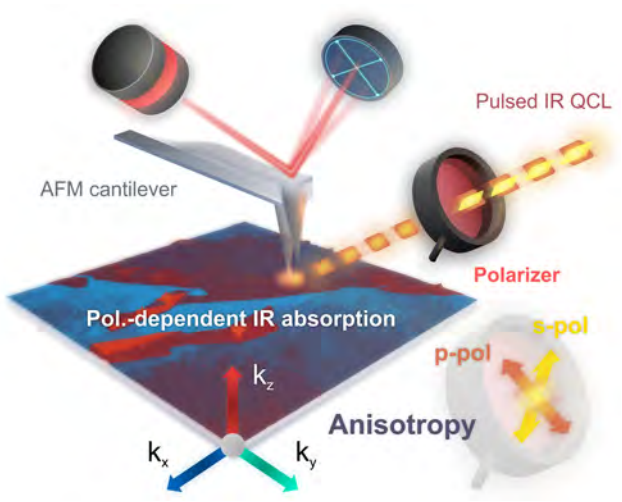

Fig. 1. Schematic of the AFM-IR nanopolarimetric setup in reflection geometry accessing in- and out-of-plane molecular anisotropy via polarization-dependent sample absorption

IR nanopolarimetry provides insights into anisotropy of thin films, surfaces, and aggregates including composition, interactions, molecular orientation, and oscillator strength induced phenomena with ≤ 30 nm spatial resolution in seconds [1–3].

This presentation will highlight the broad applicability of the method to polymer science, (bio)macromolecular research, and IR nanophotonics by focusing on the following applications: anisotropy of layered thin polyimide films [1], ordering mechanisms of supramolecular porphyrin aggregates [2], oriented protein aggregation upon adsorption [1], polaritonic modes in thin silica films [3], and polarization-dependent biosensing of a peptide nucleic acid [4] on modified graphene films [5].

The analysis of the nanoscale anisotropy is supported by vibrational and electrodynamic calculations [1].

Keywords: Nanopolarimetry; AFM-IR; Anisotropy; Molecular orientation; Light–matter interactions; Spectra-structure correlations; Thin films; Aggregates; Polymers; Proteins; Oxides; Polaritons

References

[1] K. Hinrichs, T. Shaykhutdinov, Appl.Spectr. (2018, submitted).
[2] T. Shaykhutdinov, S. D. Pop, A. Furchner, K. Hinrichs, ACS Macro Lett. 6 (2017) 598–602.
[3] T. Shaykhutdinov, A. Furchner, J. Rappich, K. Hinrichs, Opt. Mater. Express 7 (2017) 3706–3714.
[4] K. Hinrichs, T. Shaykhutdinov, C. Kratz, F. Rösicke, C. Schöniger, C. Arenz, N. H. Nickel, J. Rappich, in *Encyclopedia of Interfacial Chemistry: Surface Science and Electrochemistry*, K. Wandelt, ed. (Elsevier, 2018).
[5] F. Rösicke, M. A. Gluba, T. Shaykhutdinov, G. Sun, C. Kratz, J. Rappich, K. Hinrichs, N. H. Nickel, Chem. Comm. 53 (2017) 9308–9311.

Imaging Mueller-Matrix Ellipsometry of Anisotropic Thin-Film Semiconductors

M.Duwe[a], C.Röling[a], C.Hoffmann[a], P.H.Thiesen[a], A.J.Molina-Mendoza[b], A.Castellanos-Gomez[c], E.Y.Poimanova[d], V.V.Bruevich[e], D.Y.Paraschuk[e]

[a]Accurion GmbH, Stresemannstr.30, 37079 Goettingen, Germany
[b]Universidad Autonoma de Madrid, 28049 Madrid, Spain
[c]IMDEA Nanoscience, Campus Universitario de Cantoblanco, 28049 Madrid, Spain
[c]Donetsk National University, Department of Chemistry, Ukraine
[e]International Laser Center & Physics Faculty, M.V. Lomonosov Moscow State University, Moscow, Russia

Imaging Mueller-Matrix Ellipsometry (IMME) extends the powerful technique of Mueller-Matrix measurements into the world of microstructured samples, reaching lateral resolutions that are beyond the limits of conventional non-imaging ellipsometers. Here, we present applications of IMME for the quantitative optical analysis of microstructured anisotropic thin-film layers of semiconducting materials.

Few-layer black phosphorus features exceptional anisotropic optical and electronic properties making it an interesting option for research on 2D-semiconductors for electronic devices [1, 2]. We carried out optical measurements of the orientations and the optical dispersion of the in-plane principal axes of microscopic, mechanically exfoliated flakes of black phosphorus by means of IMME.

Thin-film crystallites of the semiconducting organic material Thiophene-phenylene were grown by a solvent-based self-assembly technique on a silicon substrate. Ellipsometric contrast micrographs revealed a vast variety of different domains on the examined sample that correspond to different layer thicknesses forming a terracelike structure (Fig.1). Rotational IMME scans of the sample yielded the in-plane orientation of the crystallites' optical axes. Combined with spectroscopic measurements, the dispersion function of Thiophene-phenylene and the terraces' layer thicknesses were obtained.

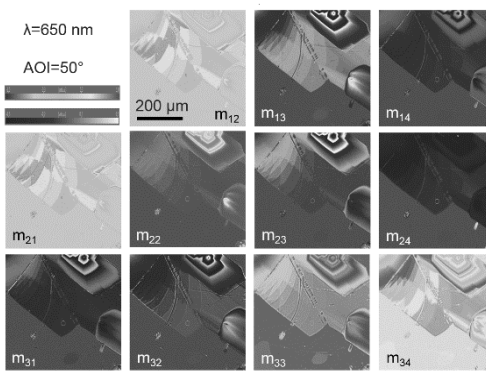

Fig. 1. 3x4-Mueller-Matrix micrographs of Thiophene-phenylene crystallites

Keywords: Mueller Matrix; Imaging Ellipsometry; 2D materials; organic semiconductors; anisotropy

References

[1] A. Castellanos-Gomez, L. Vicarelli, E. Prada, J. O. Island, K. L. Narasimha-Acharya, S. I. Blanter, D. J. Groenendijk, M. Buscema, G. A. Steele, J. V. Alvarez, H. W. Zandbergen, J. J. Palacios, and H. S. J. van der Zant, 2D Materials **1**, 025001 (2014)
[2] A. Castellanos-Gomez, J. Phys. Chem. Lett. **6**, 4280 (2015)

Ellipsometric Micromapping of Graphene grown on Copper-foil

S. Funke[a], P. Braeuninger-Weimer[b], P. H. Thiesen[a], R. Wang[b], S. Hoffmann[b]

[a]Accurion GmbH, Stresemannstraße 30, Göttingen, Germany
[b]Department of Engineering, University of Cambridge, Cambridge CB3 0FA, United Kingdom

The demand of high quality graphene e.g. for electronic applications raised the necessity for the direct growth of Graphene on Cu-foils [1]. To investigate the layer structure and coverage of Graphene, conventional methods are SEM or optical microscopy after oxidizing the foil. SEM requires high vacuum and is not suitable for the detection of defects, layer number and uniformity on large areas. To investigate Graphene with optical microscopy the foil either needs to be oxidized, hence destroyed, or the Graphene needs to be transferred to suitable substrates, e.g. Si/SiO_2.

In the talk we present, imaging ellipsometry is able to characterize the Graphene directly grown on the foil. Besides the plethora of optical properties, the combination of microscopy and ellipsometry reveals foldings of the Graphene on the Copper-foil. These foldings are induced by the different cooling coefficients of Graphene and Cu. An automatic height alignment across the whole Copper-foil allows to measure Δ and Ψ micromaps of the creased foil. The automatic stitching of all measured field of views yield to a map of Δ and Ψ of the complete sample with a lateral resolution of 4 µm (Fig.1). In [2] a flakesearch algorithm is presented, that allows the localization of regions with defined layer numbers. The algorithm is extended to pinpoint monolayer regions on the complete map of Δ and Ψ and calculate the coverage. Measuring micromaps of Δ and Ψ offers a microscopic insight to the lateral distribution of Copper-oxide layer thickness even underneath a Graphene crystallite.

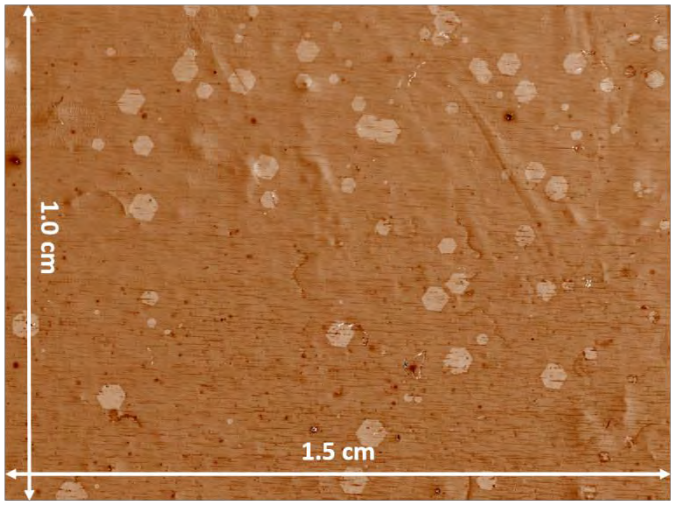

Fig. 1. Complete Δ map of Graphene on Cupper

Summing up, we will present cutting-edge technology for the characterization of Graphene directly grown on Cupper-foil including a detailed description of the substrate copper-oxide layer, altogether with the highest lateral resolution in the lower µm range.

.

Keywords: Graphene; Copper-foils; Imaging Ellipsometry

References

[1] X. Li, W. Cai, J. An, S. Kim, J. Nah, D. Yang, R. Piner, A. Welamakanni, i. Jung, E. Tutuc, S. K. Banerjee,L. Colombo, R. S. Ruoff, Science, 324(5932) (2009) 1312-1314.
[2] S. Funke, U. Wurstbauer, B. Miller, A. Matković, A. Green, A. Diebold, C. Röling, and P. H. Thiesen., Applied Surface Science, 2017.

FAST DETECTION OF WATER NANOPOCKETS UNDERNEATH WET-TRANSFERRED GRAPHENE

M. Magnozzi[a], N. Haghighian[a], V. Miseikis[b], O. Cavalleri[c], C. Coletti[b,d], F. Bisio[e], M. Canepa[a]

a OptMatLab, Dipartimento di Fisica, Università di Genova, Genova, Italy
b CNI@NEST, Istituto Italiano di Tecnologia, Pisa, Italy
c Dipartimento di Fisica, Università di Genova, Genova, Italy
d Graphene Labs, Istituto Italiano di Tecnologia, Genova, Italy
e CNR-SPIN, Genova, Italy

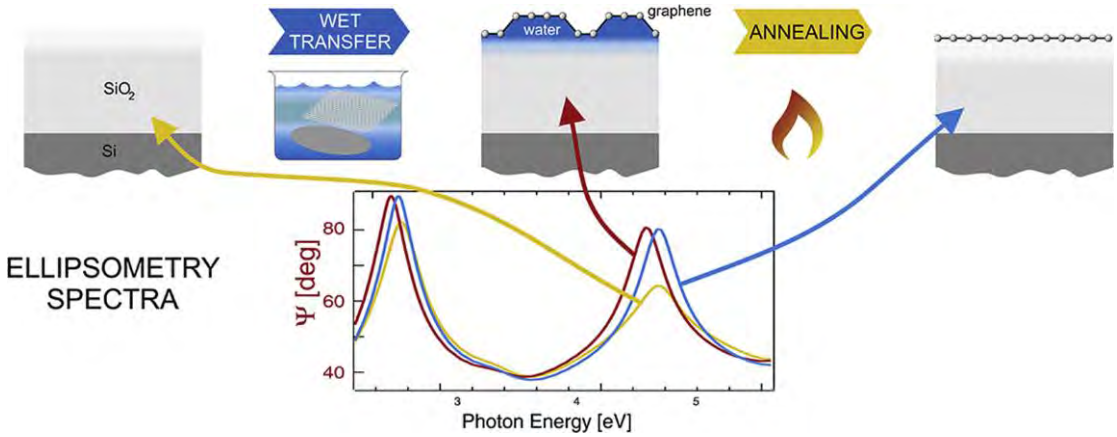

We report an investigation of the graphene/substrate interface morphology in large-area polycrystalline graphene grown by chemical-vapour deposition and wet-transferred onto Si wafers. We combined spectroscopic ellipsometry, X-ray photoelectron spectroscopy and atomic-force microscopy in order to yield morphological and chemical information about the system. The data showed that wet-transferred samples may randomly exhibit nanosized relief patterns indicative of small water nanopockets trapped between graphene and the underlying substrate. These pockets affect the adhesion of graphene to the substrate, but can be efficiently removed upon a mild annealing in high vacuum. We show that ellipsometry is capable of successfully and reliably detecting, via multilayer dielectric modelling, both the presence of such a spurious intercalation layer and its removal [1]. The fast, broadly applicable and noninvasive character of this technique can therefore promote its application for quickly and reliably assessing the degree of adhesion of graphene transferred onto target substrates, either for ex-post evaluation or in-line process monitoring.

[1] M. Magnozzi et al., Carbon, 118, 2017

Keywords: Spectroscopic ellipsometry, graphene, annealing

ELLIPSOMETRIC IMAGING OF LOW-CONTRAST SURFACE MODIFICATIONS AND DEPOLARIZATION CONTRAST IMAGING (DCI) OF PARTICULATE ACCUMULATIONS

U. Beck, J. M. Stockmann, D. Fischer, A. Hertwig, G. Hidde

BAM, division 6.7, Unter den Eichen 87, 12205 Berlin, BAM, Germany

uwe.beck@bam.de

Imaging of surfaces regarding topographical, morphological, micro-structural, and chemical features is a key requirement for quality control for the identification of contaminated, degraded, damaged or deliberately modified surface areas vs. clean, virgin, undamaged or unmodified regions. As optical functions may represent any of these changes on the micro- and nano-scale, imaging ellipsometry (IE) is the technique of choice using either intensity, phase, or/and amplitude contrast for visualization of low-contrast surface modifications [1, 2].

Defects or surface and film features whether native or artificial, intended or unintended, avoidable or unavoidable as well as surface pattern are of interest for quality control. In contrast to microscopic techniques operated at normal incidence, ellipsometry as oblique-incidence technique provides improved contrast for vertically nano-scaled add-on or sub-off features such as ultra-thin transparent films, metallic island films, carbon-based thin films, laser modification or laser induced damage, dried stain, cleaning agent or polymeric residue.

Two-sample reference techniques, i.e. referenced spectroscopic ellipsometry (RSE) may further increase sensitivity and decrease measurement time. In case of particulate accumulations depolarization contrast imaging (DCI) may improve the lateral resolution beyond the Abbe limit. This has been proven for silica spheres as reference in terms of single particles, particulate accumulations or particulate mono-layers and layer stacks. Scanning electron microscopy (SEM) and atomic force microscopy (AFM) were used for reference measurements of particle diameter, particle height, or particulate layer/accumulation thickness.

It has been shown that single silica particles of 250 nm in diameter, i.e. at least a factor of 4 better than the lateral resolution limit as of now, can be *visualized* on even substrates. However, the ellipsometric *measurement* of particle diameters of this size needs further efforts interpretation.

Keywords: low-contrast surface modifications; particulate distributions; imaging ellipsometry(IE) and depolarization contrast imaging (DCI)

References

[1] U. Beck; Imaging of Impurities and Imperfections, Micro- and Nano-scaled Pattern on Surfaces and in Films: Microscopic Techniques vs. Ellipsometry, SVC Santa Clara, CA, USA, April 2015
[2] J. M. Stockmann, A. Hertwig, U. Beck; Applied Surface Science 421(2017)807-812

Wednesday:

	N112
08:30	*Invited Talk*: T. Hofmann
09:00	L. Skowronski
09:20	M. Fried
09:40	P. Basa
10:00	L. Jansen
10:50	*Invited Talk*: S. Richter
11:20	J. Budai
11:40	A. Horn
12:00	A. Blümich
12:20	D. V. Likhachev
13:40	*Invited Talk*: S. Zollner
14:10	M. Stoica
14:30	I. Alonso
14:50	P. Kühne
15:10	*Invited Talk*: A. Furchner
15:40	Awards, Conclusion remarks

ELLIPSOMETRY AT THZ FREQUENCIES: NEW APPROACHES FOR METROLOGY AND METAMATERIAL-BASED SENSING

T. Hofmann

Department of Physics and Optical Science,
University of North Carolina at Charlotte, USA

The precise measurement of electromagnetic material properties at THz frequencies is essential for the development of increasingly advanced THz optical systems and a prerequisite for the design and manufacturing of optical elements for this spectral range. The exploration of novel physical phenomena observed in artificially structured metamaterials and the application thereof is of interest due to its relevance for the design and fabrication of novel THz optical elements and sensors. Metamaterials have attracted continued interest for almost two decades due to their unique electromagnetic properties, which can differ substantially from their constituents and often do not even exist in naturally occurring materials.

We have demonstrated that although being orders of magnitude smaller than the probing wavelength, metamaterials composed of highly-ordered 3-dimensional metal nanostructures exhibit a strong anisotropic optical response at THz frequencies. I will discuss how these interesting optical properties can be used for sensing of minute target material quantities in the THz spectral range. In addition, I will focus on a novel avenue for the fabrication of THz metamaterials using stereolithographic techniques. For the THz spectral range, where spatial resolutions in the range of several um are sufficient to create subwavelength metamaterial building blocks, stereolithography-based additive fabrication might offer a readily accessible approach which is so far unrealized. Here, metamaterials composed of spatially coherent methacrylates wires will be shown as an example. Our observations demonstrate that stereolithography may provide an alternative avenue to the fabrication of metamaterials for the terahertz spectral range and may allow tailoring of the polarizability and anisotropy of the host material by design.

Keywords: THz ellipsometry, Metamaterials, THz sensing

Ellipsometric study of the TiO_2-based decorative coatings produced using magnetron sputtering technique at industrial conditions

L. Skowronski

Institute of Mathematics and Physics, UTP University of Science and Technology, Kaliskiego 7, 85-796 Bydgoszcz, Poland

Titanium dioxide is a non-toxic, biocompatible and chemically stable material and is used as white pigment in paints and some high-tech applications including electrochromic devices, dye-sensitized solar cells (DSSC), photocatalysis, optical filters and antireflection coatings.

Moreover, due to the expressive colors of titanium oxides and oxynitrides deposited/formed on metal or metal-coated glass, these compounds can be applied as a decorative material for architecture, automotive industry, electronics and jewelry. In general, titanium dioxide is a non-absorbing material in the visible spectral range, thus the color effect is caused by the optical interference of light in the thin dielectric film.
In the last few years, the different TiO_2-based decorative coatings were produced using a industrial scale magnetron sputtering line and were analyzed at Institute of Mathematics and Physics UTP. The decorative coatings were deposited on glass, aluminum, Ti-coated aluminum, stainless steel, Ti-coated stainless steel, ceramic tiles as well as on polymer substrates. The presented results will be a summary of the last few years of research. These results show that for the opaque systems the color of sample can be related to thickness of the TiO_2 layer. The thickness of Ti film in TiO_2/Ti/glass samples is associated with their transparency, whereas in TiO_2/Ti/Al specimens - with saturation of color.

Keywords: TiO_2, decorative coatings, intereference, thin films

References

[1] L.Skowronski, AA.Wachowiak, W.Wachowiak, Appl. Surf. Sci. 421 (2017) 794-801

[2] L.Skowronski, AA.Wachowiak, K.Zdunek, M.Trzcinski, MK.Naparty, Thin Solid Films 627 (2017)1-8

[3] L.Skowronski, AA.Wachowiak, A.Grabowski, Appl. Surf. Sci. 388 (2016) 731-740

[4] L.Skowronski, M.Trzcinski, A.J.Antonczak, P.Domanowski, M.Kustra, W.Wachowiak, M.K.Naparty, T.Hiller, A.Bukaluk, A.A.Wronkowska, Appl.Surf.Sci. 322 (2014) 209-214

[5] K.Zdunek, L.Skowronski, R.Chodun, K.Nowakowska-Langier, A.Grabowski, W.Wachowiak, S.Okrasa, A.A.Wachowiak, O.Strauss, A.Wronkowski, P.Domanowski, MSP 34 (2016) 137-141

High Speed Spectroscopic Ellipsometry Technique for On-Line Monitoring in Large Area Thin Layer Production

C. Major[a], G. Juhasz[a], B. Kalas[a], P. Petrik[a], M. Schellenberger[b], M. Fried[a,c]

[a] Institute for Technical Physics and Materials Science, Centre for Energy Research (MFA), H-1525 Budapest, P.O. Box 49., Hungary

[b] Fraunhofer Institute for Integrated Systems and Device Technology IISB Schottkystrasse 10, 91058 Erlangen, Germany

[c] Institute of Microelectronics and Technology, Óbuda University, Tavaszmezo u. 17, H-1084 Budapest, Hungary

Macro imaging spectroscopic ellipsometers has been developed for high speed mapping of large area thin layer coated substrates. Non-contact and non-destructive characterization techniques based on spectroscopic ellipsometry are widely used by the photovoltaic and semiconductor industry for process or quality control in production. The commercialization of large area thin film technologies and the related increasing surfaces lead to many key problems such as reduced efficiency caused by multiple non-uniformities of the layer properties over the entire panel or wafer resulting from the technological steps of individual layer components. For these reasons, thin layer properties must be mapped by an „in-line" or „in-situ" method avoiding mistakes resulting from layer inhomogeneities. Scanning ellipsometry methods based on the conventional narrow beam spectroscopic measurements provide high accuracy but suffer from long mapping times as the polarization state of the reflected beam must be detected. **Expanded beam ellipsometry** was developed to measure rapidly the polarization state changes after reflection from bigger surfaces. Our instruments use non-collimated illumination with a special light source and an optical arrangement allowing multiple angles of incidence [1]. New prototypes have been prepared for spectroscopic measurements that provide a **line image of spectroscopic ellipsometry** data with a lateral resolution of ~10 mm over the range of 350-1000 nm [2-4]. Ellipsometric information of large areas can be collected a **couple of 10 times faster** compared to scanning methods. Prototypes have been built for structures with nominal widths of 300-450-600-900 mm (SiO2, ZnO/Mo, NiSi) **on rigid substrates**. Thin layers (ZnO/a-Si:H/Ag) on plastic foil substrates were also investigated **in roll to roll operation**. Measurements and results of different structures are presented.

We can demonstrate spectroscopic ellipsometry mapping measurements over 1800 points in ~1 min traverse of a 300-450 mm diameter Si-wafer (demonstration in clean room environment, see Fig. 1) or 600x1200 mm solar panel.

Acknowledgements: Support from OTKA K115852, M-ERA-NET 117847, and NVKP_16-1-2016-0014 projects is gratefully acknowledged.

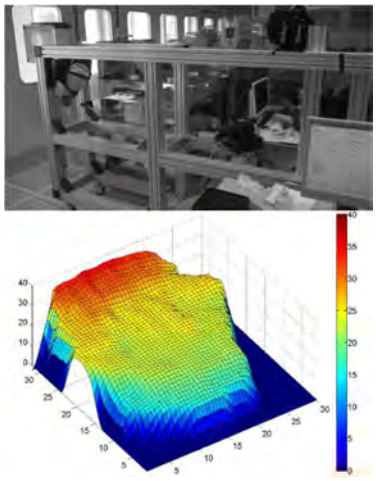

Fig. 1. Installed mapping device and thickness-map of a NiSi covered 300 mm diam. Si-wafer (complete annealing at 350° C).

Keywords: Mapping; ellipsometry, thin film

References

[1] C. Major, G. Juhasz, Z. Horvath, O. Polgar, M. Fried, physica status solidi (c) **5** (2008) 1077

[2] M. Fried, G. Juhász, C. Major, P. Petrik, O. Polgár, Z. Horváth, A. Nutsch, Thin Solid Films **519** (2011) 2730

[3] A. Shan, M. Fried, G. Juhasz, C. Major, O. Polgar, A. Nemeth, P. Petrik, L. R. Dahal, Jie Chen, Zhiquan Huang, N. J. Podraza, R. W. Collins, IEEE JOURNAL OF PHOTOVOLTAICS **4**:(1) (2014) 355

[4] Miklos Fried, Thin Solid Films **571** (2014) 345

Characterization of dielectric films on glass for the semiconductor 3D packaging process

P. Basa[a], P. Mennell[b], J. Protzman[b], A. Madan[b], J. Lubguban[b], A. Bondaz[a]

[a]Semilab Semiconductor Physics Laboratory Co. Ltd., Hungary
[b]GLOBALFOUNDRIES Inc, Hopewell Junction, NY 12533

Characterization of film homogeneity and mechanical strength of the film itself are important aspects in engineering materials for back-end of line (BEOL) semiconductor processes [1]. It is a challenge to optimize such materials both for low density and for a mechanically strong structure. In terms of device integration, thickness and composition change must be minimized during high temperature process steps [2]. These factors are especially pronounced in case of bonded wafers for 3D device structures. Such stacked plates consist of Si and glass wafers molded to each other.

The bow of the constituing glass wafer can be engineered by depositing stressful SiO2 which can be modified depending on the conditions of the deposition steps, type of precursors, or type of deposition tool. Since glass exhibits half of the modulus of Si, it can easily respond to a stressful film deposited on it. With the SiO2 stress as well as variation in thickness, the amount of bow can be calculated to be engineered on the glass that would even out the total bow when these are used as carriers.

Such characteristic samples are measured, tendencies and conclusions are drawn and will be presented.

Keywords: Si wafer; porous low-k; spectroscopic ellipsometry, ellipsometric porosimetry

References

[1] A. Bourgeois et al., ECS Transactions, 16 (3) 221-229 (2008)
[2] Z. Sun et al., AVS 60th International Symposium and Exhibition, Electronic Materials and Processing, October 31, 2013, http://www2.avs.org/symposium2013/Papers/Paper_EM+AS+PS+TF-ThM6.html

HIGH-SPEED SPRECTROSCOPIC ELIIPSOMETRY AND ITS APPLICATIONS

Lars Jansen[a], Gai Chin[b]

[a]SCHAEFER TECHNOLOGIE GmbH, Robert-Bosch-Strasse 31, 63225 Langen, Germany

[b]ULVAC Inc., Mechatronics Engineering Department, 2500 Hagisono, Chigasaki, Kanagawa, 253-8543, Japan

As a comprehensive manufacturer of metrology tools and deposition tools, ULVAC developed an innovative high-speed spectroscopic ellipsometer for many deposition applications, such as PVD, CVD, ALD and others.

This novel spectroscopic ellipsometry can measure the thickness and optical constants of thin films at a dramatically fast speed. Its data acquisition time is as short as 10ms. It does not require any active components for polarization-control, such as a rotating compensator or an electro-optical modulator.

It created great opportunities for new applications of the spectroscopic ellipsometry in which the compactness, the simplicity and the rapid response are extremely important. It can be integrated into the deposition tool and successfully measure thin films in-situ and ex-situ. Obviously, those from PVD, CVD and ALD are some promising applications for this novel spectroscopic ellipsometry.

This presentation describes the principle, system configuration and creative efforts on developing a series of high-speed spectroscopic ellipsometers. Some of the novel applications will be also introduced, such as the PVD, CVD, ALD, EUV, OLED, MEMS and some measurement data of thin films from the semiconductor, flat panel display, and other industries.

Keywords: Spectroscopic Ellipsometry; High-order Retarder; High-Speed

FS-TIME-RESOLVED SPECTROSCOPIC ELLIPSOMETRY

S. Richter[a], O. Herrfurth[a], S.J. Espinoza Herrera[b], M. Rębarz[b], M. Grundmann[a], S. Zollner[c], J. Andreasson[b,d] and R. Schmidt-Grund[a]

[a]Universität Leipzig, Felix-Bloch-Institut für Festkörperphysik,
Linnéstr. 5, 04103 Leipzig, Germany
[b]ELI beamlines/Fyzikální ústav AV ČR v.v.i.,
Za Ranicí 835, Dolní Břežany, Czech Republic
[c]New Mexico State University, Department of Physics,
P.O. Box 30001, Las Cruces, NM 88003-8001, USA
[d]Chalmers tekniska högskola,Institutionen för fysik,
Kemigården 1, 41296 Göteborg, Sweden

Implementing time-resolved ellipsometry to study effects of free charge carriers induced by pulsed laser excitation has been tried first in the 1970's [1]. However, for a long time, experimental limitations and single wavelength probes limited the ellipsometric approaches to indirect investigations of pump-induced charge carriers in the near-infrared. Today's possibilities to generate continuum white light pulses allow even spectroscopic ellipsometry with time resolution in the fs-range. Still, a number of experimental challenges as spectral fluctuations and group velocity delay remain. We demonstrate a new setup based on an amplified Ti:sapphire laser which is used to generate continuum white light in a CaF_2 crystal as probe while its fundamental, doubled or tripled frequency are applied as pump. Time-resolved spectroscopic ellipsometry measurements have been carried out in ***polarizer-sample-compensator-analyzer*** configuration by obtaining transient reflectance-difference spectra at different compensator azimuth angles.

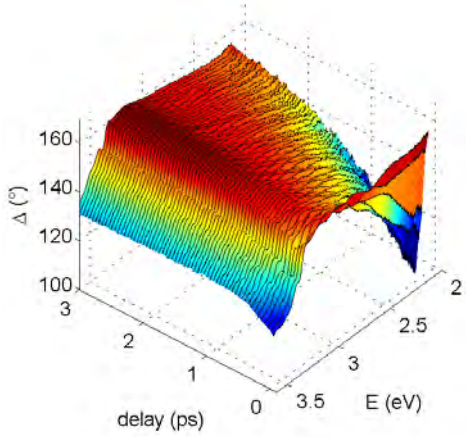

Fig. 1. Transient ellipsometric angle Δ for a ***c***-plane oriented ZnO single crystal showing the response of plasma absorption as well the damping of the excitonic and higher transitions.

We demonstrate first measurements of ZnO single crystals, films and resonators as well as Ge single crystals. In Ge, depending on the pump wavelength, band filling effects or renormalization are observed at the E1 and E1+Δ1 transitions which take place at the L point in the momentum space. In ZnO, the dynamics of UV-excited hot charge carriers can be monitored by their induced plasma absorption as well as damping of optical transitions of excitons and above the band gap. Carrier thermalization, recombination and lattice heating can be distinguished as processes on different spectral ranges and time scales ranging from fs to ns. A particular challenge to model transient ellipsometry data arises from the depth gradient of the density of excited charge carriers due to the pump laser absorption.

Keywords: dynamics; pump-probe; hot charge carriers

References

[1] D. H. Auston, C. V. Shank, Phys. Rev. Lett. **32** (1974) 1120.

ULTRAFAST IN-SITU ELLIPSOMETRY FOR STUDYING INTERACTIONS OF LASER PULSES AND MATERIAL SURFACES

J. Csontos [a,b], Z. Toth [c], Z. Pápa [a,b], J. Budai [a,b]

[a]University of Szeged, Department of Optics and Quantum Electronics, H-6720 Szeged, Dóm tér 9., Hungary
[b]ELI-ALPS Research Institute, ELI-HU Nonprofit Kft., 6720 Szeged, Hungary
[c]University of Szeged, Department of Oral Biology and Experimental Dentistry, H-6720 Szeged, Tisza Lajos krt. 64-66, Hungary

Monitoring the changes in material properties during pulsed laser excitation opens a pathway towards better understanding of the fundamental nature of laser induced processes. On one hand ultrafast single wavelength ellipsometry is an appropriate candidate for following such changes, since it provides more information than a conventional pump and probe reflection measurement. On the other hand the retrieval of the data is model based which necessitates the involvement of a broad spectral range.

Very recently, we demonstrated a unique, ultrafast pump-probe null-ellipsometry method, capable of assessing rapid changes of temperature and charge density upon femtosecond laser pulse irradiation [1]. To overcome the limitation due to the single wavelength of the probe pulse we rebuilt our measurement setup. Now it uses synchronized white light generated by femtosecond laser pulse (part of the pump) focused into a bulk glass plate, and operates as a quasi-rotating compensator ellipsometer.

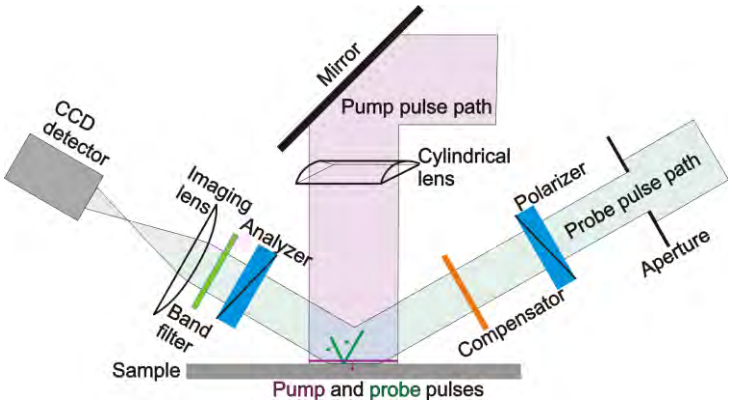

Fig. 1. Experimental setup

In this presentation, details of both experimental setups will be given. Advantages and disadvantages will be discussed through the example of silicon irradiated with fs laser pulses.

We believe that our results are not only interesting for the ellipsometric community but also represent an important contribution for applications in material science where ultrafast excitation of charge carriers is involved.

Keywords: Pump and probe method; Laser excitation; Silicon; Two-temperature model

References

[1] J. Csontos, Z. Toth, Z. Pápa, B. Gábor, M. Füle, B. Gilicze, J. Budai, Applied Surface Science 421 (2017) 325–330

ULTRAFAST ELLIPSOMETRY OF LASER-INDUCED PHASE TRANSITIONS IN MATTER

Alexander Horn, Theo Pflug, and Markus Olbrich

Laserinstitut Hochschule Mittweida, Schillerstraße 10, 09648 Mittweida, Germany

Irradiating matter with ultrafast laser radiation induces transient states with physical and chemical properties far away from any equilibrium. Thin gold film on a glass substrate (thickness $d_{\mathrm{Au}} = 200$ nm, roughness R_a =3 nm) and bulk PMMA have been excited by single pulsed femtosecond laser radiation ($\tau_{\mathrm{H}} = 40$ fs) and the temporal evolution of the complex refractive index was detected spatially- and spectroscopically-resolved by a self-developed pump-probe ellipsometer. The gold film excited at the pump wavelength $\lambda = 800$ nm exhibits for a fluence of 1 J/cm² (below gentle ablation [1]) and a probe wavelength $\lambda = 440$, 515, 550, and 600 nm a complex dynamics of the refractive index n and the extinction coefficient k (Fig.1 a). Apparently, the refractive index converges for all investigated wavelengths about 100 fs after excitation to a value close to 1 describing the heating of the electron system, in which the refractive index for $\lambda = 440$ nm demonstrates a slight decrease and for $\lambda = 515$, 550 and 600 nm the refractive index increases strongly compared to the value at rest. Thereafter, a slight decrease of the refractive index is obtained, depicting the beginning of the cooling of the electrons [2].

PMMA, an organic dielectric material, is transparent for radiation at small intensities in the VIS and IR spectral range, but at large intensities (I =3·10^{13} W/cm²) the radiation induces field ionization generating free electrons [3, 4]. Exciting above ablation threshold with a single laser pulse ($\lambda = 800$ nm) a strong increase in the refractive index and extinction coefficient is induced within 100 fs probing at the wavelength $\lambda = 440$ nm. The extinction coefficient lasts about 20 ps, then decreasing again, depicting the lifetime of the laser-induced free electrons.

Keywords: ultrafast; transient state; ablation

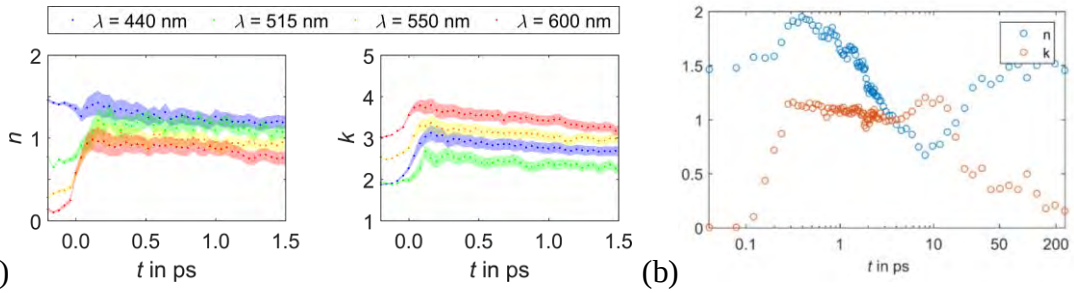

Fig. 1. Refractive index and extinction coefficient as function of time after excitation with single pulsed laser radiation ($\tau_{\mathrm{H}} = 40$ fs, $\lambda = 800$ nm) (a) of gold for different probe wavelengths, and (b) of PMMA for the probe wavelength $\lambda = 440$ nm.

References

[1] M. Olbrich, E. Punzel, R. Roesch, R. Oettking, B. Muhsin, H. Hoppe, A. Horn, Appl. Phys. A **122**, 648 (2016)
[2] S.I. Ashitkov, P.S. Komarov, V.V. Zhakhovsky, Y.V. Petrov, V.A. Khokhlov, A.A. Yurkevich, D.K. Ilnitsky, N.A. Inogamov, M.B. Agranat, J. Phys.: Conf. Ser. **774**, 12097 (2016)
[3] L.V. Keldysh, Jetp Lett. **20**, 1307 (1965)
[4] M. Garcia-Lechuga, L. Haahr-Lillevang, J. Siegel, P. Balling, S. Guizard, J. Solis, Phys. Rev. B **95** (2017)

ELLIPSOMETRY IN THE ERA OF INDUSTRY 4.0

Adrian Blümich[a], Bernd Gruska[a]

[a]Application Departement, Schwarzschildstraße 2, SENTECH Instruments, Germany

In times of Internet of Things and Industry 4.0 production lines require more automation than ever. The operators influence on the resulting product is pushed back to minimize failure. Multiple diagnostic tools are used, spinning a tight monitoring network throughout the production cycle. The vast amount of data produced by the variety of diagnostic tools must be organized, crosslinked and evaluated to maximize yield and product quality.

The data are typically processed by a host software specifically designed for the production line. The communication between the host and the large variety of equipment is performed using SECS (SEMI Equipment Communications Standard) or more specifically SECS/GEM (General Model for Communications and Control of Manufacturing Equipment). The SECS/GEM defines standard commands, replies and events allowing the host to control and monitor the manufacturing equipment.

Being a standard in microelectronics for a while now, the SECS/GEM also becomes more and more popular in other industrial fields like photovoltaics and optoelectronics. An ellipsometer designed to be placed in such a demanding environment must match these requirements as well. In addition, precision, repeatability and measurement speed are traditional challenges for production control.

Typical requirements for equipment performance, software compatibility and maintenance are presented on actual cases of major optoelectronic manufactures. Special emphasis is put on the SECS/GEM compliance. Some examples are shown of how SECS/GEM can be used either as local remote control of the measurement software or even by complete remote access via the company network. The later even allows to perform measurements with a standard tablet.

Keywords: SECS/GEM; Production;

References

USE OF P-SPLINES FOR THE DIELECTRIC FUNCTION REPRESENTATION IN THE INTERPRETATION OF SPECTROSCOPIC ELLIPSOMETRY DATA

Dmitriy V. Likhachev

GLOBALFOUNDRIES Dresden Module One LLC & Co. KG,
Wilschdorfer Landstr.101, D-01109 Dresden, Germany

About ten years ago Johs and Hale developed the Kramers–Kronig consistent B-spline formulation for the dielectric function modeling in spectroscopic ellipsometry data analysis [1]. But the actual performance of B-spline parameterization strongly depends on the number of knots (and, in general, their locations) used to describe the dielectric function. It is intuitively easy to conceive that fewer knots in the considered wavelength range may not be enough to fit all essential spectral features (underfitting). On the contrary, increasing the number of knots beyond the optimal value can result in significant overfitting of the experimental data, i.e., leads to an unrealistic result with measured noise reproduction. In previous papers [2,3], we used well-established information criteria approach for choosing a suitable B-spline model with optimal number of knots to balance fidelity to the measured data and complexity of the fit.

An alternative method to avoid overfitting by B-spline parameterization is to use one of the variants of smoothing splines called “penalized splines” or “P-splines” which include a penalty on B-spline coefficients. The amount of penalty, which based on the second- (or higher-) order finite differences of the coefficients of adjacent B-splines, is easily controlled by non-negative smoothing (or penalty) parameter α. Selection of $\alpha = 0$ leads to ordinary least-squares fit of the ellipsometric data with the B-spline model for the dielectric function. The larger the value of the smoothing parameter α, the smoother the result one can get. We will focus on application of the P-spline approach to dielectric function representation in spectroscopic ellipsometry data analysis.

The P-spline approach offers a number of advantages over well-established B-spline parameterization. First of all, it typically uses an equidistant knot arrangement which simplifies the construction of the roughness penalties and makes it computationally efficient. Since P-splines possess the “power of the penalty” property [4], the number and location of knots are no longer crucial, as long as there is a minimum knot number to capture all significant spatial variability of the data curves. We demonstrate the proposed approach by real-data case studies.

Keywords: Spectroscopic ellipsometry; Data analysis; Optical modeling; Dielectric function; Parameterization; Penalized splines; Optical metrology

References

[1] B. Johs, J.S. Hale, Dielectric function representation by B-splines, Phys. Status Solidi A 205 (2008) 715–719.
[2] D.V. Likhachev, Selecting the right number of knots for B-spline parameterization of the dielectric functions in spectroscopic ellipsometry data analysis, Thin Solid Films 636 (2017) 519–526.
[3] D.V. Likhachev, B-spline parameterization of the dielectric function and information criteria: The craft of non-overfitting, in: B. Bodermann, K. Frenner, R.M. Silver (Eds.), Modeling Aspects in Optical Metrology VI, Munich, Germany, June 25-29, 2017, SPIE Proc. 10330 2017, 103300B.
[4] P.H.C. Eilers, B.D. Marx, M. Durbán, Twenty years of P-splines, SORT-Stat. Oper. Res. Trans. 39 (2015) 149–186.

Influence of temperature, strain, alloy composition, doping, and film thickness on the dielectric function of semiconductors

Stefan Zollner
Department of Physics, New Mexico State University, Las Cruces, NM 88003, USA

Due to the pioneering work of Aspnes and Studna [1] and others following their example, the dielectric functions and interband critical point parameters of group IV semiconductors (C, Si, Ge, Sn, SiC) and III/V and II/VI compound semiconductors are fairly well established, as long as we consider these materials in bulk form, free of dopants and impurities, and at room temperature. This talk will give examples of how deviations from these ideal conditions affect the dielectric function and the interband critical points.

(1) With increasing temperature, critical points shift to lower energies and become broader. Also, excitonic enhancements become weaker, leading to a decrease of critical point amplitudes [2].
(2) Biaxial tensile stress (for example in strained epitaxial layers) shifts and splits critical points. These effects can be calculated within continuum elasticity theory using deformation potentials. The weight of the E_1 and $E_1+\Delta_1$ critical point amplitudes may also shift [3].
(3) The critical point energies in relaxed semiconductor alloys (such as $Si_{1-x}Ge_x$ or $Al_{1-x}Ga_xAs$) usually vary continuously, following Vegard's Law with small quadratic bowing corrections. Alloy composition can cause singularities, if the character of the band structure changes, for example a transition from a Ge-like to a Si-like band structure. Alloy scattering as well as statistical or macroscopic fluctuations of composition cause a broadening of the critical points. The amplitudes decrease due to a weakening of the excitonic enhancement. This also affects the excitonic phase angle. In strained semiconductor alloy layers, the effects of stress also have to be taken into account.
(4) Doping has three effects: First, the presence of free carriers adds a small Drude contribution to the undoped dielectric function. Second, the critical points red-shift, broaden, and become weaker due to the screening of the excitonic enhancement by the free carriers and scattering by ionized impurities. Third, due to band filling, the line shape of the critical points may change. We have shown this recently for heavily n-type germanium at low temperatures [4]. This effect can also be seen in transient ellipsometry spectra after femtosecond laser excitation with an 800 nm pump pulse [5].
(5) Finally, we believe that the dielectric function of ZnO varies with film thickness and depends on the choice of substrate. For example, ZnO on quartz is a type-I system, where the excitons are confined leading to an increase of the direct gap absorption. On the other hand, if ZnO thin films are grown on Si, the holes will quickly scatter into the Si substrate, which will lead to a decrease of the near-gap absorption and the refractive index. I hope to have more convincing data by October.

References:

[1] D.E. Aspnes and A.A. Studna, Phys. Rev. B **27**, 985 (1983).
[2] Carola Emminger, Linz, Austria, MS thesis (2017).
[3] N.S. Fernando *et al.*, Appl. Surf. Sci. **421 B**, 905 (2017); J. Vac. Sci. Technol. (submitted).
[4] C. Xu, N.S. Fernando, S. Zollner, J. Kouvetakis, and J. Menendez, Phys. Rev. Lett. **118**, 267402 (2017).
[5] S. Espinoza, M. Rebarz, S. Richter, and J. Andreasson (unpublished).

ELLIPSOMETRIC STUDY ON TiO_2 / ZnO BILAYER LAMINATE FILMS FOR PIEZOELECTRIC APPLICATIONS

M. Modreanu[a], I. Povey[a], M. Stoica[b], M. Gartner[b]

[a] Micro-Nanoelectronics Centre, Tyndall National Institute, University College Cork, Lee Maltings Complex Dyke Parade, Cork, Ireland
[b] Surface Science and Catalysis, Institute of Physical Chemistry "Ilie Murgulescu" of the Romanian Academy, Splaiul Independentei 202, Bucharest, Romania

Nanolaminates are multicomponent systems made up of alternating layers of specific materials, each layer being of the nanometre order [1]. Mixing a wide variety of materials makes it possible to fine-tune a material in terms of the films properties, composition and structure [2]. The applications of hybrid films range from solar cells, sensors, piezoelectric MEMS, optoelectronic devices and protective coatings [3], to name only a few. Such suitable materials to be coupled together are zinc oxide (ZnO) and titanium dioxide (TiO_2) due to their close band gap energies, in the range of 3.2 – 3.4 eV [4,5]. Both materials are photocatalysts, ZnO presents a piezoelectric effect and it is interesting to consider how their functionalities will act in a laminate system.

In this work TiO_2 / ZnO bilayer laminate films were deposited on glass and Si (111) substrates by Atomic Layer Deposition (ALD) method, through the spacing and thickness of each layer has been carefully controlled, thus a various combination of TiO_2 and ZnO multilayers were produced. The films were measured by a Woollam™ Rotating Analyzer Ellipsometer and characterized by WVASE® software. We present the ellipsometric results obtained on these laminate films in terms of layer thickness, refractive index and band gap energies, highlighting the influence of composition and layer order on optical and piezoelectric properties.

Keywords: TiO_2 / ZnO laminate films, ALD, ellipsometry, optical /piezoelectric properties

References

[1] *Atomic Layer Deposition of Nanostructured Materials*. Wiley-VCH: Weinheim, Germany (2012)
[2] H.B. Lee, V.R. Anderson, S.M. George, *Growth and properties of Hafnicone and HfO_2/Hafnicone nanolaminates and alloy films using molecular layer deposition techniques*, ACS Applied Materials & Interfaces **6** (2014) 16880-16887
[3] P. Sundberg, M. Karppinen, *Organic and inorganic-organic thin film structures by molecular layer deposition: a review*, Beilstein Journal of Nanotechnology **5** (2014) 1104-1136
[4] A. Janotti, C.G. Van de Walle, *Fundamentals of zinc oxide as a semiconductor*, Reports on Progress in Physics **72** (2009) 126501
[5] D. Reyes-Coronado, G. Rodriguez-Gattorno, M.E. Espinosa-Pesqueira, C. Cab, R. de Coss, G. Oskam, *Phase-pure TiO_2 nanoparticles: anatase, brookite and rutile*, Nanotechnology **19** (2008) 145605

Acknowledgements

The support of the project entitled "*Piezoelectric MEMS for efficient energy harvesting (PiezoMEMS)*" M-ERA.net No. 12 / 2015 is gratefully acknowledged.

SPECTROSCOPIC ELLIPSOMETRY STUDY OF HYBRID PEROVSKITE SOLID SOLUTION $FA_xMA_{1-x}PbI_3$ SINGLE CRYSTALS

M. I. Alonso[a], B. Charles[b], A. Francisco-Lopez[a], O. J. Weber[b], M. Garriga[a], M. Campoy-Quiles[a], M. T. Weller[b] and A. R. Goñi[a,c]

[a]Institut de Ciència de Materials de Barcelona (ICMAB-CSIC), Campus de la UAB, 08193 Bellaterra, Spain
[b]Department of Chemistry and Centre for Sustainable Chemical Technologies, University of Bath, Claverton Down, Bath, UK
[c]ICREA, Passeig Lluís Companys 23, 08010 Barcelona, Spain

Organic-inorganic hybrid perovskites have the generic formula ABX_3 , where X denotes a halide anion and A and B stand for an organic and a metal cation, respectively. These hybrid compounds are semiconductors with highly interesting and tunable properties and are subject of intense research for several applications, mainly in solar cells but also as LEDs and lasers. For all these applications, knowledge of the optical properties is both of fundamental and practical interest. For example, detailed knowledge of the optical constants enables the design and optimisation of light harvesting and out-coupling in the mentioned devices. Tunability of the optical properties may be accomplished by site-substituted solid solutions in A, B, or X sites. In particular, some mixed-cation systems show increased stability for these applications.

In this work, we report on the variation of the optical constants in mixed A-site cation methylammonium (MA) / formamidinium (FA) lead iodide hybrid $FA_xMA_{1-x}PbI_3$ as measured and analysed by spectroscopic ellipsometry in single crystal samples. The detailed structural phase behaviour of the samples is well established [1]. The main result in this work is the analysis of the observed electronic transitions as a function of the composition obtained from fitting the numerically built second derivatives of the dielectric function. The results are discussed together with other optical measurements (e.g., photoluminescence) by relative comparison to the electronic structures of the parent compounds [2,3].

Keywords: Ellipsometry; Hybrid Lead Halide Perovskite; Formamidinium-Methylammonium solid solution; Electronic Structure; Photovoltaics and LEDs

References

[1] O. J. Weber, B. Charles, M. T. Weller, J. Mater. Chem. A 4 (2016) 15375.
[2] A. M. A. Leguy, P. Azarhoosh, M. I. Alonso, M. Campoy-Quiles, O. J. Weber, J. Yao, D. Bryant, M. T. Weller, J. Nelson, A.Walsh, M. van Schilfgaarde and P. R. F. Barnes, Nanoscale 8 (2016) 6317.
[3] M. Kato, T. Fujiseki, T. Miyadera, T. Sugita, S. Fujimoto, M. Tamakoshi, M. Chikamatsu, H. Fujiwara, J. Appl. Phys. 121 (2017) 115501.

STEALTH TECHNOLOGY-BASED TERAHERTZ FREQUENCY-DOMAIN ELLIPSOMETRY INSTRUMENTATION

P. Kühne[a], V. Stanishev[a], N. Armakavicius[a], C. M. Herzinger[c], M. Schubert[b,a] and V. Darakchieva[a]

[a]Terahertz Materials Analysis Center, Department of Physics, Chemistry and Biology IFM, Linköping University, Sweden
[b]Department of Electrical and Computer Engineering and Center for Nanohybrid Functional Materials, University of Nebraska-Lincoln, USA
[c]J. A. Woollam Co., Inc., 645 M Street, Suite 102, Lincoln, Nebraska 68508, USA

We present a terahertz (THz) frequency-domain spectroscopic (FDS) ellipsometer design (Fig. 1) which suppresses formation of standing waves by use of stealth technology approaches. The strategy to suppress standing waves consists of three elements: geometry, coating and modulation [1]. The instrument is based on the rotating analyzer ellipsometer principle and can incorporate various sample compartments, such as a superconducting magnet, in-situ gas cells or resonant sample cavities, for example. A backward wave oscillator and three detectors are employed, which permit operation in the spectral range of 0.1–1 THz (3.3–33 cm^{-1}or 0.4–4 meV). The THz frequency-domain ellipsometer allows for standard and generalized ellipsometry at variable angles of incidence in both reflection and transmission configurations. The methods used to suppress standing waves and strategies for an accurate frequency calibration are presented. Experimental results from dielectric constant determination in anisotropic materials, and free charge carrier determination by FDS ellipsometry, and resonant-cavity enhanced optical Hall effect [2] experiments are discussed. Examples include silicon and sapphire optical constants, free charge carrier properties of two dimensional electron gas in group-III nitride high electron mobility transistor structure, and in conductive PEDOT thin polymer films.

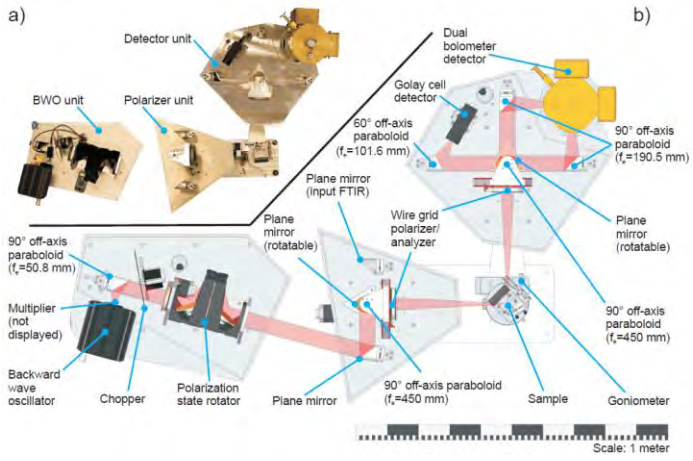

Fig. 1. a) photograph and b) schematic drawing of the THz FDS ellipsometer with major components indicated and without absorbing foam sheets and housing.

Keywords: Terahertz; Stealth technology based;

References

[1] P. Kühne, V. Stanishev, N. Armakavicius, M. Schubert and V. Darakchieva, IEEE Transactions on Terahertz Science and Technology (2018), arxiv.org/abs/1712.05283.
[2] M. Schubert, P. Kühne, V. Darakchieva and T. Hofmann, J. Opt. Soc. Am. A 33, 1553 (2016).

QUANTIFYING MOLECULAR INTERACTIONS WITH IR ELLIPSOMETRY

Andreas Furchner[a], A. Kroning[a], T. Shaykhutdinov[a], S. Adam[b], S. Rauch[b], P. Uhlmann[b], K.-J. Eichhorn[b], and K. Hinrichs[a]

[a]Leibniz-Institut für Analytische Wissenschaften – ISAS – e.V,
Schwarzschildstraße 8, 12489 Berlin, Germany
[b]Leibniz-Institut für Polymerforschung Dresden e.V.,
Hohe Straße 6, 01069 Dresden, Germany

Molecular interactions play a key role for the structural and functional properties of organic molecules at solid–liquid interfaces. Examples are ordering effects in functionalized thin films, protein aggregation at interfaces, as well as adsorption and desorption behavior of biomolecules on coated surfaces. *In situ* infrared ellipsometry (Fig. 1) accesses both film, analyte, and solvent vibrational fingerprints, and is therefore an advantageous method for measuring said properties. It provides, among other things, insights into film structure, hydration, molecular interactions, and local chemical environments, rendering it a powerful technique for detailed studies of solid–liquid interfaces, particularly of interfaces involving polymers and proteins.

Carbonyl vibrations are versitile infrared reporter modes for probing local chemical environments, that is, solvation effects and specific chemical interactions like hydrogen bonding. We employ *in situ* infrared ellipsometry to investigate structure and interactions of ultrathin polymer films and brushes containing side chain C=O moieties. The focus first lies on rather hydrophilic thermoresponsive, humidity-sensitive poly(*N*-isopropylacrylamide) [PNIPAAm] and poly(2-oxazoline) [POx] brushes whose reversible swelling–dewelling transitions in water are partially driven by a loss of water-interacting C=O groups with increasing temperature.

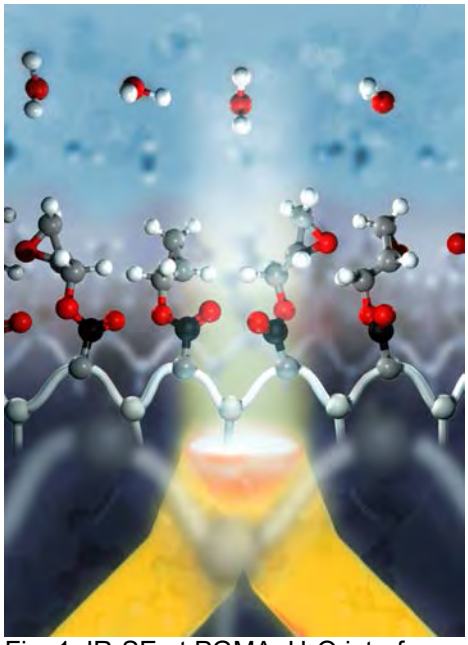

Fig. 1. IR-SE at PGMA–H_2O interface.

We then monitor and quantify interface-chromic and hydrogen-bond induced vibrational C=O band shifts of nanometer-thin hydrophobic poly(glycidylmethacrylate) [PGMA] films in contact with different solvents. The tail–train–loop structure of the covalently grafted films potentially influences film–solvent interactions. Using theoretical calculations, we find that effects from solvatochromism and interface geometry are insignificant for aprotic solvents, whereas in water the films' topmost subnanometer layer is involved in hydrogen bonds with H_2O molecules, giving rise to minor but detectable film swelling.

Keywords: In situ infrared ellipsometry; Solid–liquid interfaces; Molecular interactions

References

[1] A. Furchner, A, Kroning, S. Rauch, P. Uhlmann, K.-J. Eichhorn, K. Hinrichs, Analytical Chemistry 89 (2017) 3240.
[2] A. Kroning, A. Furchner, S. Adam, P. Uhlmann, K. Hinrichs, Biointerphases 11 (2016) 019005.

Poster Contributions

[P01] Theo Pflug
"CASE STUDY ON THE DYNAMICS OF ULTRAFAST LASER HEATING AND ABLATION OF GOLD THIN FILMS BY ULTRAFAST PUMP-PROBE ELLIPSOMETRY"

[P02] Markus Olbrich
"COMPARISON OF DIFFERENT MODELS DESCRIBING THE TEMPERATURE DEPENDENT DIELECTRIC FUNCTION: VALIDATION OF MODELS WITH TIME-RESOLVED PUMP-PROBE REFLECTOMETRY AND ELLIPSOMETRY"

[P03] Oliver Herrfurth
"PITFALLS OF TIME-RESOLVED SPECTROSCOPIC ELLIPSOMETRY"

[P04] Andreas Hertwig
"CALIBRATION SAMPLES AND THE GUM-COMPLIANT DETERMINATION OF UNCERTAINTIES IN ELLIPSOMETRY – A STANDARDIZATION INITIATIVE"

[P05] Eugene Bortchagovsky
"THE CHOICE OF OPTIMAL CONDITIONS OF ELLIPSOMETRIC MEASUREMENTS FOR ACCURATE DETERMINATION OF PARAMETERS OF INVESTIGATED SYSTEMS."

[P06] Krzysztof Dorywalski
"HYBRID GA-GRADIENT METHOD FOR THIN FILMS ELLIPSOMETRIC DATA EVALUATION"

[P07] Tobias Grunewald
"A NEW MERIT FUNCTION FOR MUELLER MATRIX ELLIPSOMETRY AND ITS APPLICATION ON SUBWAVELENGTH GRATINGS"

[P08] Andreas Furchner
"INFRARED MÜLLER MATRIX ELLIPSOMETRY OF THIN FILMS AND STRUCTURED SURFACES"

[P09] Martin Čermák
"USE OF THE EXACT APPROACH OF THE RAYLEIGH–RICE THEORY FOR CALCULATING ELLIPSOMETRIC PARAMETERS AND REFLECTANCE OF MULTILAYER SYSTEMS WITH RANDOMLY ROUGH BOUNDARIES"

[P10] Kamil Postava
"MODELING OF ELLIPSOMETRIC RESPONSE FROM PERIODIC STRUCTURE INCLUDING INCOHERENT PROPAGATION IN THICK LAYERS"

[P11] Judit Budai
"ELLIPSOMETRIC ANALYSIS OF ALIGNED CARBON NANOTUBES"

[P12] Michele Magnozzi
"SPECTROSCOPIC ELLIPSOMETRY ANALYSIS OF SELF-ASSEMBLED AU/PNIPAM CORE-SHELL NANOPARTICLES"

[P13] Francesco Bisio
"TEMPERATURE-DEPENDENT OPTICAL PROPERTIES OF PLASMONIC NANOSYSTEMS"

[P14] Sandhya Chandola
"OPTICAL CHARACTERISATION OF ELECTRONIC CONFINEMENT IN THIN METALLIC FILMS GROWN ON 1-D NANOSTRUCTURES"

[P15] Sebastian Funke
"IMAGING ELLIPSOMETRY AS A TOOL FOR THE CHARACTERIZATION OF 2D-MATERIALS ON VARIOUS SUBSTRATES"

[P16] Constance Schmidt
"IMAGING ELLIPSOMETRY WITH CON-LOCAL RAMAN SPECTROSCOPY ON 2D TRANSITION METAL DICHALCOGENIDES WITH DIFFERENT LAYER THICKNESSES"

[P17] Shun Okano
"THE INFLUENCE OF FIELD EFFECT DOPING ON THE OPTICAL PROPERTIES OF BILAYER GRAPHENE"

[P18] Premysl Marsik
"PHONON ANOMALIES IN STRAINED SRMNO3 FILMS"

[P19] Chris Sturm
"DIELECTRIC FUNCTION AND SINGULAR OPTIC AXES OF KTP"

[P20] Ievgen Voloshenko
"MUELLER MATRIX ELLIPSOMETRY INVESTIGATIONS OF INSULATOR METAL TRANSITION IN VO2"

[P21] Farzin Abadizaman
"MUELLER MATRIX ANOMALY NEAR THE CURIE TEMPERATURE OF NI"

[P22] Dmitriy V. Likhachev
"DIFFERENT PARAMETERIZATION OF THE TIN OPTICAL PROPERTIES FOR SPECTROSCOPIC ELLIPSOMETRY–X-RAY REFLECTOMETRY COMPARISON"

[P23] Tomasz Rerek
"THE INFLUENCE OF DEPOSITION RATE ON MICROSTRUCTURE AND OPTICAL PROPERTIES OF THE SN THIN LAYERS"

[P24] Saulius Tumėnas
"TEMPERATURE DEPENDENCE OF ZINC R101 ENERGY GAP"

[P25] Jiri Vohánka
"OPTICAL CHARACTERIZATION OF NON-STOICHIOMETRIC SILICON NITRIDE FILMS PREPARED BY MAGNETRON SPUTTERING"

[P26] Daniel Franta
"OPTICAL CHARACTERIZATION OF HYDROGENATED AMORPHOUS SILICON-CARBON FILMS IN A WIDE SPECTRAL RANGE"

[P27] Lukasz Skowronski
"DIELECTRIC FUNCTIONS OF TITANIUM IN THE REGIME OF THE LIMITED LIGHT PENETRATION"

[P28] Oldrich Zmeskal
"THE INFLUENCE OF BALL-MILLING ON THE OPTICAL PROPERTIES OF PRINTED TITANIA PATTERNS REINFORCED BY ORGANOSILOXANE BINDER"

[P29] Lukasz Skowronski
"THE OPTICAL TIO2 LAYERS DEPOSITED ON POLYMER SUBSTRATES"

[P30] Lukasz Skowronski
"OPTICAL AND MICROSTRUCTURAL CHARACTERIZATION OF THICK TIO2 LAYERS PRODUCED USING MAGNETRON SPUTTERING TECHNIQUE"

[P31] Przemyslaw Sedzicki
"EFFECTS OF PHOSPHOROUS IONS IMPLANTATION IN BULK CDTE CRYSTAL"

[P32] Przemyslaw Sedzicki
"OPTICAL PROPERTIES OF COBALT/CHROMIUM DOPED BULK ZNSE"

[P33] Sven Peters
"SPECTROSCOPIC ELLIPSOMETRY FOR THE ANALYSIS OF ANISOTROPIC WIDE BAND GAP SEMICONDUCTORS"

[P34] Florian Bärwolf
"SPECTROSCOPIC ELLIPSOMETRY, SIMS AND X-RAY DIFFRACTOMETRY AND REFLECTOMETRY FOR GE-GRADED SIGE HBT CONTROL"

[P35] Nerijus Armakavicius
"ELECTRON EFFECTIVE MASS IN IN0.33GA0.67N DETERMINED BY INFRARED OPTICAL HALL EFFECT"

[P36] Attila Sütő
"IMAGING SPECTROSCOPIC ELLIPSOMETER FOR OLED APPLICATION"

[P37] Peter H. Thiesen
"OPTICAL CHARACTERIZATION OF ANISOTROPIC THIOPHENE-PHENYLENE CO-OLIGOMER MICRO CRYSTALS BY SPECTROSCOPIC IMAGING ELLIPSOMETRY."

[P38] Eva Bittrich
"THE GLASS TRANSITION IN POLYIMIDE FILMS USED FOR MICROELECTRONIC PACKAGING"

[P39] Maurizio Canepa
"OPTICAL PROPERTIES OF AMORPHOUS SIO2-TIO2 MULTI-NANOLAYERED COATINGS FOR 1064-NM MIRROR TECHNOLOGY"

[P40] Peter Basa
"STABLE AND REPRODUCIBLE POROUS COATINGS FOR SMART WINDOW APPLICATIONS"

[P41] Peter H. Thiesen
"CHARACTERIZATION OF THIN FILMS AT DISADVANTAGEOUS INTERFACES BY IMAGING ELLIPSOMETRY"

[P42] Peter H. Thiesen
"IMAGING ELLIPSOMETRY AT THE AIR/WATER INTERFACE"

[P43] Benjamin Kalas
"DETECTION AND CONTROL OF SURFACE NANOSTRUCTURES AT WATER LIQUID INTERFACE FOR SENSING"

[P44] Karsten Hinrichs
"OPTOFLUIDIK PLATFORM FOR ENHANCED IR MICROSCOPIC SENSING"

[P45] Christian Hoffmann
"CHARACTERIZATION OF EXTRUDED COLLAGEN FIBRES WITH IMAGING ELLIPSOMETRY"

[P46] Elisabeth Preuße
"SPECTROSCOPIC ELLIPSOMETRY OF ADSORBED PROTEINS ON BIOCERAMIC IMPLANT MATERIAL"

Case study on the dynamics of ultrafast laser heating and ablation of gold thin films by ultrafast pump-probe ellipsometry

Theo Pflug, Markus Olbrich, and Alexander Horn

Laserinstitut Hochschule Mittweida, Schillerstraße 10, 09648 Mittweida, Germany

To increase the comprehension of the dynamics of ultrafast laser ablation it is necessary to portray the process with sufficient temporal resolution. For example, the temporal and spatial modification of the complex refractive index $\tilde{n}$ of a sample material after irradiation with ultrafast single pulsed laser radiation ($\lambda = 800$ nm, $\tau_{\mathrm{H}} = 40$ fs) can be measured, combining an ellipsometer with a pump-probe setup. This work describes the construction and the validation of a pump-probe setup (Fig. 1) enabling spatially, temporally and spectroscopically resolved ellipsometry with rotating compensator and rotating analyzer [1]. The self-constructed ellipsometer is validated by comparative measurements of the spectroscopically resolved complex refractive index of gold thin films ($d_{\mathrm{Au}} = 200$ nm, $R_a < 3$ nm) at rest with a commercial ellipsometer (nanofilm_ep4, Accurion Inc.), resulting in a deviation less than 10 %.

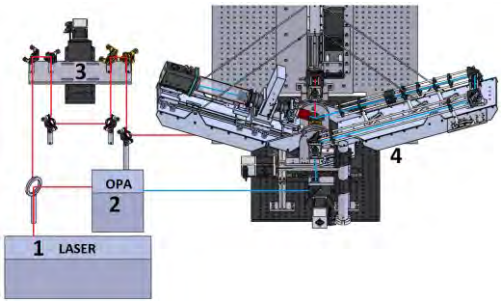

Fig. 1. Experimental setup: 1) laser emitting pump radiation at $\lambda = 800$ nm; 2) optical parametric amplifier emitting probe radiation at 250 nm $< \lambda <$ 20 µm; 3) delay line; 4) ellipsometer

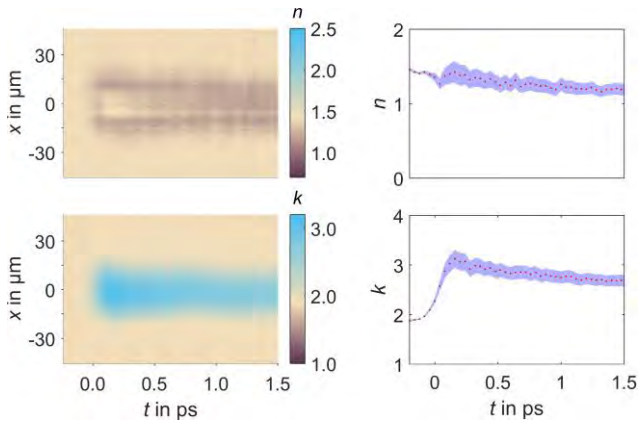

Fig. 2. Left: one-dimensional spatially resolved n and k of gold plotted as function of time after irradiation with single pulsed pump radiation; right: cross-section of n and k at $x = 0$ µm as function of time

First ellipsometric measurements at $\lambda_{\mathrm{pump}} = 800$ nm and $\lambda_{\mathrm{probe}} = 440$ nm are performed without ablating the sample material. The refractive index n slightly decreases with a spatial local maximum at $t = 0.2$ ps. The extinction coefficient k increases within the first 0.2 ps and slightly decreases afterwards (Fig.2, right). The spatial extent of the modification remains constant in the considered time range (Fig.2, left).

Keywords: pump-probe; ellipsometry; gold thin film; ultrafast; single pulsed radiation

References

[1] H. Fujiwara, *Spectroscopic Ellipsometry*, John Wiley & Sons, Ltd, Chichester, UK (2007)

Comparison of different models describing the temperature dependent dielectric function: Validation of models with time-resolved pump-probe reflectometry and ellipsometry

Markus Olbrich, Theo Pflug, and Alexander Horn

Laserinstitut Hochschule Mittweida, Schillerstraße 10, 09648 Mittweida, Germany

Irradiating thin metal films with single pulsed ultrafast laser radiation two distinguishable ablation regimes are obtained experimentally depending on the applied fluence, so called gentle and strong ablation regimes [1]. The principle mechanism causing gentle and strong ablation are studied either by hydrodynamic [2] or atomistic [3, 4] approaches. Nevertheless, time-resolved metrology [5], like ultrafast pump-probe reflectivity and ellipsometry, measuring the temporal evolution of the spatial distribution of the reflectance and complex refractive index, and thus the temperature and stress dependent dielectric function, have to be performed to validate simulations in terms of simulated and experimentally obtained changes of the dielectric function. Therefore, the temperature and stress dependence, especially for non-equilibrated electron and phonon systems, caused by heating the material with single pulsed laser radiation with a pulse duration of several 10 femtoseconds, and subsequently induced rarefaction and shock waves, must be included in a wide range model for the dielectric function.

In our approach, using the Drude-critical point model with fitted parameters to reproduce the experimentally determined complex refractive index for gold at rest and additionally modifying the model to include the temperature and stress dependence. Finally, the simulated relative reflectance change and the complex refractive index of an irradiated thin gold film ($d = 200$ nm) with ultrafast laser radiation (pump radiation: $\tau_H = 40$ fs, $\lambda = 800$ nm, probe radiation: $\tau_H = 60$ fs, $\lambda = 440$ nm) are compared with the experimentally obtained results (Fig. 1). The temperature and stress distribution are calculated by a hydrodynamic approach [4].

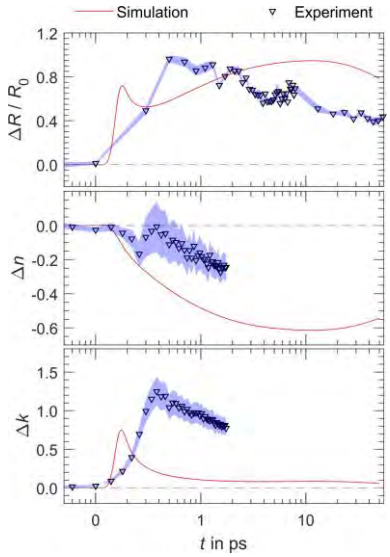

Fig. 1. Comparison of experimentally determined and simulated relative change of reflectance and complex refractive index

Keywords: pump-probe ellipsometry; pump-probe reflectometry; ultrafast material processing; thin films of gold

References

[1] M. Olbrich, E. Punzel, R. Roesch, R. Oettking, B. Muhsin, H. Hoppe, A. Horn, Appl. Phys. A **122** (2016)
[2] M.E. Povarnitsyn, N.E. Andreev, E.M. Apfelbaum, T.E. Itina, K.V. Khishchenko, O.F. Kostenko, P.R. Levashov, M.E. Veysman, Appl. Surf. Sci. **258**, 9480 (2012)
[3] M.E. Povarnitsyn, V.B. Fokin, P.R. Levashov, Appl. Surf. Sci. **357**, 1150 (2015)
[4] C. Wu, L.V. Zhigilei, Appl Phys A **114**, 11 (2014)
[5] A. Horn, *Ultra-fast material metrology* (Wiley-VCH, Weinheim, 2009)

PITFALLS OF TIME-RESOLVED SPECTROSCOPIC ELLIPSOMETRY

O. Herrfurth[a], S. Richter[a], S.J. Espinoza Herrera[b], M. Rębarz[b], M. Grundmann[a], S. Zollner[c], J. Andreasson[b,c] and R. Schmidt-Grund[a]

[a]Universität Leipzig, Felix-Bloch-Institut für Festkörperphysik,
Linnéstr. 5, 04103 Leipzig, Germany
[b]ELI beamlines/Fyzikální ústav AV ČR v.v.i.,
Za Ranicí 835, Dolní Břežany, Czech Republic
[c]Chalmers tekniska högskola,Institutionen för fysik,
Kemigården 1, 41296 Göteborg, Sweden

Time-resolved spectroscopic ellipsometry measurements have been carried out at ZnO single crystals and a film using a pump-probe setup employing UV pump and white light probe pulses. Here, we will discuss experimental details and strategies such as the choice of polarization optics in order to minimize the chirp induced by the group velocity delay, and limiting factors for the time resolution. Fluctuations of the white light spectrum are compensated by the use of two chopper plates. Further difficulties result from non-ideal optical components. Different calibration strategies have been tried when obtaining ellipsometric data from the measured intensity spectra.

The ellipsometric approach is superior to transient reflectance or transmittance experiments because it allows unambiguous distinction of effects on the real and imaginary part of the dielectric function. Furthermore, measuring transient depolarization can serve as monitor for unresolved processes faster than the time resolution of the instrument. In principal, time-resolved ellipsometry does even enable studying the dynamics of anisotropies. However, a crucial point in obtaining true dielectric function data of a pumped sample is application of an appropriate model. In particular, artificial observation of gain, indicated by a negative ε_2, is possible when neglecting that the density of excited charge carriers is highest close to the surface and decreases towards the bulk (Fig. 1). Such stimulated emission cannot be observed in reflection experiments [1], because the detected light has an opposite wave-vector component normal to the interface. Though, this aspect is hard to identify when modeling bare reflectance measurements [2].

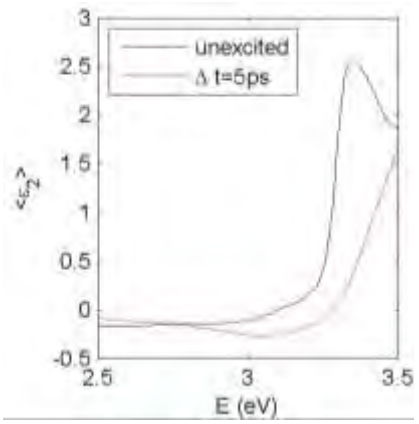

Fig. 1. As measured pseudo-dielectric function of a *c*-plane oriented ZnO single crystal before and 5ps after arrival of the UV pump pulse. Seemingly, gain is observed. (Small offset due to surface roughness)

Keywords: pump-probe; instrumentation; dynamics; modeling

References

[1] K. Bohnert, G. Schmieder, C. Klingshirn, pss B **98** (1980), 175
[2] M. A. M. Versteegh, T. Kuis, H. T. C. Stoof, J. T. Dijkhuis, Phys. Rev. B **84** (2011) 035207.

Calibration samples and the GUM-compliant determination of uncertainties in ellipsometry – a standardization initiative

Andreas Hertwig, Dana-Maria Rosu[b], Uwe Beck

[a]Division 6.7, Bundesanstalt für Materialforschung und -prüfung (BAM), Unter den Eichen 87, 12205 Berlin, Germany
[b]Physikalisch-Technische Bundesanstalt (PTB) 8.1 - Biomedical Magnetic Resonance, Abbestr. 2 - 12, D-10587 Berlin, Germany

Ellipsometry is well known as a highly sensitive and reproducible surface analysis technique. However, in a context of metrological applications, the most important property of a measurement process is accuracy, relying on statistical precision (reproducibility) and trueness (in an absolute sense versus a given standard). The latter is much more difficult to achieve. In this presentation, we discuss the possibility of establishing ellipsometry in a diverse metrological landscape by means of defining standard procedures and best practice methodologies for the measurement and for calibration purposes. The most important task of this approach is to determine the model-inherent uncertainty, originating from parameter coupling. We achieve this by means of sensitivity analysis of the parameters resulting from the fit process. We discuss the definition of reference materials by which accuracy can be made available for ellipsometry, passed along between ellipsometry laboratories and for other measurement techniques. The determination of uncertainty is presented in this work for a number of examples involving difficult analysis models employed for samples from different production environments [1].

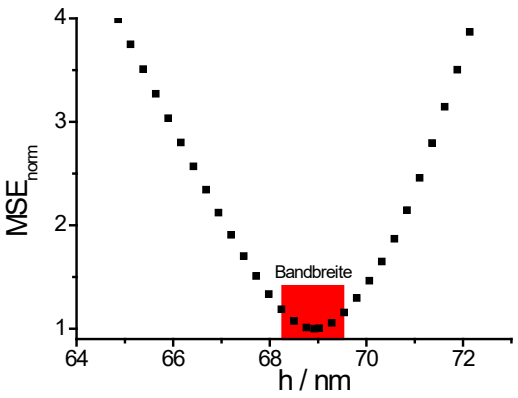

Fig. 1. Sensitivity analysis for the ellipsometric determination of a layer thickness

We present a standardization initiative with the goal to disseminate this work into an international standard alongside an inter-laboratory study comparing the results for complex samples gained by laboratories with different instrumentation. We also present the results gained within EURAMET projects focused on the metrology of materials with strong non-idealities used in photovoltaics and other energy technology.

Keywords: Ellipsometric Metrology, Reference Samples, Reference Procedures, Standardization

References

[1] D.-M. Rosu, E. Ortel, V.-D. Hodoroaba, R. Kraehnert, A. Hertwig, Ellipsometric porosimetry on pore-controlled TiO2 layers, Appl Surf Sci, 421 (2017) 487-493.

The choice of optimal conditions of ellipsometric measurements for accurate determination of parameters of investigated systems.

E. Bortchagovsky

Institute of Semiconductor Physics of NAS of Ukraine, pr.Nauki 41, Kyiv 03028, Ukraine

Ellipsometry is indirect method, which measures ellipsometric angles and not optical parameters of the investigated systems. By definition the change of any measured value $\delta\mathbf{m}$ at small change of a parameter of an investigated system $\delta\mathbf{p}$ is determined by the sensitivity of the measured parameter **m** to the system parameter **p** – $\partial\mathbf{m}/\partial\mathbf{p}$ via the expression $\delta\mathbf{m} = (\partial\mathbf{m}/\partial\mathbf{p})\,\delta\mathbf{p}$. So higher sensitivity should allow to feel smaller changes of the system parameters. It results in standard hint to make measurements at the conditions of higher sensitivity. However a simple example of a thin film on a transparent substrate demonstrates the problem of such an approach, as errors of measurements at Brewster angle make such measurements useless.

This example indicates the second element, which should be taken into account in the determination of the optimal conditions – errors of measurements. If the average magnitude of errors of measurements is $\sigma\mathbf{m}$, the minimal registered change of the system parameter **p** will be $\sigma\mathbf{p} = \sigma\mathbf{m} / (\partial\mathbf{m}/\partial\mathbf{p})$. Its inverted value $1/\sigma\mathbf{p}$ may be called “precision” of the determination of the parameter **p** and has simple interpretation, namely it is defined by the ratio of signal to noise, as the measured signal is proportional to the sensitivity.

The necessity to take into account errors at the choice of the conditions for the precise determination of parameters of the investigated system is noticed in the literature but for the analysis the constant level of errors is assumed. It turns us back to the situation with seeking for the maximal sensitivity. As the result suggestions to measure thin films on transparent substrate at angles slightly bigger than the Brewster one where the sensitivity is still high but errors are decreased may be found without any determination of the value of such angles.

At the same time expressions for the error level depending on the measurement conditions exist for long time. Those expressions with the ones for the sensitivity should be used to find the optimal condition of measurements for the accurate determination of the parameters of interest. In contrary to the qualitative hints this approach allows to determine optimal conditions of measurements quantitatively what is demonstrated in this presentation for different kinds of ellipsometers.

Keywords: Precision; Error; Optimal conditions

HYBRID GA-GRADIENT METHOD FOR THIN FILMS ELLIPSOMETRIC DATA EVALUATION

K. Dorywalski[a,b], M. Grundmann [b] and R. Schmidt-Grund [b]

[a]Faculty of Technology and Education, Koszalin University of Technology, Śniadeckich Str. 2, PL-75-453 Koszalin, Poland
[b] Universität Leipzig, Felix-Bloch-Institut für Festkörperphysik, Linnéstr. 5, 04103 Leipzig, Germany

In this work, we present application of a combined genetic-gradient algorithm in ellipsometry data analysis for samples with different structure complexity, starting with monolayer. We demonstrate that by using this method we are able to find material parameters even for limited a priori knowledge about the sample properties, where classical methods fail.

Traditionally gradient based minimization algorithms, such as Levenberg-Marquardt, are used as optimization tools in ellipsometric problems. However, similarly to other local optimizers, its performance depends on the complexity of the search space, the number of variables and a good starting point, being possible that the optimization would be trapped in a local minimum [1]. Because of the non-linearity and complexity of the model equations, the error surface in ellipsometry is mostly rough (Fig. 1). Therefore, more complex global-search optimization methods are desirable to overcome the problem of choosing initial values of the model parameters which are close enough to the real sample properties. Non-deterministic optimization algorithms, such as genetic algorithms [1], simulated annealing and others [2] have already demonstrated that in some cases they can be interesting alternative for gradient-based methods in ellipsometric data evaluation.

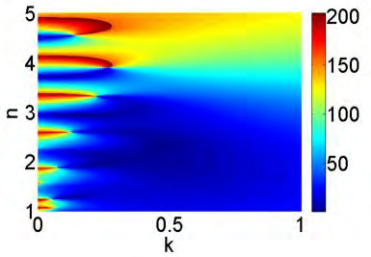

Fig. 1. An example error surface in ellipsometry: calculations for 200nm diamond-like carbon film (n = 2, k =0.25 @3.55 eV) on Si

Here we applied hybrid genetic-gradient algorithm. This method uses genetic algorithm (GA) concept to explore the objective space; hence do not make any assumptions about the underlying fitness landscape, avoiding the disadvantages of iterative improvement and, in particular, multiple descents by allowing the local search to escape from local optima. Afterward, the gradient-based algorithm is employed to explore promising part of the objective space. The method is able to determine all the parameters (complex refractive index, thickness) of any unknown layer and/or thicknesses of layers in case of a multilayer system, without need to deliver starting points.

Keywords: Thin films; Data evaluation; Genetic algorithm

References

[1] V.R. Fernandes, C.M.S. Vicente, N. Wada et. al., Opt. Exp. 16 (2010), 16586.
[2] O. Polgar, M. Fried, T. Lohner et. al., Surf. Science 457 (2000) 157-17.

A new merit function for Mueller matrix ellipsometry and its application on subwavelength gratings

Tobias Grunewald, Matthias Wurm, Bernd Bodermann

Physikalisch-Technische Bundesanstalt (PTB), Bundesallee 100, 38116 Braunschweig, Germany

Recently, Ossikovski and Arteaga have introduced a new decomposition technique for depolarizing Mueller matrices (MM), the so called integral decomposition technique [1]. We have refined this technique and derived a new merit function, which can be used in least-squares-fitting to achieve geometrical and/or optical properties of nominally nondepolarizing samples. We use in this new merit function the depolarizing parts of the measured MMs to weight the differences between all four non-depolarizing MMs (obtained from applying Cloude's sum decomposition [2]) and the simulated MMs. In this way, we obtain a physical reasonable weighting. Furthermore, also a criterion is gained whether the chosen geometry model is well suited for the sample under test or not.

In our contribution, we will present the application of this technique: we use it to derive the cross-section geometry of subwavelength gratings from Mueller matrix measurements in a wavelength range from 200 nm to 900 nm. The samples are made of silicon and provide linewidths as low as 25 nm. Note, that cross-sections of those samples are not accessible either with atomic force, top down scanning electron (SEM) or optical microscopy, for different reasons (tip size, charging, resolution). But to classify the new Mueller matrix based results we will compare them to those achieved with our DUV scatterometer and to cross-section SEM images (obtained at identically processed samples). Scatterometry and cross-section SEM results have been shown already to agree very well [3]. One example is given in Fig.1.

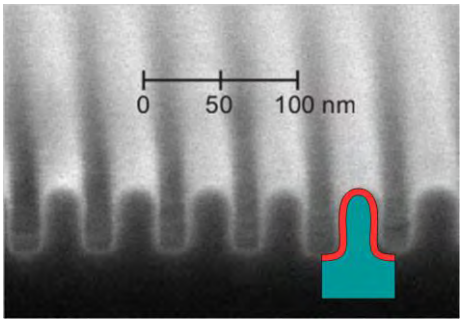

Fig. 1. Comparison of a silicon grating profile (green: silicon, red: silicon oxide) reconstructed from scatterometric measurement data with a cross-section SEM image obtained at an identically processed sample.

Keywords: subwavelength; gratings; Mueller matrix, merit function

References

[1] R. Ossikovski, O. Arteaga, Integral decomposition and polarization properties of depolarizing Mueller matrices, Optics letters 40(6),954-957 (2015).
[2] S. R. Cloude, Proc. SPIE 1166, 177 (1989).
[3] M. Wurm, J. Endres, J. Probst, M. Schoengen, A. Diener, B. Bodermann, Metrology of nanoscale grating structures by UV scatterometry, Opt. Express 25, 2460-2468 (2017)

Infrared Müller Matrix Ellipsometry of Thin Films and Structured Surfaces

Andreas Furchner[a], C. Walder[a], M. Zellmeier[b], J. Rappich[b], and K. Hinrichs[a]

[a]Leibniz-Institut für Analytische Wissenschaften – ISAS – e.V, Schwarzschildstraße 8, 12489 Berlin, Germany
[b]Helmholtz-Zentrum Berlin für Materialien und Energie GmbH, Institut für Silizium-Photovoltaik, Kekuléstraße 5, 12489 Berlin, Germany

Non-isotropic thin films can be characterized by their infrared Müller matrix (MM), which, besides anisotropy and structure, can provide information on film chemistry, composition, and molecular interactions. However, laboratory thin-film infrared MM measurements are inherently difficult, mainly because of low optical throughput, source prepolarization, and non-ideal polarizers.

We developed a novel IR Müller ellipsometer with high optical throughput that enables sensitive MM measurements of thin films below 100 nm. The measurement scheme can be restricted to a subset of defined polarizer settings, allowing one to extract quadruples of Müller matrix elements within a few 10 seconds to minutes. Tandem polarizers gurantee a sufficiently high degree of polarization necessary to accurately measure block-offdiagonal MM elements.

We demonstate MM measurements of thin polymer films and structured surfaces (trapezoidal SiO_2 gratings), the offdiagonal MM elements of which are highly sensitive towards structure and orientation, as verified by RCWA calculations.

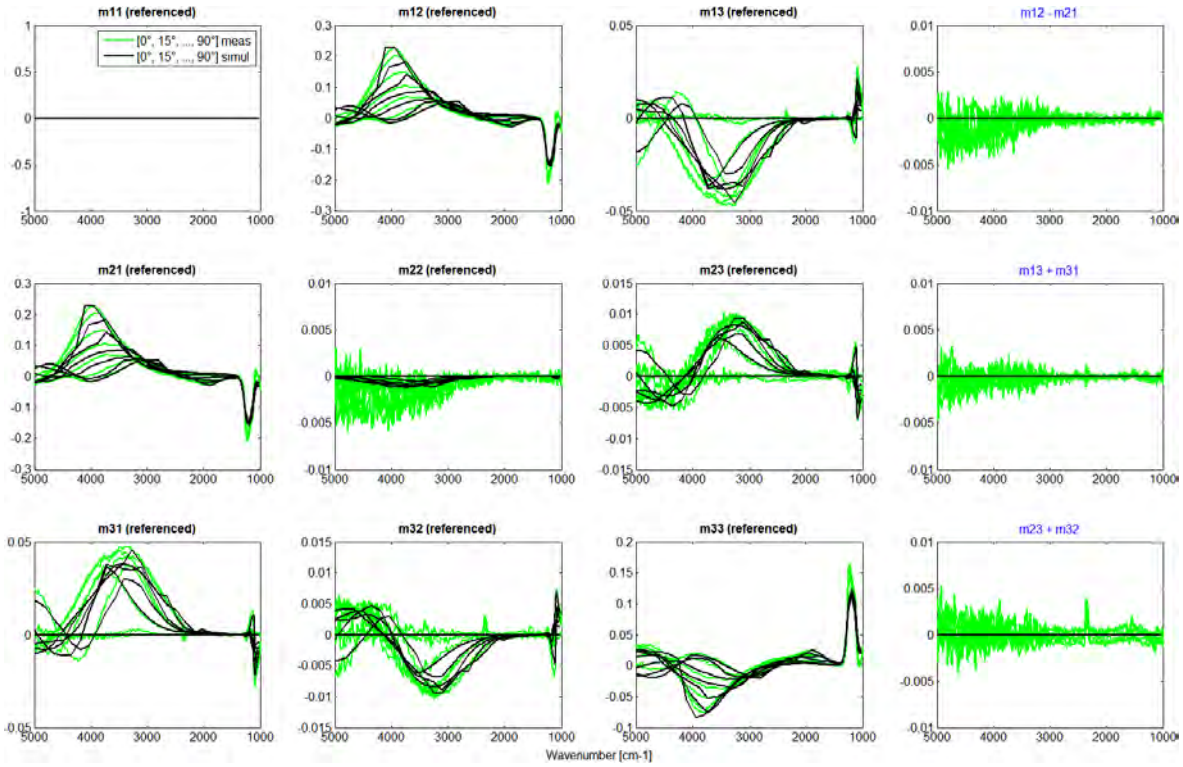

Fig. 1. Azimuth-dependent Müller matrix (measured vs. simulated) of a trapezoidal SiO_2 grating on Si.

Keywords: Infrared Mueller matrix ellipsometry; SiO_2 gratings; Thin films

USE OF THE EXACT APPROACH OF THE RAYLEIGH–RICE THEORY FOR CALCULATING ELLIPSOMETRIC PARAMETERS AND REFLECTANCE OF MULTILAYER SYSTEMS WITH RANDOMLY ROUGH BOUNDARIES

M. Čermák[a], J. Vohánka[a], I. Ohlídal[a] and D. Franta[a]

[a]Department of Physical Electronics, Faculty of Science, Kotlářská 2, 61137 Brno, Masaryk University, Czech Republic

Theoretical results concerning the optical quantities of multi-layer systems with randomly rough boundaries are presented. The exact approach of the Rayleigh–Rice theory is used to express the formulae describing optical quantities such as the ellipsometric parameters or reflectance. This approach is exact in the sense that it takes into account the propagation of perturbed electromagnetic waves among randomly rough boundaries including all cross-correlation and auto-correlation effects. The restriction to the second order of perturbation, which is the lowest order that gives nonzero corrections to coherent waves (obeying the Snell's law), represents the only approximation used in our calculations.

The presented approach represents the generalization of the exact approach for single layers and the improvement of the approximate approach for multi-layer systems published earlier [1,2].

As an example it is assumed that the layers and the substrate are formed by optically homogeneous and isotropic materials. The layered system consists of $SiO_2/HfO_2/SiO_2$ placed on Si substrate. The numerical calculations are performed for several examples differing in the total thicknesses of the layered systems.

The numerical results based on the exact approach of the Rayleigh–Rice theory are compared with those obtained by the approximate approach.

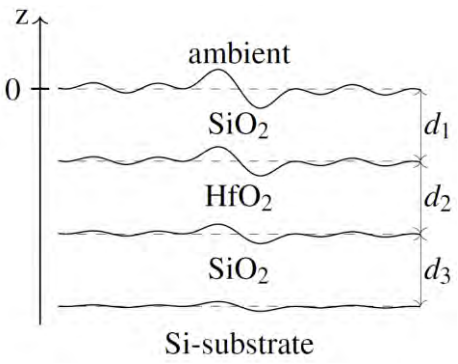

Fig.1. Schematic diagram of three-layer system with four slightly rough boundaries. The dashed lines represent the mean planes of the boundaries. The symbols d_i denote the mean thicknesses of the layers.

Keywords: multilayer systems; rough boundaries; ellipsometric parameters; reflectance

[1] D. Franta, I. Ohlídal, J. Mod. Opt. 45 (1998) 903–934.
[2] D. Franta, I. Ohlídal, D. Nečas, Opt. Express 16 (2008) 7789–7803.

MODELING OF ELLIPSOMETRIC RESPONSE FROM PERIODIC STRUCTURE INCLUDING INCOHERENT PROPAGATION IN THICK LAYERS

Kamil Postava, Premysl Ciompa, Jaromir Pistora

Nanotechnology Centre and IT4Innovations, VSB-Technical University of Ostrava, 17. listopadu 15, 708 33 Ostrava - Poruba, Czech Republic

Recently, spectroscopic ellipsometry and particularly Mueller matrix ellipsometry are widely used for characterization of structures with lateral periodicity as periodic gratings, two-dimensional dot arrays, photonic crystals, periodic metamaterials, or holographic structures. High sensitivity of spectroscopic ellipsometry to a phase change, structure induced anisotropy, and material parameters opens its applications to critical dimension monitoring, characterization of lithographic processes, and overall verification of structure model. The ellipsometric response of the structures with lateral periodicity is typically modeled using matrix formalism and Rigorous Coupled Wave Algorithm (RCWA) [1].

On the other hand, the situation becomes more complex if the structure exhibit incoherent propagation and depolarization in a transparent substrate or a thick layer. Light reflection and transmission from multilayer anisotropic structure consisting of thick layers can be calculated using a recurrent matrix approach described in Ref. [2].

In this paper we propose a general method for modeling of ellipsometric response of a system with lateral periodicity including incoherent propagation in a thick substrate (or thick layers). The approach is based on incoherent summation of transforming coherence matrices in a thick layer for all optical waves diffracting by the system periodicity. The calculation is based on the scattering matrix approach. The complete Mueller matrices of both specular and diffracted beams describing general anisotropy and depolarization are obtained.

Keywords: RCWA; Periodic structures; Thick layers, Incoherent summation

References

[1] M. Neviere and E. Popov, Light propagation in periodic media: Differential theory and design, Marcel Dekker 2003.
[2] K. Postava, T. Yamaguchi, and R. Kantor, Matrix description of coherent and incoherent light reflection and transmission by anisotropic multilayer structures, Appl. Opt. 41, (2002) 2521-2531.

ELLIPSOMETRIC ANALYSIS OF ALIGNED CARBON NANOTUBES

A. Szabó [a], Z. Pápa [b], E. Kecsenovity [a], Z. Toth [c], K. Hernadi [a], J. Budai [b]

[a]University of Szeged, Department of Applied and Environmental Chemistry, H-6720 Szeged, Rerrich Béla tér 1., Hungary
[b]University of Szeged, Department of Optics and Quantum Electronics, H-6720 Szeged, Dóm tér 9., Hungary
[c]University of Szeged, Department of Oral Biology and Experimental Dentistry, H-6720 Szeged, Tisza Lajos krt. 64-66, Hungary

Vertically aligned carbon nanotube (CNT) carpets combined with inorganic semiconductors are expected good prospect in practical applications, especially in photocatalysis. If these devices are in production, a fast and non-invasive characterization method will be required. Ellipsometry is widely used in industry as an in-line monitoring tool; therefore in this study the applicability of ellipsometry for characterizing CNT carpets is investigated.
Although the nanotubes are relatively far from each other meaning that the structure contains a lot of voids and the surface of the CNT carpet has very weak reflectivity, we could perform ellipsometric measurements on the side of the CNT carpet at different CNT orientations (Fig. 1). Due to the aligned growth of individual nanotubes, these structures exhibit strong anisotropy. It is shown based on anisotropic EMA model, that ellipsometric evaluation can provide information about the density and the optical properties of the nanotubes. However, the properties of the individual nanotubes (diameter, wall number) can not be taken into account during conventional ellipsometric modeling. To overcome these limitations, numerical simulations will also be presented [1].

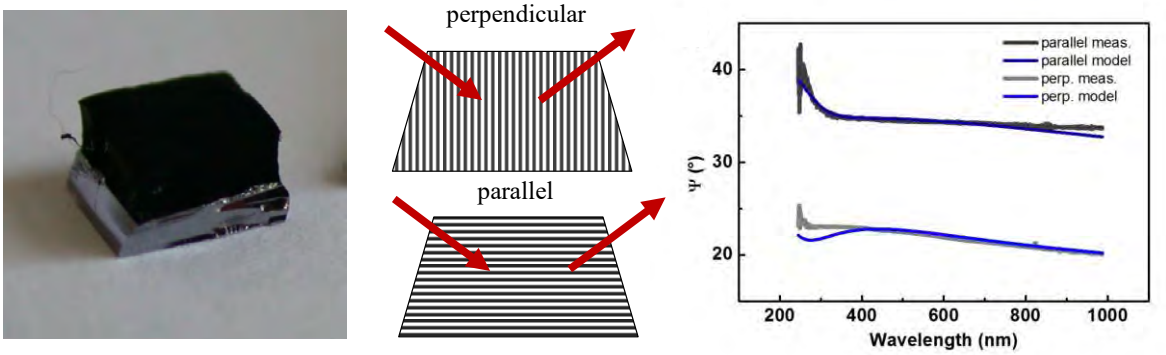

Fig. 1. Image of the investigated CNT carpet, measurement scheme and modeling with anisotropic EMA

Keywords: Vertically aligned CNT; Nanostructures; Anisotropy; Numerical methods

References

[1] Z. Pápa, E. Kecsenovity, J. Csontos, A. Szabó, Z. Toth, J. Budai, Journal of Nanoscience and Nanotechnology, submitted

SPECTROSCOPIC ELLIPSOMETRY ANALYSIS OF SELF-ASSEMBLED AU/PNIPAM CORE-SHELL NANOPARTICLES

Michele Magnozzi[a], Yannic Brasse[b], Tobias Koenig[b,c], Francesco Bisio[d], Andreas Fery[b,c], Maurizio Canepa[a]

[a] OPTMATLAB, Dipartimento di Fisica, via Dodecaneso 33, Università di Genova, Italy
[b] Leibniz-Institut für Polymerforschung Dresden e.V., Institute of Physical Chemistry and Polymer Physics, Hohe Str. 6, 01069 Dresden, Germany
[c] Cluster of Excellence Center for Advancing Electronics Dresden (cfaed), Technische Universität Dresden, 01062 Dresden, Germany
[d] CNR-SPIN, corso Perrone 24, Genova, Italy

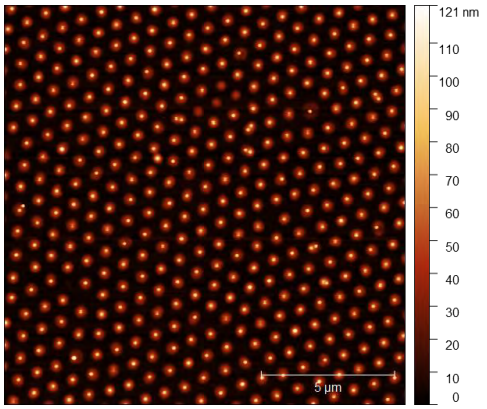

The ordered assembly of nanoparticles is a key challenge in nanoscience. A convenient approach in this regard is to use self-assembly methods, that allow to create ordered arrays of nanoparticles on a relatively large scale (cm^2) and at a low cost [1]. Such platforms of uniformly-spaced, regularly-shaped nanoparticles can find applications from sensoristics to photovoltaics, provided that their optical response is well understood.
Here, we present the spectroscopic ellipsometry (SE) data and analysis of a self-assembled system of core-shell nanoparticles, with gold as a core and the thermoresponsive polymer PNIPAM as a shell. The nanoparticles are arranged on an hexagonal lattice and deposited on glass. The interparticle distance is enough to avoid particle-particle interactions, thus the plasmonic properties of the lattice are dominated by the single-particle response. This Au/PNIPAM system is well suited to investigate the variation in the plasmonic response of Au nanoparticles when surrounded by a dielectric environment (PNIPAM), whose refractive index change with temperature.
For the data analysis and interpretation of the SE spectra, since commonly-used Effective Medium Approximations (EMA) don't provide enough accuracy, we applied a model that explicitly takes into account the key morphological parameters of our system (NPs size, shape, interparticle distance, distance from substrate) [2, 3, 4]. The main spectral feature of the SE data, caused by the plasmonic resonance, is correctly matched by the model. Thus, our approach provides detailed information about the optical properties of this system of nanoparticles, and more in general, it constitutes a flexible tool to investigate 2D arrays of plasmonic particles.

Keywords: core-shell nanoparticles; gold; PNIPAM

References

[1] M. Mueller, C. Kuttner, T. Koenig, V. Tsukruk, S. Foerster, M. Karg, A. Fery, ACS Nano, 8, 2014.
[2] L. Anghinolfi, L. Mattera, M. Canepa, F. Bisio. Phys. Rev. B., 85, 2012
[3] R. Barrera, M. del Castillo-Mussot, G. Monsivais. Phys. Rev. B, 1991
[4] E.S. Kooij, H. Wormeester, E.A.M. Brouwer, et al., Langmuir, 18, 2002

TEMPERATURE-DEPENDENT OPTICAL PROPERTIES OF PLASMONIC NANOSYSTEMS

Michele Magnozzi[a], Marzia Ferrera[a], Francesco Bisio[b], Maurizio Canepa[a]

[a] OPTMATLAB, Dipartimento di Fisica, via Dodecaneso 33, Università di Genova, Genova, Italy
[b] CNR-SPIN, corso Perrone 24, Genova, Italy

The variation of optical properties of metals with temperature is becoming an increasingly relevant issue in fields like thermoplasmonics, particle-mediated hyperthermia or heat transfer at the nanoscale. Indeed, when light-induced heating of metallic nanoparticles is performed, the systems' properties are modified, dramatically altering the heating process itself.
Whereas temperature dependencies of bulk materials are relatively well investigated, much less is known about the same phenomenon for metallic nanoparticles, where surface effects and finite-size constraints may contribute to strongly affect the temperature-dependent system response. For example, it is known that for thin Au films there is an increase of more than 100% of the imaginary part of the Au permittivity going from room temperature to 500 °C [1]. For particles, it could be in principle significantly different.
In typical laser-heating experiments on nanoparticle systems, the actual system temperature at the nanoscale is often determined *ex-post* by means of simulations that, at their best, employ the temperature-dependent permittivity of the corresponding bulk systems. Here we attempt to reverse this paradigm by measuring the optical response of a system of nanoparticles heated at a well-defined temperature, and retrieving the actual temperature-dependent system response.
We present a spectroscopic-ellipsometry study of 2D arrays of gold nanoparticles [2] at variable temperatures in the 245-1700 nm spectral range and in the 25 °C to 350 °C temperature interval. The ellipsometric spectra were acquired in-situ, under high-vacuum conditions, employing a custom-built roll-on/roll-off mini-vacuum chamber fitted to a J.A. Woollam M-2000 ellipsometer [3]. Using a dedicated effective medium approximation developed for this kind of systems [2], we are able to reproduce the SE spectra at different temperatures, noticing that contributions from surface softening or melting may play a key role as the temperature is increased.

Keywords: gold nanoparticles; in situ ellipsometry

References

[1] H. Reddy, U. Guler, A. Kildishev, A. Boltasseva, V. Shalaev. Opt. Mat. Express, 6, 2016
[2] L. Anghinolfi, R. Moroni, L. Mattera, M. Canepa, F. Bisio. J. Phys. Chem. C, 115, 2011
[3] M. Magnozzi, F. Bisio, M. Canepa, Appl. Surf. Sci., 421, 2017

OPTICAL CHARACTERISATION OF ELECTRONIC CONFINEMENT IN THIN METALLIC FILMS GROWN ON 1-D NANOSTRUCTURES

S. Chandola[a], E. Speiser[a] and N. Esser[a]

[a]Leibniz-Institut für Analytische Wissenschaften - ISAS - e.V.,
Schwarzschildstraße 8, 12489 Berlin, Germany

The quasi one-dimensional (1-D) Si(111)-(4x1)-In surface was used as an atomic scale template for the growth of thin epitaxial Ag films with thicknesses of up to 15 monolayers (ML). The electronic properties of the thin Ag films were studied *in-situ* with Reflection Anisotropy Spectroscopy (RAS) and Infrared Spectroscopic Ellipsometry in the spectral range from 0.1 eV to 6 eV, which covers both electronic single particle excitations (electronic band structure) and collective electronic excitations (ac-conductivity). The stability of the films on exposure to ambient pressures was investigated by *ex-situ* optical measurements. Such thin Ag films, up to approximately 30 ML in thickness, have previously been shown to have stripe structures with a periodicity equal to that of the Si(111)-(4x1)-In reconstruction [1]. The structural anisotropy of the striped Ag film has also been shown to lead to quasi-one-dimensional electronic states by photoemission spectroscopy [2]. The measurements reported here reveal a pronounced optical anisotropy associated with the Ag structures in the infrared spectral range. The optical spectra are analysed and the layer properties are discussed in terms of Drude and interband contributions.

Keywords: Optics; Nanostructures; One-dimensional; Anisotropy

References

[1] T. Uchihashi, C. Ohbuchi, S. Tsukamoto and T. Nakayama, Phys. Rev. Lett. **96** (2006)136104.
[2] N. Nagamura, R. Hobara, T. Uetake, T. Hirahara, M. Ogawa, T. Okuda, K. He, P.Moras, P.M. Sheverdyaeva, C. Carbone, K. Kobayashi, I. Matsuda and S. Hasegawa, Phys. Rev. B **89** (2014) 125415.

Imaging Ellipsometry as a Tool for the Characterization of 2D-Materials on various Substrates

S. Funke[a], A. Matkovic[b], P. Braeuninger-Weimer[c], P. H. Thiesen[a], S. Hoffmann[c], A. Diebold[d], U. Wurstbauer[e]

[a]Accurion GmbH, Stresemannstraße 30, Göttingen, Germany
[b]Centre for Solid State Physics and New Materials, Institute of Physics, University of Belgrade, Pregrevica 118, 11080 Belgrade, Serbia
[c]Department of Engineering, University of Cambridge, Cambridge CB3 0FA, United Kingdom
[d]College of Nanoscale Science and Engineering, State University of New York, 253 Fuller Road, Albany, New York 12203
[e]Walter Schottky Institute and Physics Department, TU München, Am Coulombwall, Garching, Germany

Imaging ellipsometry (IE) allows to measure ellipsometry on microstructured samples with a lateral ellipsometric resolution down to 1 µm. The rising field of research on 2D materials demands for techniques that enable the measurements on micron-sized flakes of 2D materials. These 2D materials often show superior behavior e.g. in optical response when monolayers are compared to multilayers. By stacking up different 2D materials, promising applications are expected. Fig. 1. shows a hetero-structure of WSe_2 and MoS_2. The poster presentation will show the IE measurements on the regions that can be seen on the SiO_2/Si substrate. In addition, the flakesearch algorithm is presented as a tool for the fast and accurate localization of flakes [1]. Detailed investigations of MoS2 on a thin, transparent sapphire substrate show the shift in the bandgap [2]. Measurements of Graphene directly on Copper-foil show the capability towards the use of imaging ellipsometry in quality control. To cover the anisotropic 2D-materials imaging Mueller-Matrix measurements are done. The in-plane dispersions for a flake of Black-phosphorous are shown.

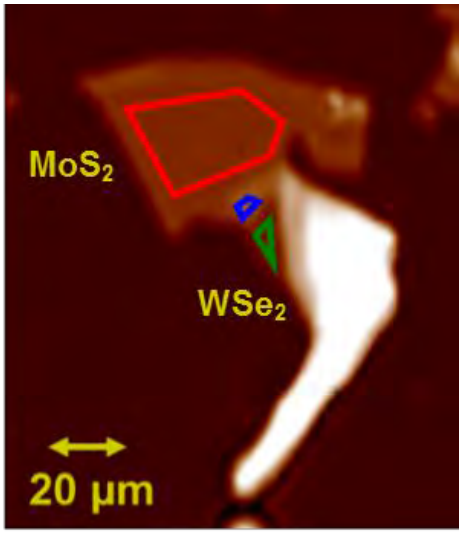

Fig. 1. Imaging ellipsometry of hetero-structure of MoS_2 and WSe_2.

Summing up, the poster presentation will show the capabilities of imaging ellipsometry in the field of 2D materials. Flakes of 2D materials can be found, investigated and orientated on various, including thin, transparent, substrates.

Keywords: Imaging Ellipsometry; Imaging Mueller Matrix, 2D Materials

References

[1] S. Funke, U. Wurstbauer, B. Miller, A. Matković, A. Green, A. Diebold, C. Röling, and P. H. Thiesen., Applied Surface Science, (2017).

[2] S. Funke, B. Miller, E. Parzinger, P. Thiesen, A. W. Holleitner, and U. Wurstbauer, J. Phys.: Condens. Matter 28, 385301 (2016).

Imaging Ellipsometry with con-local Raman Spectroscopy on 2D Transition Metal Dichalcogenides with Different Layer Thicknesses

Constance Schmidt, Mahfujur Rahaman, and Dietrich R. T. Zahn

Semiconductor Physics, Chemnitz University of Technology, 09107 Chemnitz, Germany

2D transition metal dichalcogenides are atomically thin semiconductors of the type MX_2 with M representing the transition metal, in our case Mo or W, and X stands for the chalcogen, here Selenium. Due to the direct bandgap of $MoSe_2$ and WSe_2 these materials can be used in electronic and optoelectronic applications.

2D transition metal dichalcogenide layers were prepared by mechanical exfoliation. As a substrate we use Si wafer pieces with native oxide. The layer thickness ranges from monolayer to bulk.

Using an Accurion nanofilm_ep4 setup, we performed imaging ellipsometry. For the measurements we used two different objectives: 12.5 x with an operation range from 250 – 1700 nm and 50 x, which operates in the visible spectral range. An optical image of $MoSe_2$ flakes taken with the nanofilm_ep4 can be seen in Figure 1. Ψ- and Δ-maps of a $MoSe_2$ flake are shown in Figure 2, taken at a wavelength of 435 nm. By choosing different regions of interest (ROIs) we can investigate different parts with different thicknesses of the transition metal dichalcogenide.

Besides the optical properties obtained from the analysis of the ellipsometry spectra we also investigate the samples with Raman spectroscopy (532 nm). For this purpose a Horiba Raman head was mounted in the ellipsometer setup, so that ellipsometry and Raman spectroscopy can be measured con-locally.

We determine the dielectric function of the 2D transition metal dichalcogenide by using imaging ellipsometry with the thickness of the different flakes determined by modeling the data obtained and confirmed by the con-local Raman spectra.

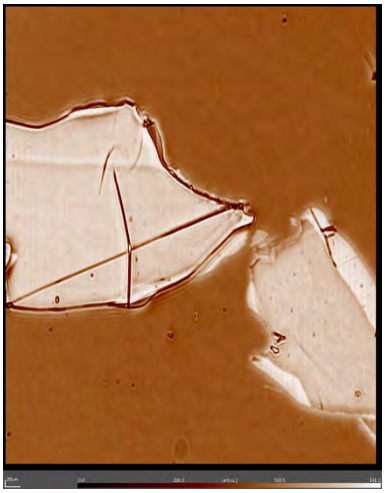

Figure 1 Optical image of $MoSe_2$ flakes with different thicknesses taken with the Accurion nanofilm_ep4

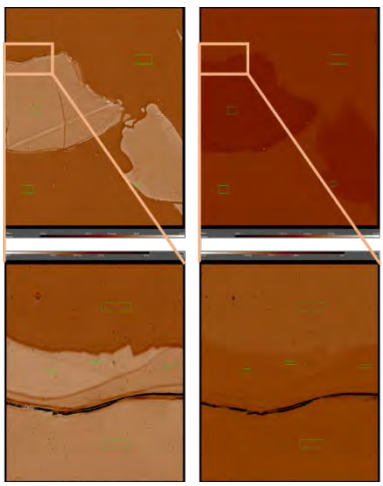

Figure 2 Ellipsometry maps of $MoSe_2$ flakes. The marked green areas show the ROIs: a) Ψ-map with 12.5 x objective, b) Δ-map with 12.5 x objective; c) Ψ-map map with 50 x objective, and c) Δ- map with 50 x objective taken at 435 nm.

Keywords: Imaging ellipsometry, spectroscopic ellipsomtry, 2D Transition Metal Dichalcogenides, Raman spectroscopy

The Influence of Field Effect Doping on the Optical Properties of Bilayer Graphene

S. Okano[a], C. Günther[a], A. Nishimura[b], O. D. Gordan[a], V. Dzhagan[a], K. Ikushima[b], and D. R. T. Zahn[a]

[a]Semiconductor Physics, Chemnitz University of Technology, D-09107 Chemnitz, Germany
[b]Department of Applied Physics, Tokyo University of Agriculture and Technology, 2-24-16 Nakacho, Koganei, Tokyo 184-8588, Japan

Graphene is currently one of the most intensively investigated materials due to its unique properties like linear dispersion at the K-point of the Brillouin zone and the presence of 2D electron system [1]. The carrier concentration of graphene can be controlled by field effect doping [1] leading to changes in the optical reflection in the mid-infrared range by applying a back gate voltage as demonstrated recently [2]. We show here that this effect which is important from an application point of view also markedly affects the visible range. We thus demonstrate the tuning of the optical properties of bilayer graphene on a Si/SiO_2 substrate in both the visible and near-infrared range by applying a back gate voltage. The bilayer graphene sample was prepared by mechanical exfoliation and transferred onto a highly n-doped Si substrate covered with a 300 nm thick SiO_2 layer. The electrodes consisting of a 10 nm NiCr / 30nm Au bilayer were prepared by electron beam lithography. The measurement of the dielectric function was performed by a microscopic imaging ellipsometer nanofilm_ep4 (Accurion GmbH) under ambient conditions. The experimental geometry is shown in Figure 1(a). The dielectric function of graphene was modelled using an anisotropic model including one Lorentzian oscillator, corresponding to a transition at the Γ point, and the Drude function accounting for the free carrier contributions. The evolution of the real and imaginary parts of the in-plane dielectric function of bilayer graphene as a function of applied back gate voltage is shown in Figure 1(b). The changes in the carrier concentration and the related changes in optical reflectivity and Drude model in 2D system will be discussed.

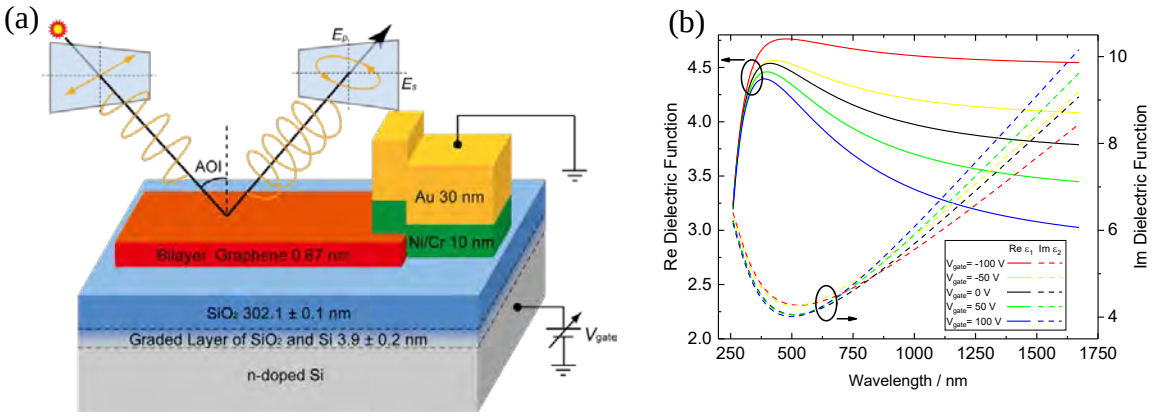

Figure 1: (a) Sketch of the experimental geometry. (b) Evolution of the real and imaginary parts of the in-plane dielectric function of the bilayer graphene as a function of back gate voltage.

[1] K. S. Novoselov, *et al. Nature* **438**, 197-200 (2005).

[2] F. Wang, *et al. Science* **320**, 206 (2008).

PHONON ANOMALIES IN STRAINED $SrMnO_3$ FILMS

P. Marsik[a], R. de Andres Prada[a], F. Lyzwa[a] and C. Bernhard[a]

[a]Physics Department, Chemin du Musee 3, 1700 Fribourg,
University of Fribourg, Switzerland

Using Fourier-transformed far-infrared (FTIR) and Time Domain – Terahertz (TD-THz) ellipsometry, we investigated epitaxial thin films of $SrMnO_3$ grown by pulsed laser deposition (PLD) on various substrates.

$SrMnO_3$ in bulk is a cubic perovskite with antiferromagnetic ordering under T_N=~230-260 K. Under epitaxial strain it is possible to stabilize ferroelectric order caused by off-center displacement of the central magnetic Mn^{4+} ion [1]. Such multiferroic state is expected to show large magnetoelectric coupling. The strong interaction between the spin ordering and lattice phonons has been demonstrated on bulk $Sr_{1-x}Ba_xMnO_3$ (x = 0-0.3) [2,3].

We will present temperature dependent, 10 K – 400 K, THz-FIR optical response of 30 nm $SrMnO_3$ films with varying epitaxial strain driven by lattice mismatch of $SrMnO_3$ with respect to substrate. The substrates were chosen accordingly: cubic $LaAlO_3$ causing small compressive strain (-0.3%), tetragonal $SrLaGaO_4$ (001) with moderate 1.1% tensile strain and cubic LSAT with tensile strain of 1.8% that should be sufficient for the ferroelectric instability [4].

In our films we observe the three characteristic phonons of cubic perovskite, with dominant lowest-energy mode that shows softening with increasing strain and anomaly at temperature of the antiferromagnetic transition.

Keywords: THz ellipsometry; Ultrathin films; Ferroelectrics

References

[1] J.H. Lee and K.M. Rabe, Phys. Rev. Lett. **104**, 207204 (2010).
[2] S. Kamba *et al*., Phys. Rev. B **89**, 064308 (2014).
[3] H. Sakai *et al.*, Phys. Rev. B **86**, 104407 (2012).
[4] C. Becher *et al*., Naure Nanotechnology **10** (2015).

DIELECTRIC FUNCTION AND SINGULAR OPTIC AXES OF KTP

C. Sturm and M. Grundmann

Felix-Bloch-Institut für Festkörperphysik, Linnéstr. 5, Universität Leipzig, Germany

Potassium titanyl phosphate ($KTiOPO_4$, KTP) is an optically biaxial material which is widely used in applications such as for second harmonic generation (SHG) in general and in diode pumped lasers. Although the components of the dielectric tensor in the transparent spectral range are well known there are only few reports for the absorption spectral range, limited to the onset of the absorption.

Here we present the full dielectric tensor in the spectral range from 0.5eV up to 8.4eV. From a line shape analysis of the dielectric tensor components, the properties of the electronic transitions were deduced and the fundamental band gap energy was determined to 4.2eV for dipoles polarized along the *c*-axis. For the transitions polarized along the *a* and *b* direction, the gaps are blue-shifted by 0.70eV and 0.05eV, respectively.

Based on the determined dielectric tensor, the orientation and dispersion of the (singular) optic axes are investigated (Fig.1). As soon as the absorption sets in at an energy of about 3.5eV, both optic axes split into two singular axes [1] and thus, KTP can be considered as optically four-axial in this spectral range. Along such a singular optic axis, either a left or right-hand circular polarized wave can propagate without changing its polarization state. For energies of about 5.55 eV, 6.54 eV, 7.39 eV and 8.22 eV, KTP exhibits a biaxial behaviour since two of the singular optic axes coincide with each other forming a classical optic axis.

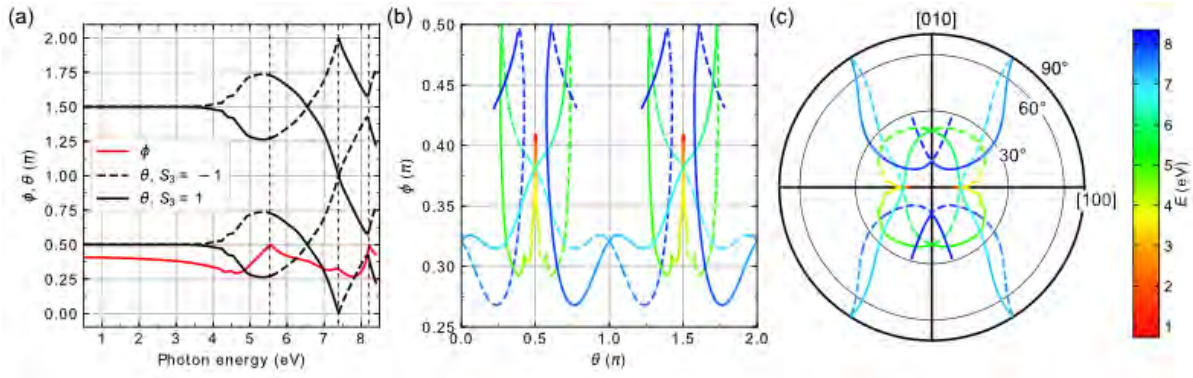

Fig.1. (a) The polar (f) and azimuthal angle (q) of the (singular) optic axes as a function of the energy. The vertical dashed lines indicate the energetic position of the classical optic axes in the absorption spectral range. (b,c) The orientation of the singular optic axis by (b) means of the polar and azimuthal angle ϕ and θ, i.e. the unit vector of the direction is given by $(a, b, c)^T = (\cos\phi, \cos\theta \sin\phi, \sin\theta \sin\phi)^T$ and (c) in the stereographic projection from the upper hemisphere onto the (a,b) plane.

Keywords: singular optic axes; dielectric function; optical anisotropy

References

[1] C. Sturm and M. Grundmann, Phys. Rev. A 93 (2016) 053839.

MUELLER MATRIX ELLIPSOMETRY INVESTIGATIONS OF INSULATOR METAL TRANSITION IN VO_2

I. Voloshenko[a], B. Gompf[a], A. Berrier[a], G.Schnoering[a] and M. Dressel[a]

[a]1st Physikalisches Institute, Pfaffenwaldring 57, Universität Stuttgart, Germany

The nature of insulator to metal transition in VO_2, after more than half a century of investigations still remains under debate, though the convenient temperature of the transition attracts people to utilize it in many applications, especially in the field of plasmonics, as for example all-optical modulation or sensing. Thus there is a need for a precise prediction of temperature dependent optical properties in this material.

In this study, we concentrate on the macroscopic model which would describe the temperature dependence of optical constant over the transition in thin film VO2. We confirm the Bruggeman effective medium approximation [1] as a proper model describing the temperature dependence of optical constants of the material in visible and near infrared range even around the transition temperature. Using depolarization factor, which is related to the shape of the inclusions, as a free parameter, we obtain an improvement in overall mean square error of the model.

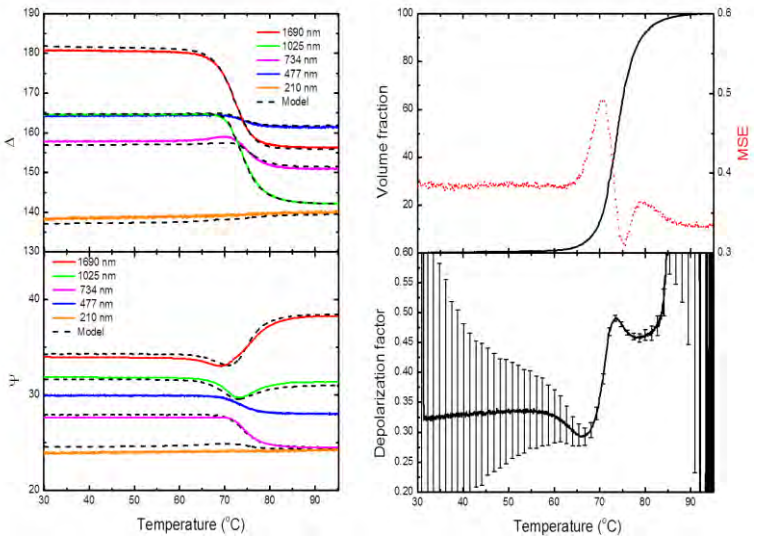

Fig. 1: Result of the BEMA

In addition, we observe that the depolarization of light in the sample is also temperature dependent. Moreover, it is linked to the observed transition and correlates with the filling fraction of metallic phase derived from the BEMA model. Thus it is an interesting observable to investigate the transition in terms of disorder induced by shape and size in the granular thin films.

Keywords: Insulator-metal transition; Ellipsometry; Effective medium approximation, Depolarization

References

[1]J. Rozen et al., Applied physics letters (2006), **88**, 081902.

MUELLER MATRIX ANOMALY NEAR THE CURIE TEMPERATURE OF NI

F. Abadizaman, S. Zollner

Department of Physics, New Mexico State University, Las Cruces, NM, USA

The temperature dependence of the optical constants of magnetized bulk Ni and Ni(111) films demonstrates an anomaly near the Curie temperature (T_c=627 K). We investigate this anomaly by taking measurements of the temperature dependent Mueller Matrix (MM). Using spectroscopic ellipsometry at an energy of 1.97 eV, the MM measurement was taken as a series of four runs, going up and down from 400 K to 800 K. The MM data of magnetized Ni reveal very small changes in the anisotropic portion of the MM compared to the windows effect while passing T_c. However, very large changes in the isotropic MM elements were found.

After the first series of measurements, the sample was magnetized again and went through the same series of four runs. However, the second series does not demonstrate any changes near T_c. The authors believe that the large change in the first series of measurements near T_c indicates a relation between magnetization and the morphology of the sample, yet the second series contradicts the statement.

Furthermore, powder XRD data of the sample before and after the measurements do not show any observable variation of the out of plane grain sizes.

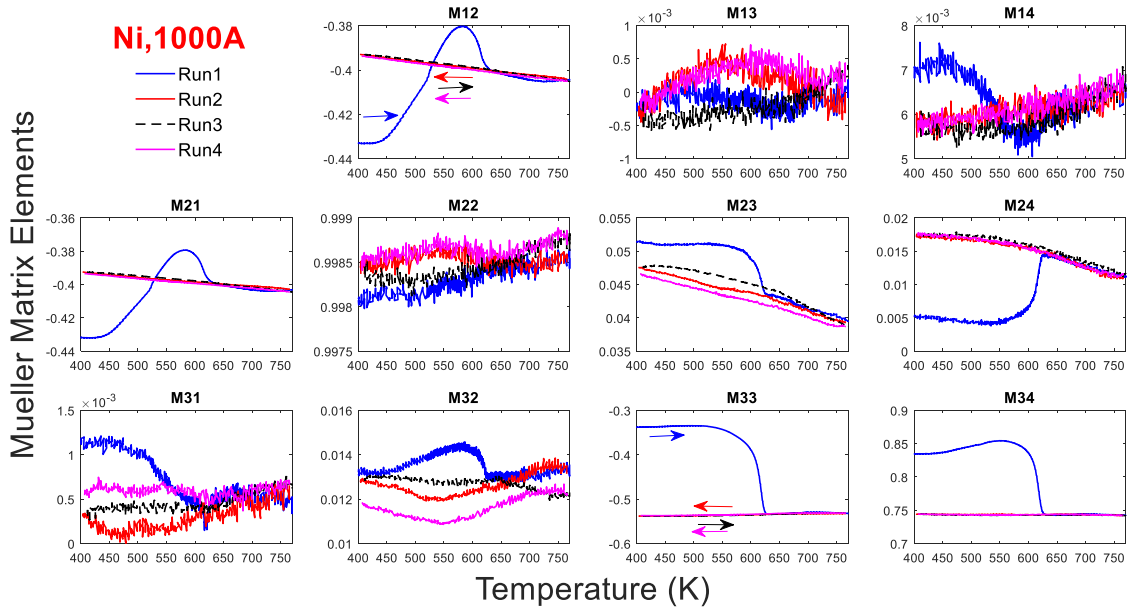

Fig. 1. Mueller Matrix measurements of a 1000 Å thick Ni film on thick SiO_2 at 1.97 eV as function of temperature.

DIFFERENT PARAMETERIZATION OF THE TIN OPTICAL PROPERTIES FOR SPECTROSCOPIC ELLIPSOMETRY–X-RAY REFLECTOMETRY COMPARISON

Dmitriy V. Likhachev

GLOBALFOUNDRIES Dresden Module One LLC & Co. KG,
Wilschdorfer Landstr.101, D-01109 Dresden, Germany

Typical dispersion model used for description of the titanium nitride (TiN) dielectric function in the optical range is a combination of the Drude model (free electrons at energy up to the plasma energy) with a dual Lorentz oscillator model (bound electrons at higher energy), sometimes called a “D2L model” [1,2]. Also, some researchers describe the TiN dielectric function using, say, D1L model with single Lorentz oscillator [3] or D*n*L model with the number of Lorentz oscillators $n > 2$ to cover a very broad spectral range [4,5]. There are also other physics-based optical dispersion parameterizations which can be applied to describe the TiN dielectric function.

In this study, the thickness-dependent TiN optical properties were represented by the multiple-oscillator Drude–Lorentz (DL), Forouhi–Bloomer (FB) and Lorentz optical dispersions with different numbers of parameters. The dielectric function of thin TiN films with intermediate behavior can be appropriately expressed in terms of 9 to 13 model parameters.

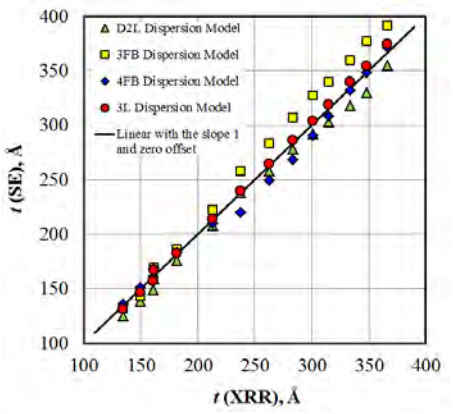

Fig. 1. Comparisons of film thickness using SE and XRR measurements

Using X-ray reflectometry (XRR) as a reference technique and taking into account surface roughness on the TiN films, it has been shown that three-term Lorentz (3L) model provides not only the best fit quality for the nominal thicknesses ranging from 125 Å to 350 Å but also an extremely good correlation between the thickness values obtained by spectroscopic ellipsometry (SE) and XRR and the following linear equation was established between the thickness measurements: t_{SE}(Å) = 1.038×t_{XRR}(Å) – 7.532 Å with R^2 = 0.9994 (see Fig. 1). Use of other models results in the worst correlation between XRR and SE measurements.

Thus, an appropriate modeling of the film’s optical properties is one of the factors needed to be taken into account to establish well-grounded and credible SE and XRR correlation.

Keywords: Titanium nitride; Thin films; Optical modeling; Dielectric function; Spectroscopic ellipsometry; X-ray reflectometry

References

[1] K. Postava, M. Aoyama, T. Yamaguchi, Appl. Surf. Sci. 175–176 (2001) 270–275.
[2] P. Patsalas, S. Logothetidis, J. Appl. Phys. 90 (2001) 4725–4734.
[3] J. Humlíček, A. Nebojsa, J. Hora, M. Stránský, J. Spousta, T. Šikola, Thin Solid Films 332 (1998) 25–29.
[4] P.E. Schmid, M. Sato Sunaga, F. Levy, J. Vac. Sci. Technol. A 16 (1998) 2870–2875.
[5] N. White, A.L. Campbell, J.T. Grant, R. Pachter, K. Eyink, R. Jakubiak, G. Martinez, C.V. Ramana, Appl. Surf. Sci. 292 (2014) 74–85.

THE INFLUENCE OF DEPOSITION RATE ON MICROSTRUCTURE AND OPTICAL PROPERTIES OF THE Sn THIN LAYERS

T. Rerek[a], L. Skowronski[b], R. Szczesny[c], M.K. Naparty[b], A. Wronkowski[b] and B.Derkowska-Zielinska[a]

[a]Institute of Physics, Faculty of Physics, Astronomy and Informatics, Grudziadzka 5, 87-100 Torun, Nicolaus Copernicus University in Torun, Poland
[b]Institute of Mathematics and Physics, Kaliskiego 7, 85-796 Bydgoszcz, UTP University of Science and Technology, Poland
[c]Faculty of Chemistry, Gagarina 7, 87-100 Torun, Nicolaus Copernicus University in Torun, Poland

The 30 nm - tin (Sn) layers were deposited on the Al_2O_3 coated Si substrates using the physical vapor deposition (PVD) method. It was noticed that the microstructure and optical properties of thin films strongly depend on the deposition conditions (e.g. temperature, deposition rate). Therefore, the studied layers were prepared at five different deposition rates (0.05 A/s, 0.15 A/s, 0.50 A/s, 2.50 A/s, 5.00 A/s) at room temperature.

The AFM results show that the deposition rate has a major influence on the surface topography obtained of the Sn films. It was observed that the Sn layers prepared at deposition rates 2.50 Å/s and 5.00 Å/s are definitely less rough than Sn films grown at the deposition rates lower than 0.50 Å/s.

Changes in the microstructure of the Sn layer affect changes in their optical properties. This influence is clearly visible in the determined dielectric functions of the Sn films, which exhibit the largest differences for photon energies lower than 2.5 eV (see Fig.1.). This fact is associated with varied formation of metallic layers (their microstructure), thereby with different response of free electrons on the incident light and thus with different contribution of the Drude term to the complex dielectric function of the Sn layers.

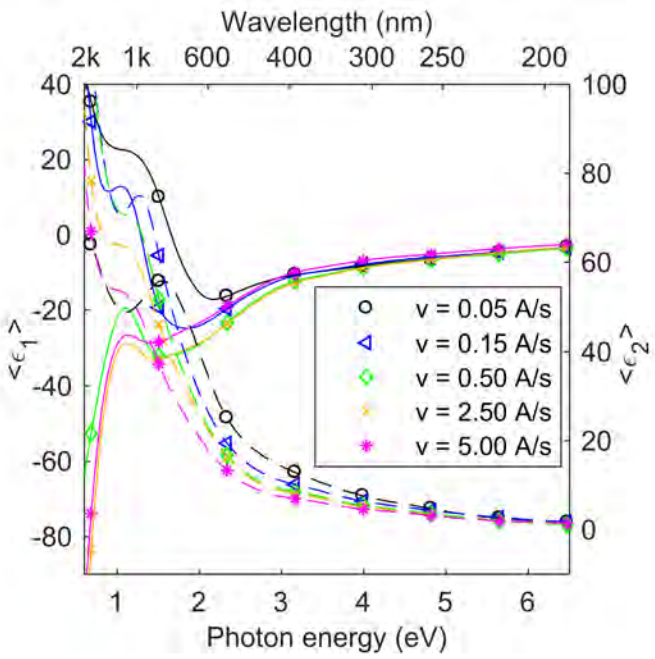

Fig.1. Real part $< \varepsilon_1 >$ (solid line) and imaginary part $<\varepsilon_2>$ (dashed line) of the effective complex dielectric function of Sn films.

Keywords: Sn thin layers; Microstructure; Optical properties

TEMPERATURE DEPENDENCE OF ZINC Δ_{101} ENERGY GAP

S. Tumėnas and V. Karpus

Semiconductor Optics Laboratory, LT-01108 Vilnius,
Center for Physical Sciences and Technology, Lithuania

We present experimental results of spectroscopic ellipsometry (SE) and modulation spectroscopy study of the (001) single-crystal zinc in the 10-500 K temperature range.

The clean (001) optical surfaces of Zn samples were disclosed by cleaving crystals. The SE measurements, in the 0.73–6 eV spectral range, were performed with a dual rotating compensators ellipsometer RC2 (J. A. Woollam Co., Inc.) equipped with the standard heat stage HTC-100 (incident angle of 70°) for high-temperature measurements and the closed-cycle cryostat CTI-Cryogenics (incident angle of 45°) for low-temperature measurements. The dielectric functions of zinc were determined from SE data by an iteration procedure [1]. A theoretical analysis of the obtained dielectric function spectra allowed for a determination of the temperature dependence of the interband optical transitions across the Δ_{101} energy gap. Alternatively, to follow the low-temperature dependence of the gap, the λ-modulated reflectance measurements were carried out, making use of a Δ_{101}-related minimum of Zn reflectance spectrum (at $\boldsymbol{E} \perp \boldsymbol{c}$).

The temperature dependence of the zinc energy gap Δ_{101} (presented by dots in Fig. 1) is similar to that of band-gaps of semiconductors. In the present work we succeeded to show that the *T*-dependence of Zn Δ_{101}-gap is solely due to the Debye–Waller factor. Indeed, making use of literature data [2] for Zn mean-square displacements and having calculated the Debye–Waller factor for the $\boldsymbol{g}_{101}$ reciprocal lattice vector, we obtained an excellent agreement between the experimental $\Delta_{101}(T)$ dependence and the temperature dependence of the Debye–Waller factor (Fig. 1).

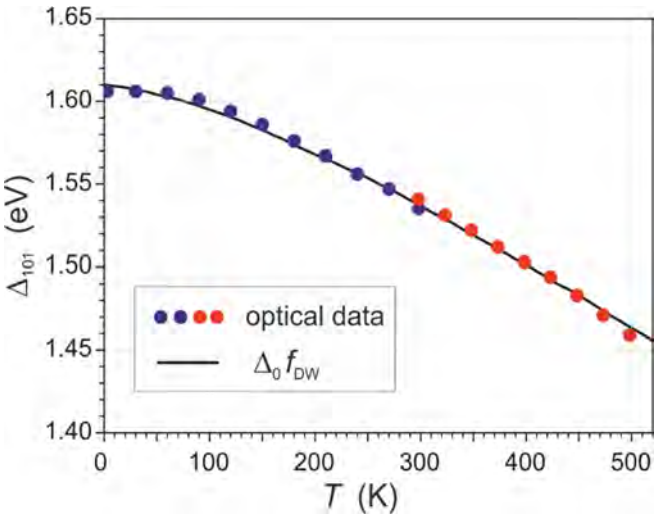

Fig. 1 Temperature dependence of the Zn Δ_{101} energy gap. Dots present experimental optical data and curve corresponds to *T*-dependence of the Debye–Waller factor f_{DW} (at Δ_0 = 1.63 eV).

The present study has been supported by the Research Council of Lithuania (grant MIP-081/2012).

Keywords: Zinc; Spectroscopic Ellipsometry

References

[1] V. Karpus, S. Tumėnas, A. Eikevičius, and H. Arwin, Phys. Status Solidi B 253 (2016) 419.
[2] E.F. Skelton and J.L. Katz, Phys. Rev. 171 (1968) 801.

OPTICAL CHARACTERIZATION OF NON-STOICHIOMETRIC SILICON NITRIDE FILMS PREPARED BY MAGNETRON SPUTTERING

J. Vohánka[a], I. Ohlídal[a], P. Vašina[a], J. Ženíšek[a], M. Čermák[a] and D. Franta[a]

[a]Department of Physical Electronics, Faculty of Science, Kotlářská 2, 61137 Brno, Masaryk University, Czech Republic

The optical characterization of several samples of non-stoichiometric silicon-nitride films deposited on double-side polished silicon single crystal wafers is performed. The silicon nitride films are prepared by magnetron sputtering. By changing the amount of nitrogen used during the deposition it is possible to prepare silicon nitride films with different stoichiometric ratio. Our main goal is to determine how the optical constants of the silicon nitride films depend on the deposition conditions (e.g. on the nitrogen flow rate). The deposition rate can also be estimated from the determined thicknesses of layers and deposition times.

The optical characterization is based on simultaneous processing of ellipsometric data measured in the spectral range 0.6–6.5 eV for five incidence angles within the range 55–75° and reflectometric data measured in the spectral range 0.7–6.5 eV at near normal angle of incidence.

The dielectric response of the non-stoichiometric silicon nitride is described by a simple three-parametric model of interband transitions. In this model, the imaginary part of the dielectric function is given as

$$\varepsilon_{\mathrm{i}}(\mathrm{E}) = \frac{\mathrm{N}\left(\mathrm{E}-\mathrm{E_g}\right)^2(\mathrm{E}-\mathrm{E_h})^2}{\mathrm{CE}^2} \text{ for } \mathrm{E_g} < E < \mathrm{E_h}\ ,$$

where the symbols $\mathrm{E_g}$ and $\mathrm{E_h}$ denote the minimum and maximum energy of interband transitions, the symbol N determines the strength of these transitions. Outside of the interval $\mathrm{E_g}<\mathrm{E}<\mathrm{E_h}$ we define $\varepsilon_{\mathrm{i}}(\mathrm{E})=0$. The normalization constant C is calculated using the sum rule. The real part of the dielectric function is calculated from the imaginary part using the Kramers–Kronig relation.

Since the films are placed on top of double-side polished silicon wafers the depolarization due to the back side reflections must be taken into account in the infrared region, where the silicon wafer is transparent. The possibility of the presence of defects influencing the optical quantities of the silicon nitride film such as the random roughness of the upper boundary, overlayer, slight inhomogeneity (refractive index profile) is also investigated.

As the results achieved the dependencies of the optical constants and dispersion parameters of the characterized non-stoichiometric silicon nitride films on quantities describing the technological conditions such as the nitrogen flow rate are presented. An attempt at interpretation of these results is also made.

Keywords: Ellipsometry; Reflectometry; Silicon nitride films; Optical characterization

OPTICAL CHARACTERIZATION OF HYDROGENATED AMORPHOUS SILICON-CARBON FILMS IN A WIDE SPECTRAL RANGE

Daniel Franta[a], Martin Bránecký[b], Martin Čermák[a], Pavel Franta[a], Jiří Vohánka[a], Ivan Ohlídal[a], Vladimír Čech[b]

[a]Department of Physical Electronics, Faculty of Science, Masaryk University, Kotlářská 2, 61137 Brno, Czechia
[b]Institute of Materials Science, Faculty of Chemistry, Brno University of Technology, Purkyňova 118, 61200 Brno, Czechia

The optical characterization of hydrogenated amorphous silicon-carbon (a-SiC:H) films has been performed in the wide spectral range from far IR to vacuum UV.

The films were prepared from tetravinylsilane on double-sided polished float-zone silicon wafers (100) by plasma-enhanced chemical vapor deposition process operated in a pulsed mode. Dielectric response of the a-SiC:H films were described by Universal dispersion model containing several contributions: excitations of valence electrons, Urbach tail, absorption on localized states and phonons.

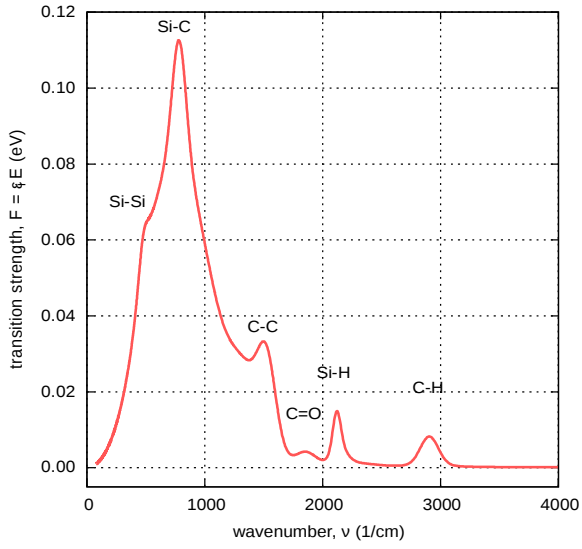

Fig.1: Transition strength function of a-SiC:H in IR region modeled using Voigt peaks.

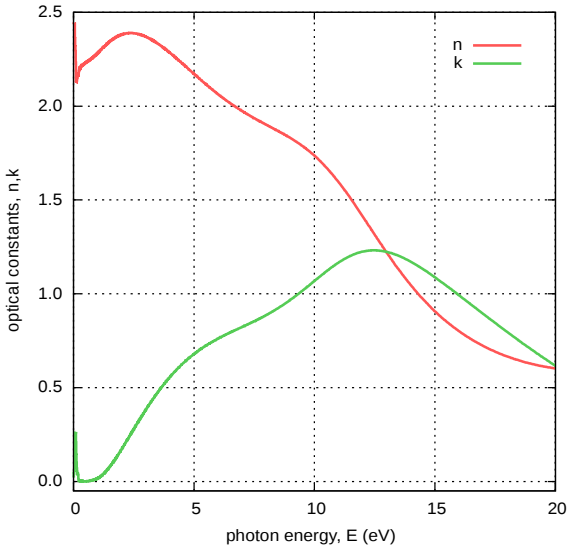

Fig.2: Optical constants of a-SiC:H in UV region described by Campi-Coriasso dispersion model.

Five models combining the Tauc law with Lorentz functions were tested for valence electron excitations. The Urbach tail was described by recently developed model. Phonon excitations were described using broadened discrete spectrum. The Voigt distribution function for broadening was compared with the linear combination of Gaussian and Lorentzian distribution functions. Films have exhibited a refractive index profile, roughness, and oxide transition or overlayers. All these effects were taken into account in the interpretation of experimental spectrophotometric and ellipsometric data.

Keywords: Silicon-carbon films; Universal dispersion model; Dielectric response

Dielectric functions of titanium in the regime of the limited light penetration

L. Skowronski, A. Wronkowski, M.K. Naparty, W. Wachowiak, A.A. Wronkowska

Institute of Mathematics and Physics, UTP University of Science and Technology, Kaliskiego 7, 85-796 Bydgoszcz, Poland

Titanium films with a thickness in the range from about 10 nm to 2.1 um were deposited using a gas impulse injection magnetron sputtering technique [1,2] on the Bk7 glass plates (1 mm thick).

To determine the complex dielectric function of Ti coatings, the three-phase (or four-phase - for the thinnest layers) optical model was used: ambient / rough layer / Ti layer / (Bk7 glass). To determine optical constants of the rough layer, the three component Effective Medium Approximation (EMA) model was used as a linear combination of optical properties of void, native titanium dioxide and titanium (the assumed volume fraction of each medium was 1/3). The optical response of titanium films was parameterized using the semi-classical Drude-Lorentz model of dielectric function.

The Drude parameters $\hbar\omega_p$ and $\hbar\Gamma$ are associated with the concentration and scattering frequency of free electrons, respectively. The obtained results show gradual decrease in the free-carrier damping from 2.4 eV (d_{Ti}=12 nm) to 0.98 eV (d_{Ti} =2100 nm). Based on the values of Drude parameters the mean relaxation time of conduction (τ) and the optical resistivity (ρ_{opt}) were calculated. The mean relaxation time increases with the increase of the titanium layer thickness (from 0.27 fs to 0.67 fs). However the plasma energy exhibits the other trend: increases from 6.48 eV (d_{Ti} =12 nm) to ~8 eV (d_{Ti} =50 nm) and then decreases to 5.4 eV (d_{Ti} =2100 nm). This behavior of Drude parameters directly affects the optical resistivity of titanium films. The lowest value of optical resistivity was observed for Ti films of thickness 50-100 nm (about 200 $\mu\Omega\mathrm{cm}$). The dc- (ρ_{dc}) and optical resistivity take similar values for thinner Ti films, however for thicker coatings significant discrepancies can be observed.

The behavior of the plasma energy, optical resistivity and discrepancies between ρ_{opt} and ρ_{dc} values for thicker titanium coatings can be explained as an effect of limited light penetration.

Keywords: Magnetron Sputtering, Ti layers, Drude parameters, limited penetration of light

References

[1] K. Zdunek, et. al. Surf. Coat. Technol. 228 (2013) S367-S373
[2] L. Skowronski, et. al. Surf. Coat. Technol.282, (2015) 16-23

THE INFLUENCE OF BALL-MILLING ON THE OPTICAL PROPERTIES OF PRINTED TITANIA PATTERNS REINFORCED BY ORGANOSILOXANE BINDER

Oldrich Zmeskal[a], Veronika Schmiedova[a], Petr Dzik[b], Jakub Tkacz[a] and Michal Vesely[b]

[a]Center fo Materials Research, Faculty of chemistry, Brno University of Technology, Purkynova 118, 612 00 Brno, Czech Republic
[b]Department of Physical and Applied Chemistry, Faculty of Chemistry, Brno University of Technology, Purkynova 118, 612 00 Brno, Czech Republic

Transition metal oxide and silica mixtures represent a perspective group of active materials that have recently been proposed as for various heterogeneous photocatalysis processes. Surprisingly, silica present in minor amount isn't dentrimental for charge transfer in the hybrid semiconductor-silica layer and among other applications allows for the fabrication of titania-silica photoanodes and other photonic components [1].
In this paper, we report about the influence of ball-milling on the optical properties of silica-bonded particulate titania patterns fabricated by inkjet printing. A previously optimized printing protocol [2] was used to fabricate composite titania-silica patterns of various area and thickness. The employed „ink", consisted of a commercial titania nanoparticles (Evonik P-25) and a recently reported organo-silica binder [3]. The previous studies proved the binder presence is beneficial for a number of reasons (stability of the stock suspension, rheological behavior during inkjet printing and bonding the printed nanoparticles). However, the soluble organo-silica binder needs to be mineralized in order to render it fully insoluble and significantly improve the printed layer mechanical properties. As reported recently [4], three different processes can be employed for this purpose: (a) thermal annealing, (b) UV-curing, and (c) atmospheric plasma treatment in a coplanar dielectric barrier discharge.
All three processes yield composite titania-silica patterns with interesting photonic functionality. However, the way the two components interact is to a great extend depending on the texture of the titanium dioxide, which can be conveniently controlled by ball-milling the liquid formulation prior to printing it. Since the titania texture has a direct impact on the optical properties, spectroscopic ellipsometry can be used to extract valuable information about the extent of milling. By correlating ellipsometric data with measurements obtained by other methods (nitrogen sorption, mechanical profilometry), we have shown that as the titania aggregates are broken into smaller fragments and eventually primary crystallites, the porosity and surface roughness is decreasing. Thus ellipsometric measurement can be employed as quick process control tool.

Keywords: materials printing, titanium dioxide, texture, porosity, ball milling

References

[1] P. Dzik, M. Veselý, M. Kete, E. Pavlica, U.L. Štangar, M. Neumann-Spallart, ACS Appl. Mater. Interfaces, 7 (2015) 16177-16190.
[2] M. Králová, P. Dzik, V. Kašpárek, M. Veselý, J. Cihlář, Molecules, 20 (2015) 16582-16603.
[3] D. Gregori, I. Benchenaa, F. Chaput, S. Therias, J.L. Gardette, D. Leonard, C. Guillard, S. Parola, J. Mater. Chem. A, 2 (2014) 20096-20104.
[4] T. Homola, P. Dzik, M. Veselý, J. Kelar, M. Černák, M. Weiter, ACS Appl. Mater. Interfaces, 8 (2016) 33562-33571.

The optical TiO_2 layers deposited on polymer substrates

R. Chodun[a], L. Skowronski[b], S. Okrasa [a], B. Wicher [a], K. Nowakowska – Langier [c], K. Zdunek [a]

[a] Faculty of Materials Science and Engineering, Warsaw University of Technology, Woloska 141, 02 – 507, Warsaw, Poland
[b] Institute of Mathematics and Physics, UTP University of Science and Technology, Kaliskiego 7, 85-796 Bydgoszcz, Poland
[c] National Centre for Nuclear Research, Andrzeja Soltana 7, 05-400, Otwock-Swierk, Poland

Plasma Surface Engineering methods meet the limitation of efficient synthesis of layers on the thermally unstable substrates, i. e.: HSS, electronic materials, polymers, etc. During the process of synthesis, an exchange of energy between the plasma and the substrate surface occurs. Overheating the substrate material leads to its decomposition, phase transition, structural changes, etc. Polymers are materials characterizing by relatively low melting temperature, so the process of layer deposition is very challenging. Overheated polymers degrade easily by breaking bonds in chain, so among the PSE methods only a few are predestinated to use.

Couple of years ago, we introduced a novel approach to control the plasma pulses in the magnetron sputtering method – Gas Injection Magnetron Sputtering (GIMS) [1]. In this technique the plasma is generated by pressure oscillations controlled by pulse gas valve. Our previous study showed that, using the GIMS technique, the synthesis of TiO_2 rutile phase is possible [2]. Taking into account the pulsed distribution of energy during the process of synthesis by GIMS, we predicted that the efficient deposition of coatings on polymer substrates is possible, thanks to favorable conditions of the energy dissipation on the substrate between each of the plasma pulse.

In this work, we present the optical TiO_2, TiO_2/Al, TiO_2/Cu layers deposited on PMMA substrates. Metallic and TiO_2 layers were synthesized by GIMS technique, operating with 1Hz frequency of gas injection for 7 min (metallic sub – layer) and 1,5 – 5 min (TiO_2).

The prepared samples were investigated by means of spectroscopic ellipsometry and spectrophotometry. To extract optical constants of TiO_2 layers and their thicknesses the multiple sample analysis approach was applied. Optical constants of metallic films were determined in a separate experiment.

Keywords: Magnetron Sputtering, TiO_2 layers, polymer substrates, optical properties

References

[1] K Zdunek, et. al. Surf. Coat. Technol. 228 (2013) S367-S373
[2] L Skowronski, et. al. Surf. Coat. Technol.282, (2015) 16-23

Optical and microstructural characterization of thick TiO_2 layers produced using magnetron sputtering technique

L. Skowronski [a], R.Chodun [b], K. Nowakowska – Langier [c], S. Okrasa [b], K. Zdunek [b]

[a] Institute of Mathematics and Physics, UTP University of Science and Technology, Kaliskiego 7, 85-796 Bydgoszcz, Poland
[b] Faculty of Materials Science and Engineering, Warsaw University of Technology, Woloska 141, 02 – 507, Warsaw, Poland
[c] National Centre for Nuclear Research, Andrzeja Soltana 7, 05-400, Otwock-Swierk, Poland

Optical and microstructural properties of materials synthesized using magnetron sputtering technique strongly depend on the growth conditions (i.e. temperature of substrate, pressure of inert and reactive gases, bias voltage).

The thick (a few hundred of nm) titanium dioxide layers were synthesized applying two techniques: pulsed magnetron sputtering and, lately developed, gas injection magnetron sputtering at variable argon/oxygen plasma composition. The two deposition methods have allowed the production of coatings in two completely different gas conditions in the vacuum chamber.

Optical and microstructural properties of the produced TiO_2 films were investigated using spectroscopic ellipsometry (V-VASE, J.A.Woollam Co., Inc.) and scanning electron microscopy (ZEISS Ultra Plus). To extract optical constants of the thick titanium dioxide layers different optical models of samples (with different complexity) were prepared. These models allowed to estimate the average values of optical constants of TiO_2 layers of as well as to perform detailed analysis of variable optical constants of TiO_2 through the axis perpendicular to the substrate. These results are confirmed by SEM measurements (cross-sections of TiO_2 layers).

Keywords: TiO_2, gradient model

EFFECTS OF PHOSPHOROUS IONS IMPLANTATION IN BULK CdTe CRYSTAL

Przemyslaw Sedzicki[a], Lukasz Skowronski[b], Robert Szczesny[c], Hans-Werner Becker[d], Detlef Rogalla[d], Michal Pawlak[a], Beata Derkowska-Zielinska[a,*]

[a]Institute of Physics, Faculty of Physics, Astronomy and Informatics, Nicolaus Copernicus University, Grudziadzka 5, 87-100 Torun, Poland
[b]Institute of Mathematics and Physics, UTP University of Science and Technology, S. Kaliskiego 7, 85-796 Bydgoszcz, Poland
[c]Faculty of Chemistry, Nicolaus Copernicus University, Gagarina 7, 87-100 Torun, Poland
[d]RUBION, Central Unit for Ion Beams and Radionuclei, Ruhr-University of Bochum, Germany

The CdTe monocrystals were grown from the melt by the modified high-pressure Bridgman method. The phosphorus particles flux in a range of $5 \cdot 10^{13}$ to $5 \cdot 10^{16}$ ions per cm^2 were used to dope the host material.
Ellipsometric azimuths, Ψ and Δ, were measured for three angles of incidence (65º, 70º and 75º) in UV-VIS spectral range (0.5-6.5 eV) by the V-VASE ellipsometer (J.A.Woollam Co., Inc.). The transmittance spectra were recorded applying Cary 5000 spectrophotometer.
The changes in the optical constants of studied materials have been observed with transmittance measurements and spectrometric ellipsometry. Variations in refractive index (n) and extinction coefficient (k), which depends on the implantation of phosphorus ions in CdTe, are shown in Fig. 1.

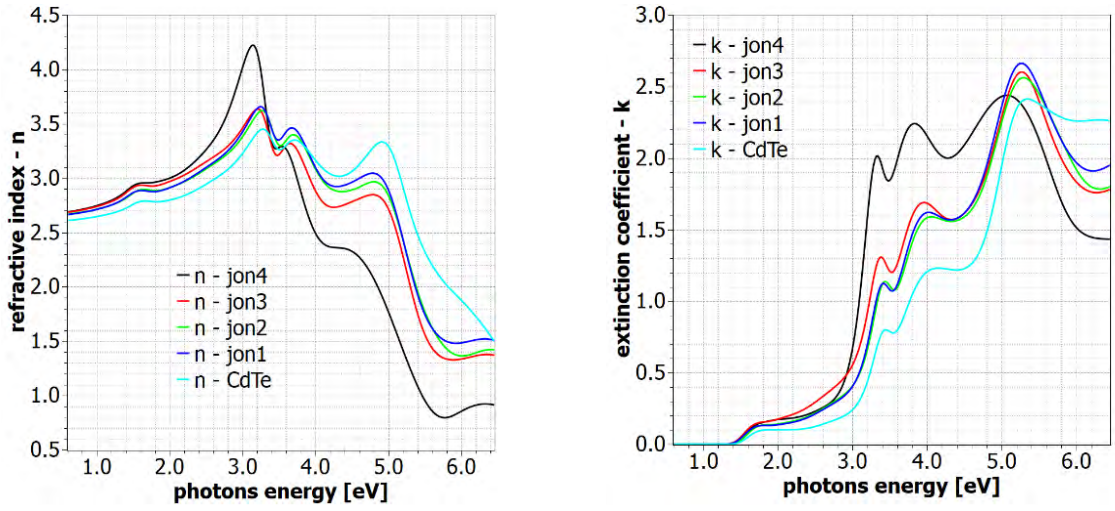

Fig. 1. Changes in refractive index (n) and extinction coefficient (k) for CdTe:P.

Keywords: bulk CdTe; ions implantation; ellipsometry

* Corresponding author: Beata Derkowska-Zielinska, e-mail address: beata@fizyka.umk.pl, Institute of Physics, Faculty of Physics, Astronomy and Informatics, Nicholas Copernicus University, Grudziadzka 5/7, 87-100 Torun, Poland Tel.: +48 56 611 32 01; Fax: +48 56 622 53 97

OPTICAL PROPERTIES OF COBALT/CHROMIUM DOPED BULK ZNSE

Przemyslaw Sedzicki[a], Łukasz Skowronski[b], Robert Szczesny[c], Beata Derkowska-Zielinska[a,*]

[a]Institute of Physics, Faculty of Physics, Astronomy and Informatics, Nicolaus Copernicus University, Grudziadzka 5, 87-100 Torun, Poland
[b]Institute of Mathematics and Physics, UTP University of Science and Technology, S. Kaliskiego 7, 85-796 Bydgoszcz, Poland
[c]Faculty of Chemistry, Nicolaus Copernicus University, Gagarina 7, 87-100 Torun, Poland

Spectroscopic ellipsometry combined with transmittance measurements have been used to estimate the optical constants of ZnSe:Co and ZnSe:Cr crystals, which were grown from the melt by the modified high-pressure Bridgman method. Fig. 1 presents the changes in refractive index (n) and extinction coefficients (k). One can see that these variations depend on the chosen dopant.

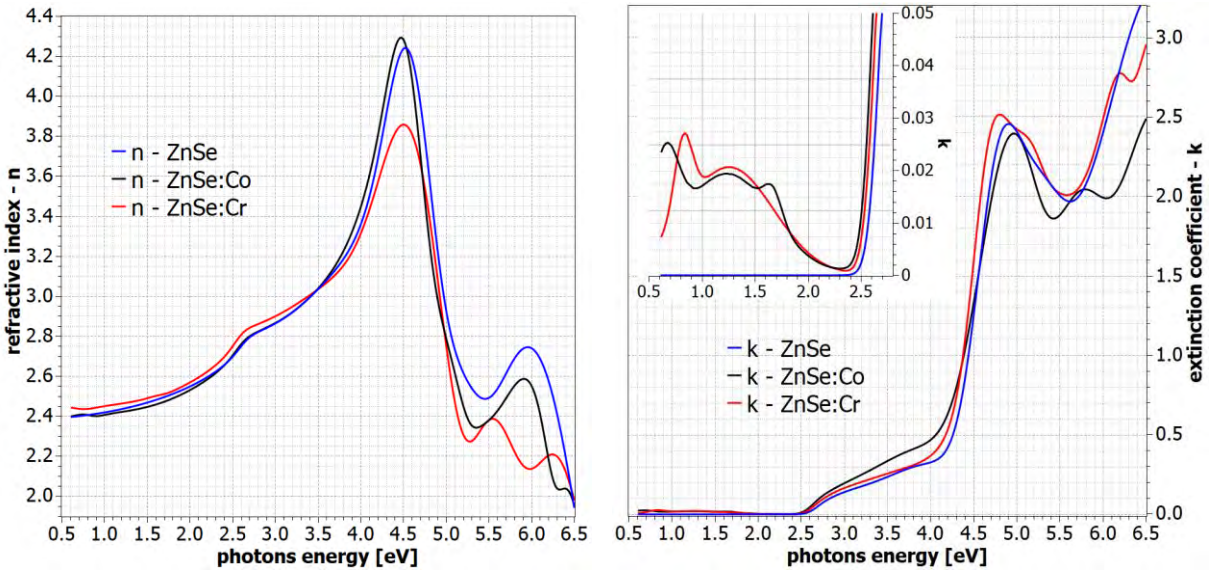

Fig. 1. Change in refractive index (n) and extinction coefficient (k) for ZnSe, ZnSe:Co, ZnSe:Cr crystals obtained from samples models fitted to ellipsometric measurements.

Moreover, transmission measurements also show the additional bands at around 1400-2000 nm for ZnSe:Cr, as well as at around 700-800 nm and 1400-1900 nm for ZnSe:Co compared to ZnSe.

Keywords: bulk ZnSe chromium, cobalt; ellipsometry, transmission

* Corresponding author: Beata Derkowska-Zielinska, e-mail address: beata@fizyka.umk.pl, Institute of Physics, Nicholas Copernicus University, Grudziadzka 5/7, 87-100 Torun, Poland Tel.: +48 56 611 32 01; Fax: +48 56 622 53 97

SPECTROSCOPIC ELLIPSOMETRY FOR THE ANALYSIS OF ANISOTROPIC WIDE BAND GAP SEMICONDUCTORS

S. Peters

Schwarzschildstr. 2, 12489 Berlin, SENTECH Instruments GmbH, Germany

Ellipsometry is used in many different applications fields from fundamental research to industrial applications in micro- and optoelectronics, photovoltaics, metal, and glass industry. We are presenting a selection of sophisticated R&D applications emphasizing the capability of spectroscopic ellipsometry analyzing the dielectric functions ε for selected anisotropic wide band gap semiconductors: wurtzite-ZnO, 6H-SiC, and β-Ga_2O_3.

The ellipsometric measurements were performed using a SENTECH SENresearch 4.0 SER850 DUV spectroscopic ellipsometer.

The (10-10) plane of a **wurtzite ZnO** crystal was measured parallel and perpendicular to the optical c-axis. The dispersion of ε_1, ε_2 of ZnO was parameterized using an oscillator model describing the bandgap structure as well as the excitonic structures in the band gap region (Fig. 1).

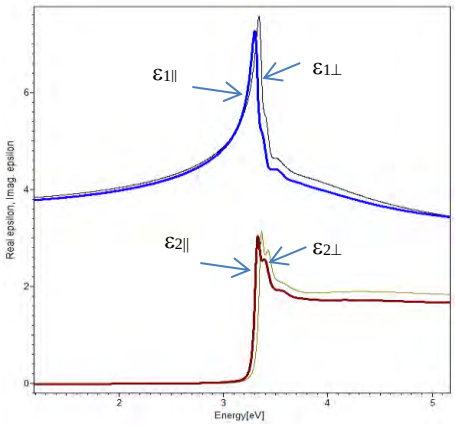

Fig. 1. ε_1, ε_2 of ZnO

The (000-1) plane of a double side polished **6H-SiC** sample was measured by Muller Matrix (MM) ellipsometry in the energy range from 0.5 to 3.0 eV. The beam, refracted into the wafer is split into two beams due to the anisotropy of the SiC wafer. When exiting the wafer after being reflected at the polished backside, both components show a phase shift due to different travel length. This causes interference fringes in the MM spectra. The superposition of these two interfering beams with the directly reflected beam is incoherent causing depolarization of the light. Muller matrix measurements must be applied for modeling anisotropy and depolarization simultaneously.

β-Ga_2O_3 shows a monoclinic crystalline structure. This causes biaxial anisotropic behavior. Here a simpler cubic crystal was modeled neglecting the xz component of the dielectric tensor. As a result, only three crystallographic directions a, b, c* can be measured. c* is the perpendicular component of the c-axis perpendicular to the crystallographic a-b-plane. An (010) β-Ga_2O_3 crystal was measured along the c*-axis and an (001) β-Ga_2O_3 crystal was measured along its a- and b-axes by Muller Matrix ellipsometry in the energy range from 1.2 to 6.5 eV. The resulting dielectric function is shown in Fig. 2.

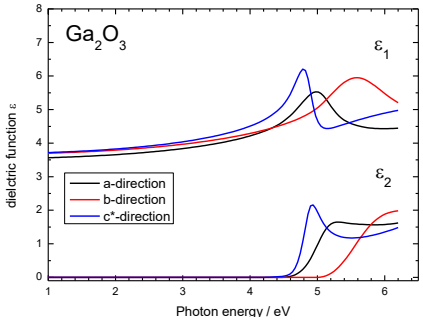

Fig. 2. ε_1, ε_2 of β-Ga_2O_3

Keywords: Ellipsometry, Muller Matrix, Anisotropy, Wide band gap, semiconductor, Ga_2O_3

Spectroscopic ellipsometry, SIMS and X-ray diffractometry and reflectometry for Ge-graded SiGe HBT control

F. Bärwolf, O. Fursenko, P. Zaumseil and Y. Yamamoto

IHP, Im Technologiepark 25, D-15236 Frankfurt (Oder), Germany

SiGe BiCMOS process technologies require precise, fast, nondestructive and in-line thickness and composition control of Ge-graded HBT (Heterojunction Bipolar Transistor) layer stacks. In this contribution we demonstrated advantages and shortcomings of different characterization techniques such as spectroscopic ellipsometry (SE), dynamic secondary ion mass spectroscopy (DSIMS) and X-ray diffractometry (XRD) and reflectometry (XRR) for SiGe HBT with Ge graded profile up to 40%. Starting point of our investigation were HBT profiles described in [1, 2].

Thickness of Si-cap and SiGe base, splited into the gradient and plateau part, maximum Ge content, and shape of the Ge gradient part are measured and the error limits of the different techniques are discussed. The spectroscopic ellipsometry measurements were realized using automated KLA-Tencor SpectraFilm F1 ellipsometer with rotating polarizer and compensator at 3 angles of incidence (59, 65 and 71 deg). The sensitivity of spectroscopic ellipsometry to different shapes of the gradient part is demonstrated. DSIMS measurements were done with oxygen bombardment at low impact energy and compared with XRD.

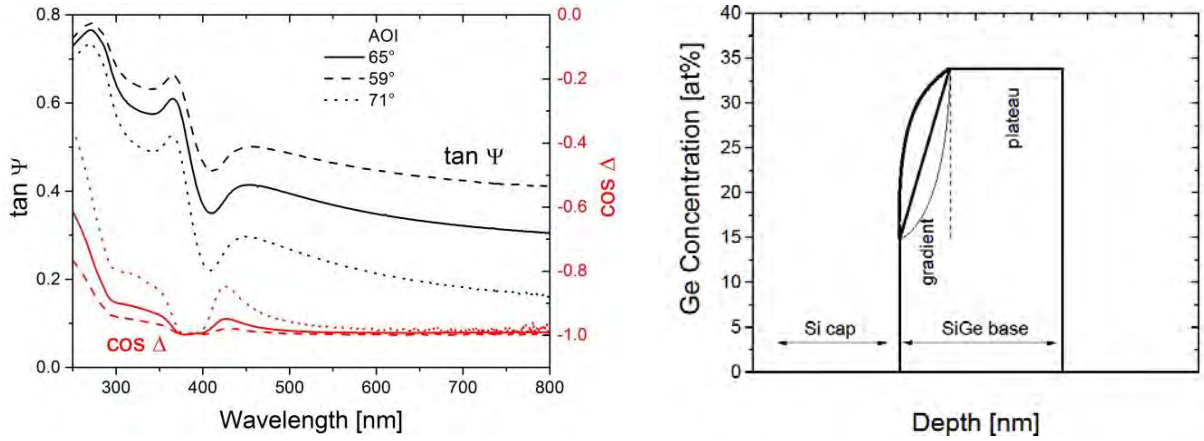

Keywords: spectroscopic ellipsometry, SIMS; X-ray diffraction (XRD), X-ray reflection (XRR), SiGe HBT

References

[1] O. Fursenko, J. Bauer, P. Zaumseil, D. Krüger, A. Goryachko, Y. Yamamoto, K. Köpke, B. Tillack, Mat. Science in Semicond. Proces. 8 (2005) 273.
[2] P. Zaumseil, D. Krüger, R. Kurps, O. Fursenko, P. Formanek, Solid State Phenomena 95-96 (2004) 473.

ELECTRON EFFECTIVE MASS IN $In_{0.33}Ga_{0.67}N$ DETERMINED BY INFRARED OPTICAL HALL EFFECT

N. Armakavicius[a], V. Stanishev[a], S. Knight[b], P. Kühne[a], M. Schubert[a,b], V. Darakchieva[a]

[a]Terahertz Materials Analysis Center, Department of Physics, Chemistry and Biology IFM, Linköping University, Sweden
[b]Department of Electrical and Computer Engineering and Center for Nanohybrid Functional Materials, University of Nebraska-Lincoln, USA

Due to its band gap tunability and high electron saturation drift velocity, InGaN is very attractive for optoelectronic, high frequency and high power applications. Knowledge of free charge carrier effective mass parameter in InGaN is important for modelling the device performance and developing new designs. Typically, cyclotron resonance and Shubnikov-de Haas measurements are used to determine the effective mass. However, they require high carrier mobilities and thus low temperatures with high external magnetic fields. Due to difficulties in growth of high In content $In_xGa_{1-x}N$ ($x > 0.3$), material suffer from high concentration of defects and low mobility parameters. Thus, the reports of the effective mass parameter in $In_xGa_{1-x}N$ are scarce.

External magnetic fields alter the optical response of the free charge carriers in conductive materials that results in optical birefringence called optical Hall effect (OHE) [1]. Probing of the OHE by Mueller matrix ellipsometry at infrared and terahertz spectral ranges allows the determination of effective mass at room temperatures together with free carrier concentration and mobility parameters in bulk materials and thin layers.

Mid-infrared OHE measurements are used to determine the free charge carrier parameters of wurtzite structure *c*-plane oriented $In_{0.33}Ga_{0.67}N$ epitaxial layer [2]. Room temperature electron effective mass parameters of $m_{\perp}^{*} = (0.205 \pm 0.013)m_0$ and $m_{\parallel}^{*} = (0.204 \pm 0.016)m_0$ for polarization perpendicular and parallel to the *c*-axis, respectively, were determined. The free electron concentration was obtained as $(1.7 \pm 0.2) \times 10^{19}\ \mathrm{cm}^{-3}$. Within our uncertainty limits we detect no anisotropy for the electron effective mass and we estimate the upper limit of the possible effective mass anisotropy as 7%. We discuss the influence of band nonparabolicity on the electron effective mass parameter as a function of In content. The effective mass parameter is consistent with a linear interpolation scheme between the conduction band mass parameters in GaN and InN when the strong nonparabolicity in InN is included. The $In_{0.33}Ga_{0.67}N$ electron mobility parameters were found to be anisotropic supporting previous experimental findings for wurtzite structure GaN, InN, and AlGaN epitaxial layers with *c*-plane growth orientation. In addition, our data analysis reveals a surface charge depleted layer confirming previous findings showing that depletion of the electrons at the surface occurs in $In_xGa_{1-x}N$ with *x* below 0.4.

Keywords: effective mass; free charge carriers; optical Hall effect; III group nitrides; epitaxial graphene

References

[1] M. Schubert, P. Kühne, V. Darakchieva, T. Hofmann, J. Opt. Soc. Am. A 33, (2016), 1553-1568.
[2] N. Armakavicius, V. Stanishev, S. Knight, P. Kühne, M. Schubert, V. Darakchieva, (2017), arXiv:1712.01738 [cond-mat.mtrl-sci].

IMAGING SPECTROSCOPIC ELLIPSOMETER FOR OLED APPLICATION

A. Sütő, Sz. Bíró, A. Bölcskei-Molnár

Semilab Semiconductor Physics Laboratory Co. Ltd., Budapest, Hungary

Flat panel display technology demands the layer characterization within small areas. OLED technology uses multi-layer stack that is why ellipsometry is mandatory metrology for characterization.

Considered that the layer structure is complex and extremely small that is why the high lateral resolution spectroscopic ellipsometry (SE) is preferred to determine the optical properties of the layers.

To get 2D thickness map and 2D refractive index map simultaneously at high lateral resolution, imaging SE metrology is developed. Metrology is based on microscope type arrangement including polarization state elements. By using basically microscope and extended with spatial filter to define the incidence plane and using polarization element to define the incidence polarization state in the illumination path. Moreover, compensator and analisator are used in the detection path to get ellipsometry data on 2D CCD device. Ellipsometry data is calculated from Fourier components at given compensator positions.

In this work, we present the preliminary result of unique iSE metrology on multi-layer stack.

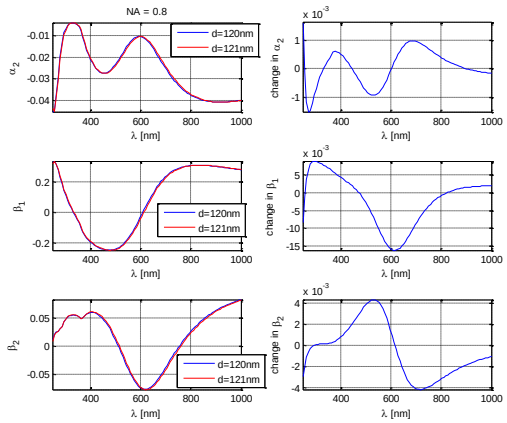

Fig. 1. Sensitivity on 1200A SiO2/Si structure using iSE metrology

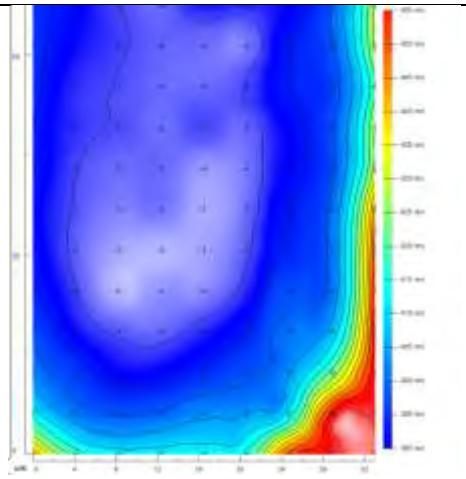

Fig. 2. 2D total THK map of multi-layer structure

Keywords: ellipsometry, imaging

References

[1] High-resolution imaging ellipsometer, Qiwen Zhan and James R.Leger, 1 August 2002 / Vol. 41, No. 22 / APPLIED OPTICS [2]

Optical Characterization of Anisotropic Thiophene-Phenylene Co-oligomer Micro Crystals by Spectroscopic Imaging Ellipsometry.

Christian Röling[a)], Peter H. Thiesen[b)], Matthias Duwe[b)], Elena Y. Poimanova[c)], and Vladimir V. Bruevich[d)]

[a)] Institute of Physical Chemistry, Georg-August-University Göttingen, Germany
[b)] Accurion GmbH, Stresemannstr. 30, 37079 Göttingen, Germany
[c)] Donetsk National University, Department of Chemistry, Ukraine
[d)] International Laser Center & Physics Faculty, M.V. Lomonosov Moscow State University, Vorobyevy gory, Moscow

Here we demonstrate Imaging Ellipsometry as a combination of microscopy and ellipsometry to characterize even micro-sized thin film crystals on plane surface regarding anisotropy, optical properties, crystalline domains and thickness. The semiconducting thiophene phenylene co-oligomer 1,4-bis(5'-hexyl-[2,2'-bithiophen]-5-yl)benzene (dHex-TTPTT) crystals were grown by solvent based self-assembly technique on silicon substrate with 300 nm thermally-grown silicon dioxide (Fig. 1).

The ellipsometric measurements were performed with an Ep4-SE (Accurion). In an ellipsometric high-contrast image of the complete sample we have localized high quality single crystals. After characterization of the biaxial anisotropy of the crystal by using Mueller-Matrix imaging ellipsometry, we performed spectroscopic measurements (λ = 400-700 nm in intervals of 5 nm) at the pseudo-isotropic orientations of the sample.

Fig. 1. Ellipsometric contrast micrograph of the complete sample with thin thiophene crystals on silicon with SiO_2 (d =300 nm).

The optical properties were described by using a Lorentz term in the Ep4-Model. After determining the dispersion of the crystals we converted a recorded Delta and Psi-map into a 2D thickness image. Based on a quantitative analysis of the resulting thickness map we have calculated the height of a molecular layer (3.49 nm).

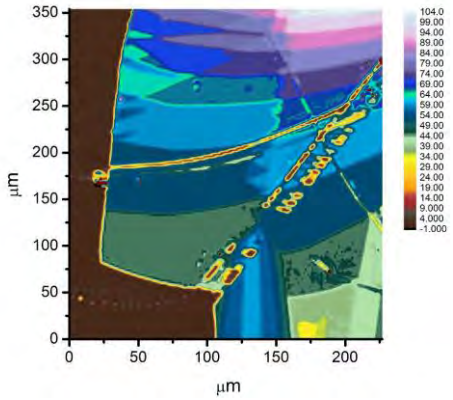

Fig. 2. Thickness map of the multi-layered thiophene based micro crystals.

Acknowledgments. The authors thanks Y.N. Luponosov for synthesis of dHex-TTPTT and D.Yu. Paraschuk for discussions.

Keywords: Spectroscopic Imaging Ellipsometry, Organic electronics, anisotropic micro crystals, Microscopic Müller Matrix maps

THE GLASS TRANSITION IN POLYIMIDE FILMS USED FOR MICROELECTRONIC PACKAGING

E. Bittrich[a], F. Windrich[b,c], D. Martens[d], L. Bittrich[a], L. Häussler[a] and K.-J. Eichhorn[a]

[a]Leibniz-Institut für Polymerforschung Dresden e.V., Hohe Str. 6, Dresden, Germany
[b]Center "All Silicon System Integration Dresden", Fraunhofer IZM, Moritzburg, Germany
[c]Organic Chemistry of Polymers, Technische Universität Dresden, Dresden, Germany
[d]New Mexico State University, Las Cruces, NM, USA

Thin polyimide films are commonly used as interlayer dielectric and for microelectronic packaging. New materials with low curing temperatures were developed in recent years to address the demand for low processing temperatures due to the increased complexity of material combinations in today's advanced packaging technologies.

We report on the glass transition temperature T_g of thin films made from photosensitive low-temperature cure ester-type polyimide, and analyze the effect of different curing temperatures T_{cure} on T_g as well as on the thermal expansion $\alpha(T) = \partial d(T)/\partial T$ by temperature-dependent spectroscopic ellipsometry [1]. We found considerably lower T_g in the bulk than in the thin film, and the T_g values of the films increased about 34 °C with increasing curing temperature in the range of T_{cure} = 230 – 380 °C.

These observations are attributed to the temperature sensitive release of the imidization by product 2-hydroxyethyl methacrylate (HEMA) and crosslinker components as well as decomposition products from the material [2,3].

Ellipsometric data evaluation was adapted to account for the release of low molecular weight compounds during the heating process and to model the T_g of the thin films more precisely.

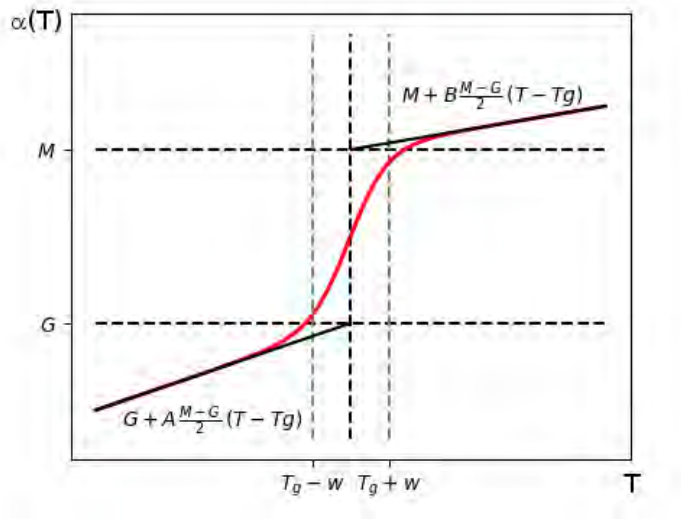

Fig. 1: Sketch to illustrate the trends in the thermal expansion α(T) and the fit parameters *G, M, A, B* as well as the glass transition temperature T_g and the width of transition *w*.

Keywords: T-SE; glass transition temperature; polyimide

References

[1] E. Bittrich, F. Windrich, D. Martens, L. Bittrich, L. Häussler, K.-J. Eichhorn, Polymer Testing, 64 (2017) 48.
[2] F. Windrich, E. J. Kappert, M. Malanin, K.-J. Eichhorn, L. Häussler, N. E. Benes, B. Voit, Eur. Polym. J. 84 (2016) 279.
[3] F. Windrich, M. Malanin, K.-J. Eichhorn, B. Voit, K. D. Lang, Mat. Res. Soc. Symp. Proc. 1692 (2014) 1.

OPTICAL PROPERTIES OF AMORPHOUS SiO_2-TiO_2 MULTI-NANOLAYERED COATINGS FOR 1064-NM MIRROR TECHNOLOGY

M. Magnozzi[a], S. Terreni[a], L. Anghinolfi[a], S. Uttiya[a], M.M. Carnasciali[b], G. Gemme[c], M. Neri[a,c], M. Principe[d], I. Pinto[d], L.-C. Kuo[e], S. Chao[e], M. Canepa[a,c]

[a] OPTMATLAB, Dipartimento di Fisica, Università di Genova, Italy
[b] Dipartimento di Chimica e Chimica Industriale, Università di Genova, Italy
[c] Istituto Nazionale di Fisica Nucleare, Sezione di Genova, Italy
[d] Dept. of Engineering, University of Sannio, Italy
[e] Institute of Photonics Technologies & E.E. Dept., National Tsing Hua University, Taiwan

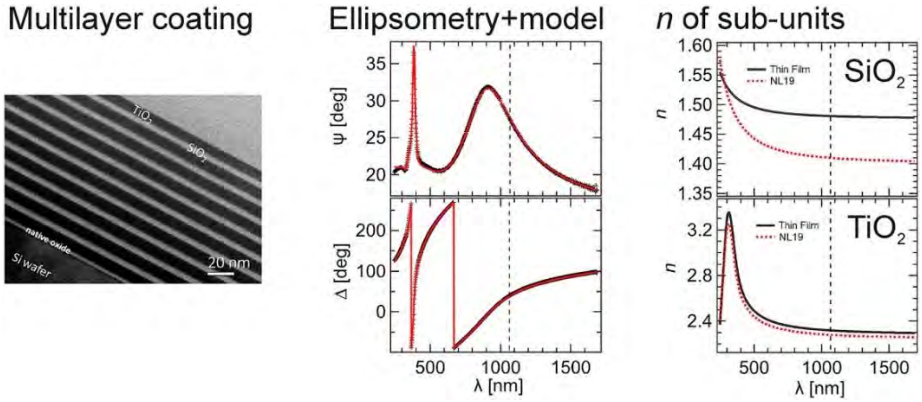

The use of amorphous, SiO_2-TiO_2 nanolayered coatings has been proposed recently for the mirrors of 3rd generation interferometric detectors of gravitational waves, to be operated at low temperature. The optimization of mirror designs based on such coatings requires a detailed knowledge of the optical properties of sub-units at the nm-thick scale. To this aim we have performed a Spectroscopic Ellipsometry (SE) study of amorphous SiO_2-TiO_2 nanolayered films deposited on Si wafers by Ion Beam Sputtering. We have analyzed films that are composed of 5 and 19 nanolayers (NL5 and NL19 samples) and have total optical thickness nominally equivalent to a quarter of wavelength at 1064 nm. By flanking SE with ancillary techniques, such as TEM and AFM, we built optical models that allowed us to retrieve the broadband (250-1700 nm) optical properties of the nanolayers in the NL5 and NL19 composite films [1]. Regarding the NL5 sample, with thickness of 19.9 nm and 27.1 nm for SiO_2 and TiO_2 sub-units, respectively, the optical properties presented limited variations with respect to the thin film counterparts. For the NL19 sample, which is composed of ultrathin sub-units (4.4 nm and 8.4 nm for SiO_2 and TiO_2, respectively) we observed a significant decrease of the IR refraction index for both types of subunits; this points to a lesser mass density with respect to the thin film reference.

[1] M. Magnozzi et al., Optical Mat., 75, 2018

Keywords: Spectroscopic ellipsometry, Coatings, Multilayer, SiO2 thin film, TiO2 thin film

Stable and reproducible porous coatings for smart window applications

P. Basa[a], L. Kócs[b], E. Albert[b], B. Tegze[b], Cs. Major[c], A. Szalai[c], Gy. Sáfrán[d], Z. Hórvölgyi[b]

[a]Semilab Semiconductor Physics Laboratory Co. Ltd., Hungary
[b]Budapest University of Technology and Economics, Department of Physical Chemistry and Materials Science, Hungary
[c]Hungaro Lux Light Ltd., Hungary
[d]Hungarian Academy of Sciences, Institute of Technical Physics and Materials Science, Hungary

The reported work is concerning porous silica dielectric coatings which are exhibiting improved light transmittance properties. These anti-reflective (AR) coatings are increasingly popular in various research areas and applications [1]. One of their most important basic requirements is that they maintain their optical stability during the time of their utilization. Attaining sustainable long-lasting porous thin films with AR properties is a major challenge, especially in optically transparent windows and in related applications, for instance regarding preparation of self-cleaning surfaces or solar energy conversion. In order to improve the temporal stability of the films, a custom network strengthening chemical treatment is suggested.

Measurement results of spectroscopic ellipsometry, ellipsometric porosimetry [2], transmission electron microscopy and optical spectroscopic transmission are presented and discussed.

Keywords: glass; ellipsometric porosimetry; porous coating, smart windows

References

[1] L. Kócs et al., Periodica Polytechnica Chemical Engineering, 62 (1) 21-31 (2018), and references therein.
[2] A. Bourgeois et al., Adsorption, 14 (4-5) 457-465 (2008)

Characterization of Thin Films at Disadvantageous Interfaces by Imaging Ellipsometry

Peter H. Thiesen, Matthias Duwe, Sebastian Funke, Stefan Schneider

Accurion GmbH, Stresemannstr. 30, 37079 Göttingen, Germany

The characterization of thin films at disadvantageous surfaces like technical metal surfaces, curved surfaces, natural mineral surfaces, liquid surfaces or thin transparent substrates can be an issue. A number of new developments in the field of Imaging ellipsometry as well as established techniques like knife edge illumination enable new characterization methods for thin films on disadvantageous surfaces. In case of technical surfaces (Fig. 1), a pre-evaluation of the surface before the selection of the area that is represented by the measurement, increases the data quality. Ellipsometric contrast micrographs are the method of choice, because they can be recorded very fast and the contrast can be optimized to make inhomogeneities and thickness changes in the nanometer range visible. Moreover the micrographs are recorded with the same detector and the optical contrast is increased by the same optical high quality components as the following ellipsometric measurements. This circumstance helps minimizing errors caused by the mismatching between microscopic images and the measurement area.

Microscopic Müller-Matrix maps and isotropic/ anisotropic imaging enable a higher quality level in pre-evaluating of inhomogeneous surfaces and new characterization tools for surfaces that are disadvantageously regarding optical thin film metrology from the geometrical point of view.

Fig. 1. Ellipsometric contrast micrograph of an oil film on a technical metal surface.

Disturbances caused by back reflections are a main issue in thin film metrology at the interface of thin transparent substrates. Knife edge illumination is dedicated to suppress these disturbances. The technique makes use of the fact that the cut partial beam, reflected from the back of the substrate is passing the surface of the substrate with a certain distance from the blade. This area between the blade and the edge of the back-reflected beam is not disturbed by back-reflected light. With an imaging ellipsometer, where the region represented by the measurement is selected on the detector side, the thin film characterization can be performed in the area that is not hidden and disturbed by the back-reflected light (Fig. 2).

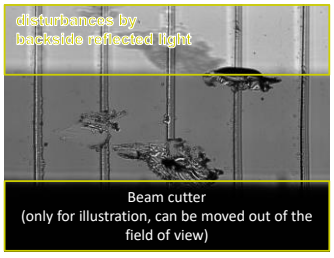

Fig. 2. Nanoparticles strips on a glass substrate. Image recorded under knife edge illumination.

The contribution will illustrate different approaches with examples from practical applications and take up new developments.

Keywords: thin transparent substrates; technical surfaces, Imaging Ellipsometry, knife edge illumination.

Imaging Ellipsometry at the air/water interface

Peter H. Thiesen, Christian Hoffmann

Accurion GmbH, Stesemannstr. 30, 3079 Göttingen, Germany

Conventional ellipsometry is well established in the field of thin film metrology due to the exceptionally high resolution in the z-axis, enabling very accurate thickness measurements for nano- and microfilms. However, conventional ellipsometry does not have a sufficient lateral resolution for a number of current developments nor a direct microscopic visualization with highest contrast for thin films. The approach of Imaging Ellipsometry (SIE) differs from conventional ellipsometry in that the measurements are based on a series of micrographs taken at dedicated orientations of the optical components. The primary measurements are microscopic maps of the ellipsometric angles Delta and Psi. The data were transferred into thickness maps by optical modelling (EP4_model software package, Accurion). In literature, maps of ellipsometric parameters at the air water interface were for example reported by Rottke et al.[1].

Microscopic Delta and Psi maps were recorded with a single wavelength imaging ellipsometer, equipped with a red laser ($^{IE}EP4_{L658nm}$). The instrument was mounted on a Halcyonics_vario40 active vibration isolation system on top of a halcyonics support frame. A water-filled round Teflon trough equipped with a wedge shaped black glass plate was used. Droplets of a Ethylstearate (solution of 1 mg/ml in Hexane) were spread with a microliter syringe at a cleaned water surface. Delta and Psi maps were recorded continuously with maximum speed at the laser wavelength of 658 nm and an angle of incidence of 50°.

The experimental results are discussed in the context of new developments in the field of Gibbs, LB and related thin films at the air water interface.

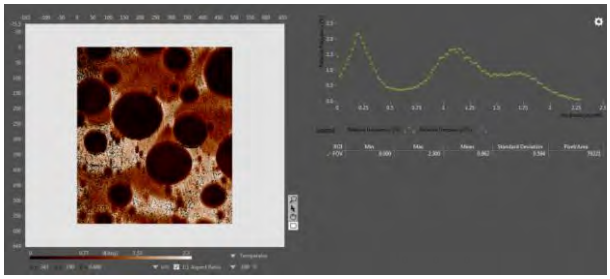

Fig. 1. Ethyl stearate film at the air water interface without compression - Delta map and distribution of Delta values.

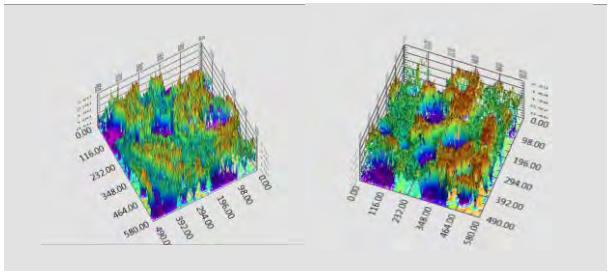

Fig.2. Thickness maps of the Ethyl stearate films at the air/water interface.

Air/Water interface, Imaging ellipsometry, active vibration isolation

References

[1] F.O. Rottke, B. Schulz, K. Richau, K. Kratz, A. Lendlein, Beilstein J. Nanotechnol. 2016, 7, 1156–1165.

Detection and control of surface nanostructures at water liquid interface for sensing

B. Kalas[a], J. Nador[a], A. Saftics[a], C. Moldovan[b], M. Gartner[c], M. Gheorghe[d], M. Fried[a], F. Vonderviszt[a, e], P. Petrik[a]

[a]Institute for Technical Physics and Materials Science, Centre for Energy Research, Hungarian Academy of Sciences, Budapest, Hungary

[b]National Institute for Research & Development in Microtechnologies, Bucharest, Romania

[c]„Ilie Murgulescu" Institute of Physical Chemistry of the Romanian Academy, Bucharest, Romania

[d]NANOM MEMS SRL, Brasov, Romania

[e]University of Pannonia, Veszprém, Hungary

The detection of contamination in natural water gains increasing importance due to health concerns. Real time monitoring of contamination can significantly reduce the health risk. Optical methods are preferred in these applications since they offer sensitive, *in situ* and non-destructive measurement possibilities. To identify the contamination, specific binding has to be realized.
Our approach is to use genetically modified bacterial filaments to ensure this specific detection. Using *in situ* ellipsometry measurements our aim is to understand the adsorption process and the 3D evolution of the filament sensor layer. To achieve high sensitivity *in situ* ellipsometry measurements we have built a Kretschmann-Raether cell [1,2].
With the help of the surface plasmon resonance (SPR) phenomenon combined with spectroscopy in a broad wavelength range, the sensitivity of the detection was largely increased. The phase information of the reflected beam enabled the increase of the sensitivity compared to traditional SPR devices [3,4].
The main goal of these investigations is to get a more comprehensive understanding about the adsorption of genetically modified flagellar filaments (FFs) since they have the potential of gaining an increasing application in future biosensors.

Keywords: Protein adsorption; Surface plasmon resonance; Biosensor

References

[1] H. Raether, *Surface Plasmons on Smooth and Rough Surfaces and on Gratings*, Springer-Verlag Berlin Heidelberg (1988).
[2] H. Arwin, M. Poksinski, K. Johansen, *Total internal reflection ellipsometry: principles and applications*, Appl. Opt. **43**, 3028–3036, (2004).
[3] J. Homola, *Surface Plasmon Resonance Sensors for Detection of Chemical and Biological Species*, Chem. Rev. **108**, 462-493 (2008).
[4] P. Petrik, E. Agocs, B. Kalas, P. Kozma, B. Fodor, J. Nador, C. Major, and M. Fried, *Multiple angle of incidence, spectroscopic, plasmon-enhanced, internal reflection ellipsometry for the characterization of solid-liquid interface processes*, SPIE Proc. **9529**, 95290W (2015).

OPTOFLUIDIK PLATFORM FOR ENHANCED IR MICROSCOPIC SENSING

C. Kratz[a], T. W. H. Oates[a], D. Janasek[b], K. Hinrichs[a]

[a] ISAS — e.V., Schwarzschildstr. 8, 12489 Berlin, Germany
[b] ISAS — e.V., Otto-Hahn-Str. 6b, 44227 Dortmund, Germany

An optofluidic platform for in situ enhanced infrared (IR) microscopic biosensing is presented enabling structural and chemical analysis of biomolecules in nanoliter samples. The platform combines enhancement substrates and microfluidic chips of arbitrary material and is designed for applications in conventional IR microscopes. [1] Metallic island film covered templates for Surface Enhanced IR Absorption (SEIRA) exhibit a specific enhancement behaviour. For quantitative evaluation the surfaces were characterized by UV-VIS ellipsometry, IR Ellipsometry/Microscopy and AFM-IR.

Potential applications for the developed optofluidic platform are lab-on-chip, organ-on-chip, cell analytics, bio-analytics or diagnostics. In situ IR spectroscopy enables label free and non-destructive molecular identification and can provide detailed information on interactions and reactions *e.g.* changes in protein folding or receptor-ligand interactions. The presented optofluidic platform circumvents the challenge of strong IR absorption of common polymeric materials used for microfluidic chips employing a single-reflection geometry under non-ATR (attenuated total internal reflection) conditions. This development allows for the usage of commercially available chips facilitating the application of the method. Utilization of optimized enhancement substrates of metal island films [2] offers a signal enhancement by a factor of 10-100.[3]

Submonolayer sensitivity of the developed platform is demonstrated by studying the formation of 1.2 nm thin monolayer of the tripeptide glutathione (GSH) in an aqueous environment. The potential to study interactions and reactions at the solid–liquid interface is shown by monitoring chemical changes in the monolayer as response to changes in environmental pH. Time-resolved (2.5 min) measurements of GSH monolayer formation show that dynamic processes can be monitored in situ. The determined detection limit of 0.03 nmol/cm^2 emphasize the potential of the platform in biosensing applications as well as in the study of dynamic processes *e.g.* enzymatic reactions, receptor–ligand interactions or conformational changes of molecules due to environmental stimuli with sub-monolayer sensitivity under in situ conditions.

Keywords: metal island films, infrared ellipsometry/microscopy, submonolayer, nanoliter, sensing

References

[1.] C. Kratz, A. Furchner, T. W. H. Oates, D. Janasek and K. Hinrichs, submitted
[2.] C. Kratz, T. W. H. Oates, and K. Hinrichs, Thin Solid Films 617 (2016) 33-37
[3.] M. Osawa, in S. Kawata (eds): “Near-Field Optics and Surface Plasmon Polaritons” p. 163-187, Springer (2001)

Characterization of extruded Collagen Fibres with Imaging Ellipsometry

Christian Hoffmann[a], Peter H. Thiesen[a], Karsten Stapelfeldt[b], Naiana Suter[b] and Dorothea Brüggemann[b]

[a] Accurion GmbH, Stresemann Str. 30, D-37079 Göttingen, Germany
[b] nanoBiomaterials – Emmy Noether research group, Institute for Biophysics (FB1) – University of Bremen, Otto-Hahn-Allee 1, D-28359 Bremen, Germany

Manufacturing biocompatible surfaces has evolved into a cornerstone for downstream biomedical and pharmaceutical applications. In live tissues the structural and biochemical support for cells is maintained by various secreted extracellular matrix (ECM) components. The *ex vivo* deposition and network formation of these components on various scaffolds is crucial for subsequent cellular adhesion processes, thus vital for the production of tissue-like implants or effective cell-seeding on prostheses.

Here we focus on collagen, a highly abundant protein and key component of the ECM. The purified protein was extruded through a nanoporous filter, like dough in a pasta machine, and deposited as a drop onto a conventional glass microscope slide [1]. The sample was a kind gift from the Emmy Noether research group for nanoBiomaterials of Prof. Dorothea Brüggemann. We used imaging ellipsometry for the analysis of the extruded collagen fibres. A total sample overview covering 2.7 cm^2 was generated by the integrated image stitching algorithm combining 1008 single contrast micrographs into one image (Fig. 1 A). Back reflections of the glass slide are suppressed using the unique knife-edge illumination (B). Regions of interest were selected upon this pre-screening and Δ/Ψ maps were recorded spectroscopically from 400 to 760 nm (C). After applying an ellipsometric model, we analyzed the thickness and optical properties of the collagen network.

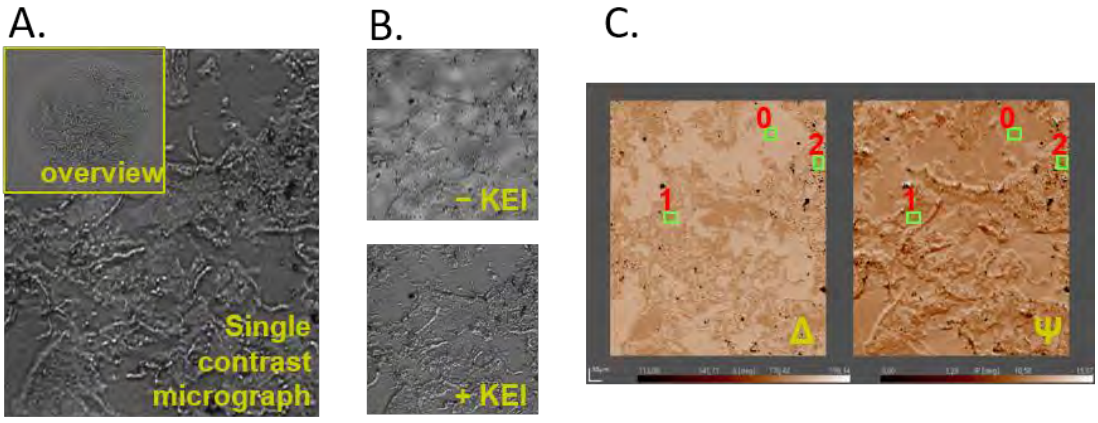

Fig. 1. Ellipsometric characterization of extruded collagen fibres. A) Total sample overview realized by stitching of contrast micrographs. B) Back reflection suppression by knife-edge illumination. C) Exemplary Δ/Ψ maps of the collagen network at 400nm with depicted ROIs (Regions of interest).

Keywords: Imaging Ellipsometry; Collagen; Biocompatible Surfaces; Transparent Substrates

References

[1] Raoufi, M. et al., Integr Biol (Camb) 8 (2016) 1059–1066.

SPECTROSCOPIC ELLIPSOMETRY OF ADSORBED PROTEINS ON BIOCERAMIC IMPLANT MATERIAL

Elisabeth Preußeª, Sven Petersᵇ, Adrian Blümichᵇ, Susanne Kurzª, Jörg Opitzª, and Juliane Spohnª

ªBio- and Nanotechnology, Maria-Reiche Straße 2, 01109 Dresden, Fraunhofer Institute for Ceramic Technologies and Systems IKTS, Germany
ᵇThin Film metrology, Schwarzschildstr. 2, 12489 Berlin, SENTECH Instruments GmbH, Germany

Ceramic materials like zirconium oxide have gained increased interest as a biomaterial for dental implants. They provide not only better aesthetical properties but also an improved biocompatibility and a mechanical strength comparable to standard titanium implants. Bioceramics do not oxidize or corrode, giving them an advantage over metal implants. There are many factors, like material surface characteristics, protein adsorption, cell adhesion and type of surrounding tissue, influencing the interaction at the biointerface between a biological system and a material surface.

The primary adhesion of proteins, e.g. from the blood of the patient, is crucial for cell attachment and an associated problem-free integration of the implant in the body. To date, there are only a few immunological, standardized diagnostic tests so that the extent of a clinically acute immune reaction cannot be estimated sufficiently, especially with regard to innovate implant materials.

We present results on a work-in-progress Ellipsometry investigation about the adsorption of serum albumin, a typical blood protein, on zirconium oxide. Our aim is to investigate the protein adsorption on polished (Ra=0.01µm) zirconium oxide by means of thickness measurement of the protein layer. Even with the polishing there still remains a roughness influencing the protein adsorption (Figure 1) which is important to know to correctly evaluate the amount of adsorbed proteins on the ceramic.

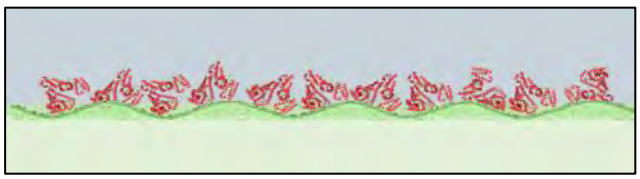

Fig. 1. Modell of adsorbed BSA on zirconium oxide

We used a liquid cell for the in-situ Spectroscopic Ellipsometry (240-900nm) to analyse the optical and structural properties of the protein layer and the zirconium oxide roughness. For a first approach the influence of the pH-value has been studied under various buffer conditions. The adsorbed protein layers were measured after 1h incubation of the material in the corresponding protein solution.

By determining the thickness of the protein layer we were able to quantify the amount of the adsorbed protein on the polished zirconium oxide.

We acknowledge and thank SENTECH Instruments GmbH for their help with the measurements and for providing the liquid cell.

Keywords: Protein adsorption, serum albumin, liquid cell; bioceramic

List of Authors

Legend:

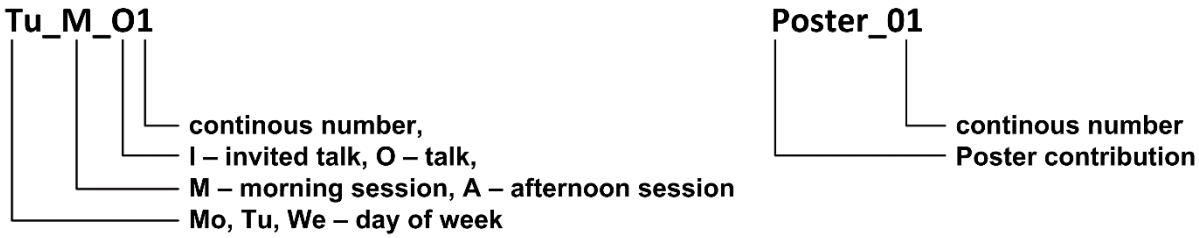

Abadizaman, F.
Contribution(s): P21

Adam, S.
Contribution(s): We_A_I2

Albert, E.
Contribution(s): P40

Almeida, M.
Contribution(s): Mo_A_O2

Alonso, M. I.
Contribution(s): We_A_O2

Andreasson, J.
Contribution(s): We_M_I2, Mo_A_O1, P03

Andres Prada, de R.
Contribution(s): P18

Anghinolfi, L.
Contribution(s): P39

Armakavicius, N.
Contribution(s): We_A_O3, P35

As, D. J.
Contribution(s): Mo_A_O3

Baron, E.
Contribution(s): Mo_A_O3

Basa, P.
Contribution(s): We_M_O3, P40

Beck, U.
Contribution(s): Tu_M_O8, P04

Becker, H.-W.
Contribution(s): P31

Bernhard, C.
Contribution(s): P18

Berrier, A.
Contribution(s): P20

Bisio, F.
Contribution(s): Mo_M_O3, Tu_M_O7, P13, P12

Bittrich, E.
Contribution(s): Mo_M_O6, P38

Bittrich, L.
Contribution(s): P38

Blümich, A.
Contribution(s): We_M_O7, P46

Bodermann, B.
Contribution(s): P07

Bondaz, A.
Contribution(s): We_M_O3

Bonholzer, M.
Contribution(s): Mo_A_O7

Bortchagovsky, E.
Contribution(s): P05

Braeuninger-Weimer, P.
Contribution(s): Tu_M_O6, P15

Brasse, Y
Contribution(s): P12

Colette, C.
Contribution(s): Tu_M_O7

Csontos, J.
Contribution(s): We_M_O5

Darakchieva, V.
Contribution(s): We_A_O3, Mo_A_O8, P35

Denecke, R.
Contribution(s): Mo_A_O7

Deppe, M.
Contribution(s): Mo_A_O3

Derkowska-Zielinska, B.
Contribution(s): P23, P31, P32

Diebold, A.
Contribution(s): P15

Dorywalski, K.
Contribution(s): P06

Dressel, M.
Contribution(s): P20

Duwe, M.
Contribution(s): Tu_M_O5, P41, P37

Dzhagan, V.
Contribution(s): P17

Dzik, P.
Contribution(s): P28

Ecke, R.
Contribution(s): Mo_A_O2

Eichhorn, K.-J.
Contribution(s): We_A_I2, Mo_M_O6, P38

Espinoza, S.
Contribution(s): Mo_A_O1, P03

Espinoza, S.,
Contribution(s): We_M_I2

Esquinazi, P.
Contribution(s): Mo_A_O7

Esser, N.
Contribution(s): P14

Feneberg, M.
Contribution(s): Mo_A_O3

Ferrera, M.
Contribution(s): P13

Fery, A.
Contribution(s): P12

Fischer, D.
Contribution(s): Tu_M_O8

Franta, D.
Contribution(s): P09, P26, P25

Franta, P.
Contribution(s): P26

Franzisco-Lopez, A.
Contribution(s): We_A_O2

Fried, M.
Contribution(s): We_M_O2, P43

Funke, S.
Contribution(s): Tu_M_O6, P15, P41

Furchner, A.
Contribution(s): We_A_I2, Mo_M_O1, P08

Fursenko, O.
Contribution(s): P34

Garriga, M.
Contribution(s): We_A_O2

Gartner, M.
Contribution(s): We_A_O1, P43

Gawek, M.
Contribution(s): Mo_M_O4

Gemme, G.
Contribution(s): P39

Ghanem, B.
Contribution(s): Mo_M_O2

Gheorghe, M.
Contribution(s): P43

Goldhahn, R.
Contribution(s): Mo_A_I2

Goldmann, R.
Contribution(s): Mo_A_O3

Gompf, B.
Contribution(s): Tu_M_I1, P20

Gordan, O. D.
Contribution(s): P17

Goñi, A. R.
Contribution(s): We_A_O2

Grundmann, M.
Contribution(s): We_M_I2, Mo_A_O4, Mo_A_O6, Mo_A_O7, P06, P03, P19

Grunewald, T.
Contribution(s): P07

Gruska, B.
Contribution(s): We_M_O7

Günther, C.
Contribution(s): P17

Haghighian, N.
Contribution(s): Tu_M_O7

Hammerschmidt, M.
Contribution(s): Tu_M_O1

Hansen, P.-E.
Contribution(s): Tu_M_O3

Hernadi, K.
Contribution(s): P11

Herrfurth, O.
Contribution(s): We_M_I2, P03

Hertwig, A.
Contribution(s): Tu_M_O8, Mo_M_O4, Tu_M_O3, Tu_M_O4, P04

Herzinger, M. C.
Contribution(s): We_A_O3

Hidde, G.
Contribution(s): Tu_M_O8

Hingerl, K.
Contribution(s): Mo_M_I1

Hinrichs, K.
Contribution(s): We_A_I2, Tu_M_I2, Mo_M_O5, Mo_M_O1, P44, P08

Hodoroaba, V.-D.
Contribution(s): Tu_M_O4

Hoffmann, C.
Contribution(s): Tu_M_O5, P45, P42

Hoffmann, S.
Contribution(s): Tu_M_O6, P15

Hofmann, T.
Contribution(s): We_M_I1

Horn, A.
Contribution(s): We_M_O6, P02, P01

Hu, C.
Contribution(s): Tu_M_O2

Hu, X.
Contribution(s): Tu_M_O2

Huo, S.
Contribution(s): Tu_M_O2

Huth, P.
Contribution(s): Mo_A_O7

Häussler, L.
Contribution(s): P38

Hórvölgyi, Z.
Contribution(s): P40

Ikushima, K.
Contribution(s): P17

Janasek, D.
Contribution(s): P44

Janietz, S.
Contribution(s): Mo_M_O5

Jansen, L.
Contribution(s): We_M_O4

Jensen, S. A.
Contribution(s): Tu_M_O3

Juhasz, G.
Contribution(s): We_M_O2

Kaehnert, R.
Contribution(s): Tu_M_O4

Kalas, B.
Contribution(s): We_M_O2, P43

Karpus, V.
Contribution(s): P24

Kecsenovity, E.
Contribution(s): P11

Ketelsen, H.
Contribution(s): Mo_M_O1

Knight, S.
Contribution(s): Mo_A_O8, P35

Koenig, T.
Contribution(s): P12

Korlacki, R.
Contribution(s): Mo_A_O8

Kratz, C.
Contribution(s): Mo_M_O5, P44

Kroning, A.
Contribution(s): We_A_I2

Krüger, E.
Contribution(s): Mo_A_O4

Kuo, L.-C.
Contribution(s): P39

Kurz, S.
Contribution(s): P46

Kócs, L.
Contribution(s): P40

Kühne, P.
Contribution(s): We_A_O3, P35

Lenzner, J.
Contribution(s): Mo_A_O6, Mo_A_O7

Li, S.
Contribution(s): Tu_M_O2

Likhachev, D. V.
Contribution(s): We_M_O8, P22

Lorenz, M
Contribution(s): Mo_A_O6

Lubguban, J.
Contribution(s): We_M_O3

Lyzwa, F.
Contribution(s): P18

Ma, X.
Contribution(s): Mo_M_O2

Madan, A.
Contribution(s): We_M_O3

Madkour, S.
Contribution(s): Mo_M_O4

Magnozzi, M.
Contribution(s): Tu_M_O7, P13, P39, P12

Major, C.
Contribution(s): We_M_O2, P40

Marsik, P.
Contribution(s): P18

Martens, D.
Contribution(s): P38

Matkovic, A.
Contribution(s): P15

Matthes, P.
Contribution(s): Mo_A_O2

Mennell, P.
Contribution(s): We_M_O3

Miseikis, V.
Contribution(s): Tu_M_O7

Mock, A.
Contribution(s): Mo_A_O8

Modreanu, M.
Contribution(s): We_A_O1

Moldovan, C.
Contribution(s): P43

Molina-Mendoza, A. J.
Contribution(s): Tu_M_O5

Münch, A.
Contribution(s): Mo_M_O6

Naas, C.
Contribution(s): Mo_M_O6

Nador, J.
Contribution(s): P43

Naparty, M. K.
Contribution(s): P23, P27

Neri, M.
Contribution(s): P39

Neubert, T. J.
Contribution(s): Mo_M_O5

Nickel, N. H.
Contribution(s): Mo_M_O5

Nishimura, A.
Contribution(s): P17

Nowakowska-Langier, K.
Contribution(s): P30, P29

Oates, T. W. H.
Contribution(s): P44

Ogieglo, W.
Contribution(s): Mo_M_O2

Ohlídal, I.
Contribution(s): P09, P26, P25

Okano, S.
Contribution(s): P17

Okrasa, S.
Contribution(s): P30, P29

Olbrich, M.
Contribution(s): We_M_O6, P02, P01

Opitz, J.
Contribution(s): P46

Paraschuk, D. Y.
Contribution(s): Tu_M_O5

Parisse, P.
Contribution(s): Mo_M_O3

Pawlak, M.
Contribution(s): P31

Pazidis, A.
Contribution(s): Mo_A_O5

Peters, S.
Contribution(s): P33, P46

Petrik, P.
Contribution(s): We_M_O2, P43

Pflug, T.
Contribution(s): We_M_O6, P02, P01

Pinnau, I.
Contribution(s): Mo_M_O2

Pinto, G.
Contribution(s): Mo_M_O3

Pinto, I.
Contribution(s): P39

Pistora, J.
Contribution(s): P10

Poimanova, E. Y.
Contribution(s): Tu_M_O5, P37

Postava, K.
Contribution(s): P10

Povey, I.
Contribution(s): We_A_O1

Preuße, E.
Contribution(s): P46

Pápa,Z.
Contribution(s): We_M_O5

Pápa, Z.
Contribution(s): Mo_M_I2, P11

Rahaman, M.
Contribution(s): P16

Rappich, J.
Contribution(s): Mo_M_O5, Mo_M_O1, P08

Rauch, S.
Contribution(s): We_A_I2

Rebarz, M.
Contribution(s): We_M_I2, Mo_A_O1, P03

Reineke-Koch, R.
Contribution(s): Mo_A_O5

Rerek, T.
Contribution(s): P23

Richter, S.
Contribution(s): We_M_I2, Mo_A_O1, P03

Rogalla, D.
Contribution(s): P31

Rosu, D.-M.
Contribution(s): Tu_M_O3, P04

Röling, C.
Contribution(s): Tu_M_O5, P37

Rösicke, F.
Contribution(s): Mo_M_O5

Sachse, R.
Contribution(s): Tu_M_O4

Saftics, A.
Contribution(s): P43

Salvan, G.
Contribution(s): Mo_A_I1, Mo_A_O2

Santiago, X. G.
Contribution(s): Tu_M_O1

Schellenberger, M.
Contribution(s): We_M_O2

Schmidt, C.
Contribution(s): P16

Schmidt-Grund, R.
Contribution(s): We_M_I2, Mo_A_O4, Mo_A_O6, Mo_A_O7, P06, P03

Schmiedova, V.
Contribution(s): P28

Schneider, P.-I.
Contribution(s): Tu_M_O1

Schneider, S.
Contribution(s): P41

Schnoering, G.
Contribution(s): P20

Schubert, M.
Contribution(s): We_A_O3, Mo_A_O8, P35

Schulz, S. E.
Contribution(s): Mo_A_O2

Schönhals, A.
Contribution(s): Mo_M_O4

Sedzicki, P.
Contribution(s): P31, P32

Setzer, A.
Contribution(s): Mo_A_O7

Sharma, A.
Contribution(s): Mo_A_O2

Shaykhutdinov, T.
Contribution(s): We_A_I2, Tu_M_I2

Shaykhutdinova, T.
Contribution(s): Mo_M_O5

Shen, W.
Contribution(s): Tu_M_O2

Skowronski, L.
Contribution(s): We_M_O1, P23, P31, P32, P30, P27, P29

Solano, I.
Contribution(s): Mo_M_O3

Speiser, E.
Contribution(s): P14

Splith, D.
Contribution(s): Mo_A_O6

Spohn, J.
Contribution(s): P46

Stanishev, V.
Contribution(s): We_A_O3, P35

Stapelfeldt, K.
Contribution(s): P45

Stockmann, J. M.
Contribution(s): Tu_M_O8

Stoica, M.
Contribution(s): We_A_O1

Sturm, C.
Contribution(s): Mo_A_O6, P19

Sun, G.
Contribution(s): Mo_M_O5

Sun, L.
Contribution(s): Tu_M_O2

Sun, Z.
Contribution(s): Tu_M_O2

Suter, N.
Contribution(s): P45

Szabó, A.
Contribution(s): P11

Szalai,A.
Contribution(s): P40

Szczesny, R.
Contribution(s): P23, P31, P32

Sáfrán, G.
Contribution(s): P40

Sütő, A.
Contribution(s): P36

Tegze, B.
Contribution(s): P40

Terreni, S.
Contribution(s): P39

Thiesen, P. H.
Contribution(s): Tu_M_O5, Tu_M_O6, P15, P45, P42, P41, P37

Tkacs, J.
Contribution(s): P28

Toth, Z.
Contribution(s): We_M_O5, P11

Tumėnas, S.
Contribution(s): P24

Uhlmann, P.
Contribution(s): We_A_I2, Mo_M_O6

Uttiya, S.
Contribution(s): P39

Vašina, P.
Contribution(s): P25

Vesely, M
Contribution(s): P28

Vohánka, J.
Contribution(s): P09, P26, P25

Voit, B.
Contribution(s): Mo_M_O6

Voloshenko, I.
Contribution(s): P20

Vonderviszt, F.
Contribution(s): P43

Wachowiak, W.
Contribution(s): P27

Walder, C.
Contribution(s): Mo_M_O1, P08

Wang, R.
Contribution(s): Tu_M_O6

Weber, J. O.
Contribution(s): We_A_O2

Weller, M. T.
Contribution(s): We_A_O2

Wenckstern, von H.
Contribution(s): Mo_A_O6

Werner, A.
Contribution(s): Mo_A_O6

Wessling, M.
Contribution(s): Mo_M_O2

Wicher, B.
Contribution(s): P29

Windrich, F.
Contribution(s): P38

Wronkowska, A. A.
Contribution(s): P27

Wronkowski, A.
Contribution(s): P23, P27

Wurm, M.
Contribution(s): P07

Wurtsbauer, U.
Contribution(s): P15

Yamamoto, Y.
Contribution(s): P34

Yang, C.
Contribution(s): Mo_A_O4

Zahn, D. R. T. *Contribution(s):* Mo_A_O2, P17, P16

Zaumseil, P.
Contribution(s): P34

Zdunek, K.
Contribution(s): P30, P29

Zellmeier, M.
Contribution(s): Mo_M_O1, P08

Zmeskal, O.
Contribution(s): P28

Zollner, S.
Contribution(s): We_M_I2, We_A_I1, P03, P21

Zschiedrich, L.
Contribution(s): Tu_M_O1

Zviagin, V.
Contribution(s): Mo_A_O4, Mo_A_O8, Mo_A_O7

Čech, V.
Contribution(s): P26

Čermák, M.
Contribution(s): P09, P26, P25

Ženíšek, J.
Contribution(s): P25


CHEMNITZ
STADT DER
MODERNE
1
2
3
4
Chemnitz Hbf
An der Johanniskirche
Sonnenberg
Augustusburger Straße
Zietenstraße
Fürstenstraße
Sonnenstraße
Jakobstraße
Hainstraße
Uferstraße
Karl-Liebknecht-Straße
Brückenstraße
Mühlenstraße
Theaterstraße
Markt
Am Wall
Rosenhof
Schloßteich
Schloßteichpark
Reichsstraße
Chemnitz Mitte
B 173
B 169
B 174
S 236
B 95

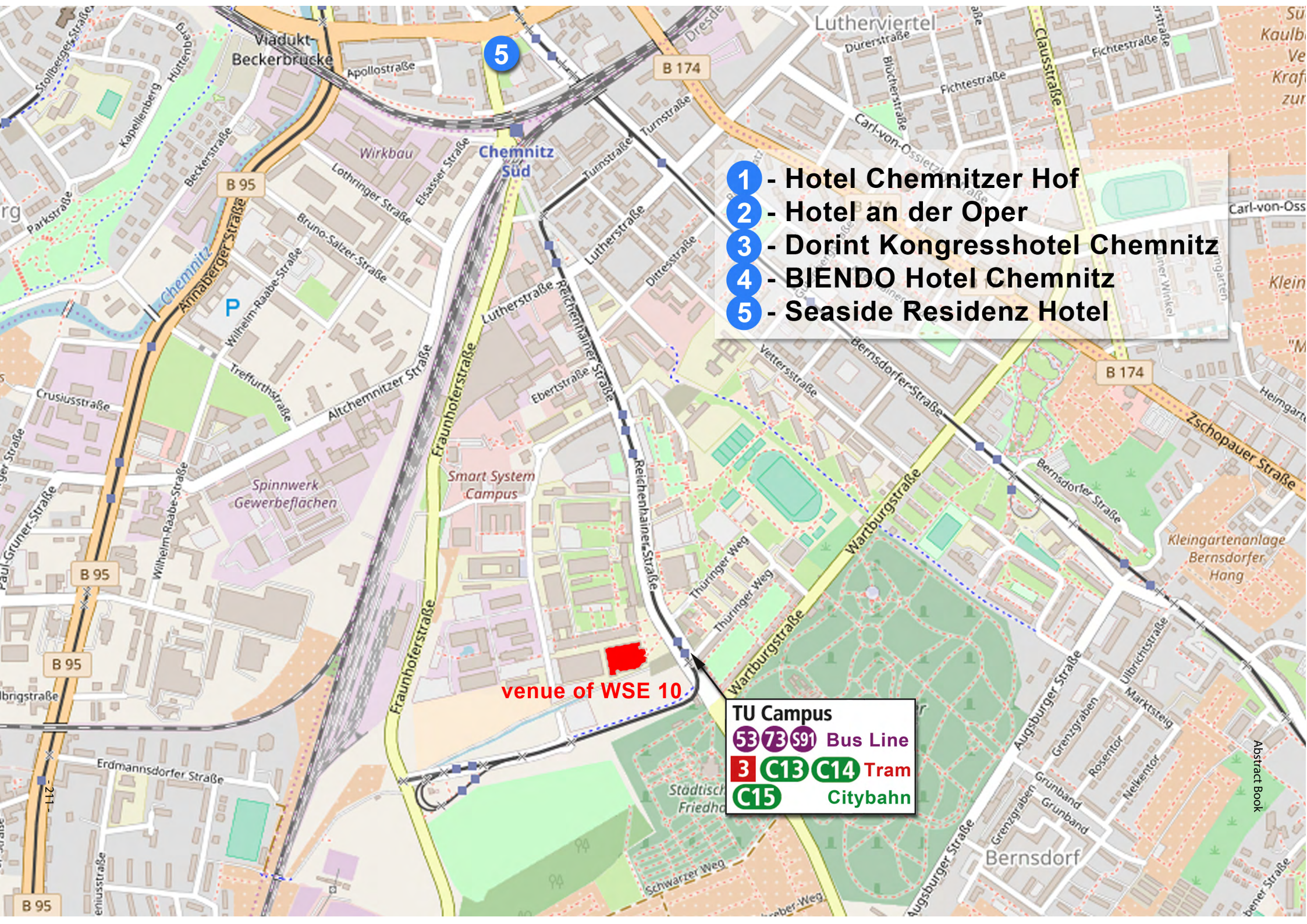
1 - Hotel Chemnitzer Hof
2 - Hotel an der Oper
3 - Dorint Kongresshotel Chemnitz
4 - BIENDO Hotel Chemnitz
5 - Seaside Residenz Hotel
venue of WSE 10
TU Campus
53 73 S91 Bus Line
3 C13 C14 Tram
C15 Citybahn
Chemnitz Süd
Lutherviertel
Viadukt Beckerbrücke
Wirkbau
Spinnwerk Gewerbeflächen
Smart System Campus
Bernsdorf
B 95
B 174
Fraunhoferstraße
Reichenhainer Straße
Wartburgstraße
Bernsdorfer Straße
Zschopauer Straße
Annaberger Straße
Altchemnitzer Straße
Lutherstraße
Turnstraße
Augsburger Straße
Erdmannsdorfer Straße
Schwarzer Weg
Kleingartenanlage Bernsdorfer Hang
Abstract Book
-211-

Campus Map

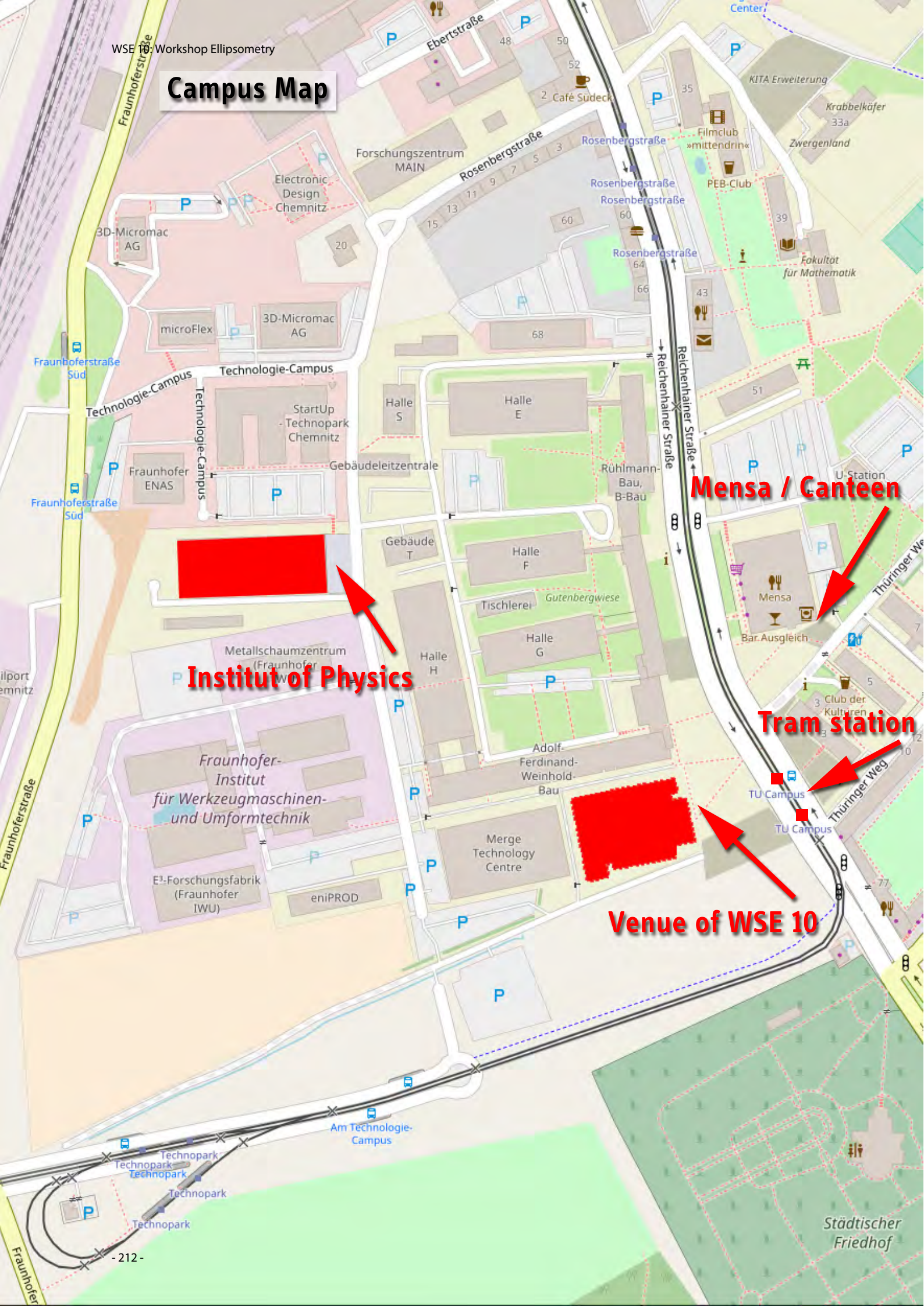
Mensa / Canteen
Institut of Physics
Tram station
Venue of WSE 10
Fraunhoferstraße
Ebertstraße
Rosenbergstraße
Forschungszentrum MAIN
Electronic Design Chemnitz
3D-Micromac AG
microFlex
Technologie-Campus
StartUp - Technopark Chemnitz
Fraunhofer ENAS
Gebäudeleitzentrale
Halle S
Halle E
Halle F
Halle G
Halle H
Gebäude T
Rühlmann-Bau, B-Bau
Reichenhainer Straße
Tischlerei
Gutenbergwiese
Mensa
Bar Ausgleich
U-Station
Thüringer Weg
TU Campus
Club der Kulturen
Adolf-Ferdinand-Weinhold-Bau
Merge Technology Centre
Fraunhofer-Institut für Werkzeugmaschinen- und Umformtechnik
E³-Forschungsfabrik (Fraunhofer IWU)
eniPROD
Metallschaumzentrum (Fraunhofer
Café Südeck
Filmclub »mittendrin«
PEB-Club
KITA Erweiterung
Krabbelkäfer
Zwergenland
Fakultät für Mathematik
Am Technologie-Campus
Technopark
Städtischer Friedhof

www.WSE10.de

secretary@WSE10.de

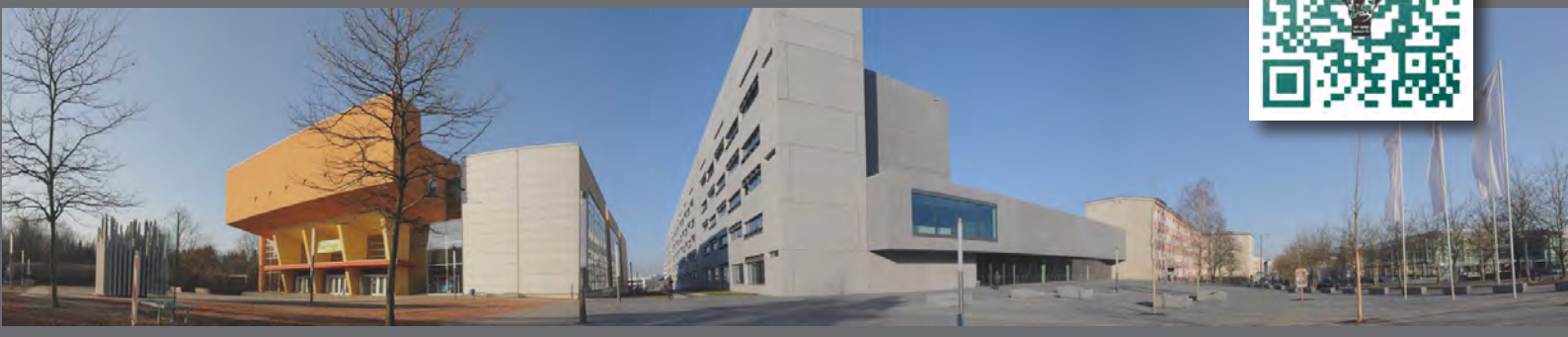

conference venue: Central Lecture Hall Building on the campus